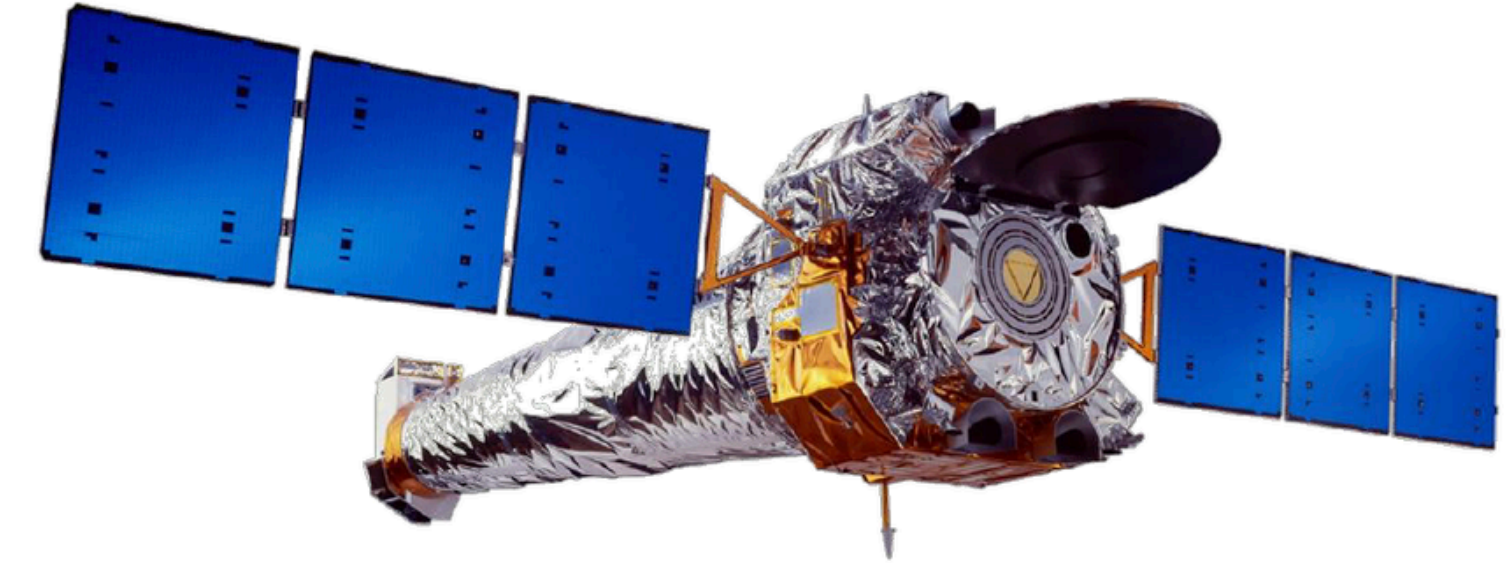
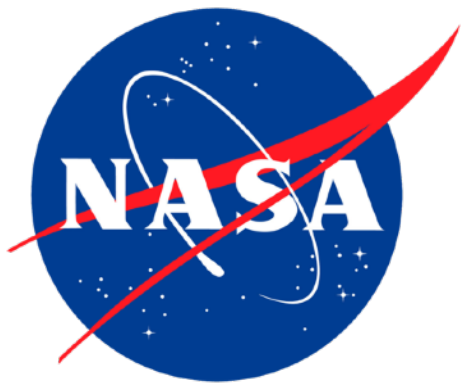
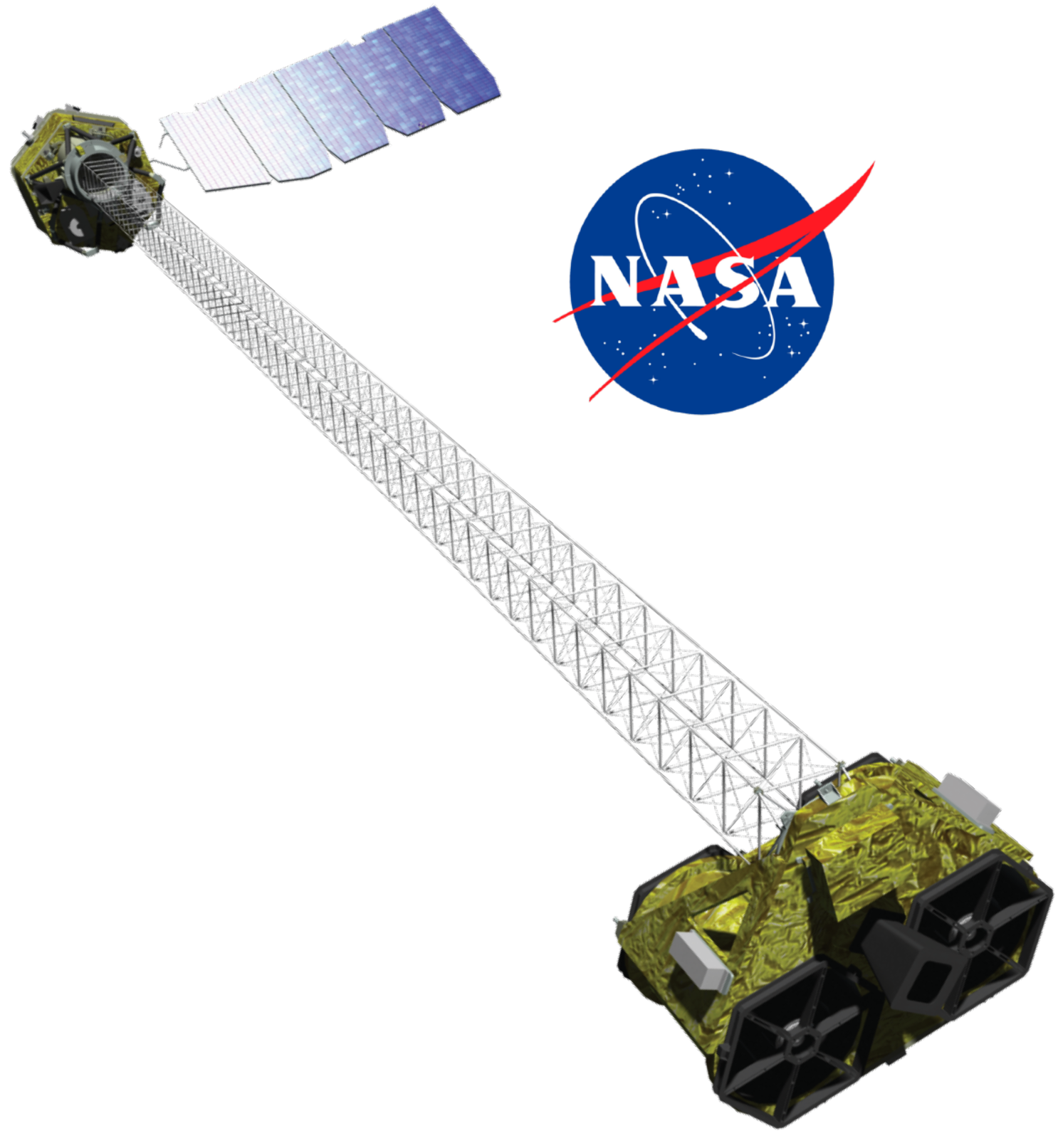


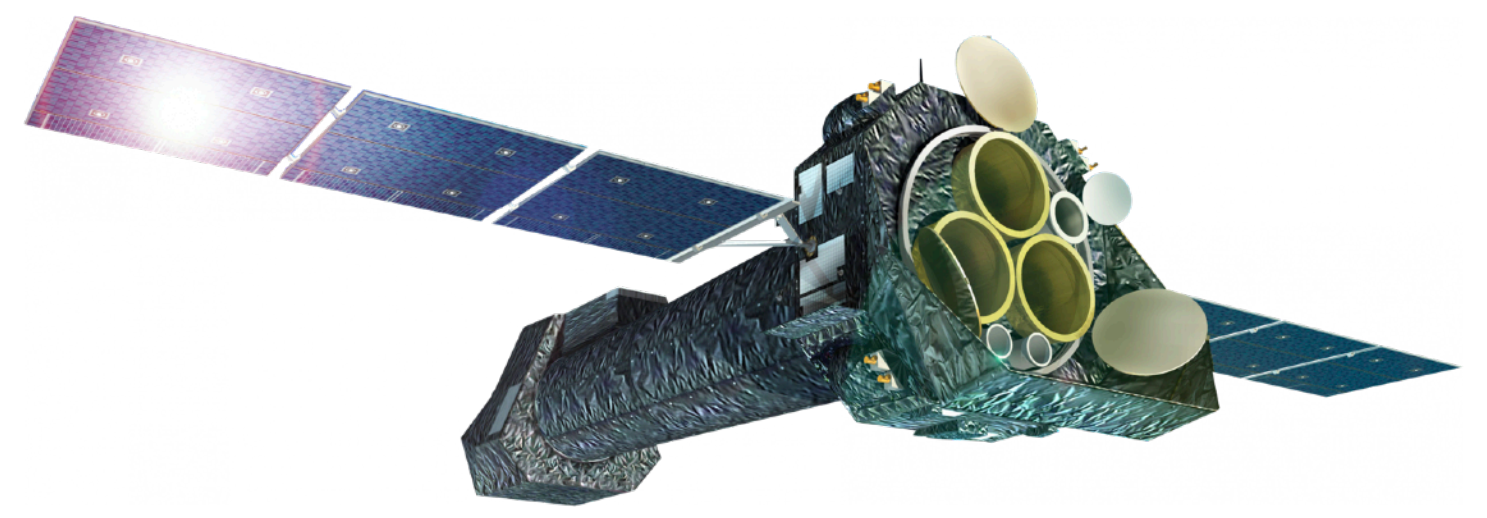
Galaxy Cluster-based Evidence for Conflicting Calibrations between *NuSTAR* and *XMM-Newton/Chandra* at 3-10 keV Energies



CHANDRA X-RAY OBSERVATORY

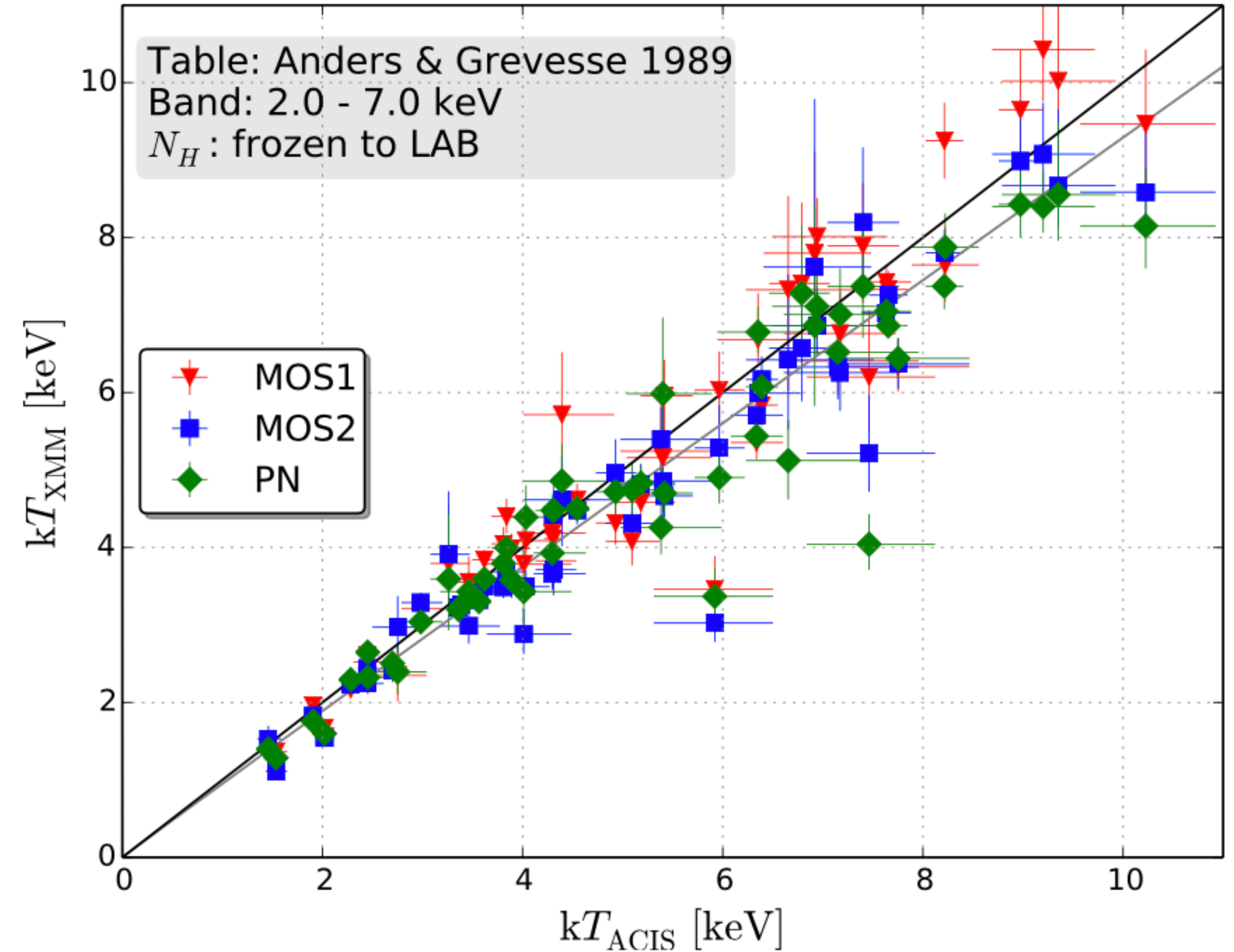
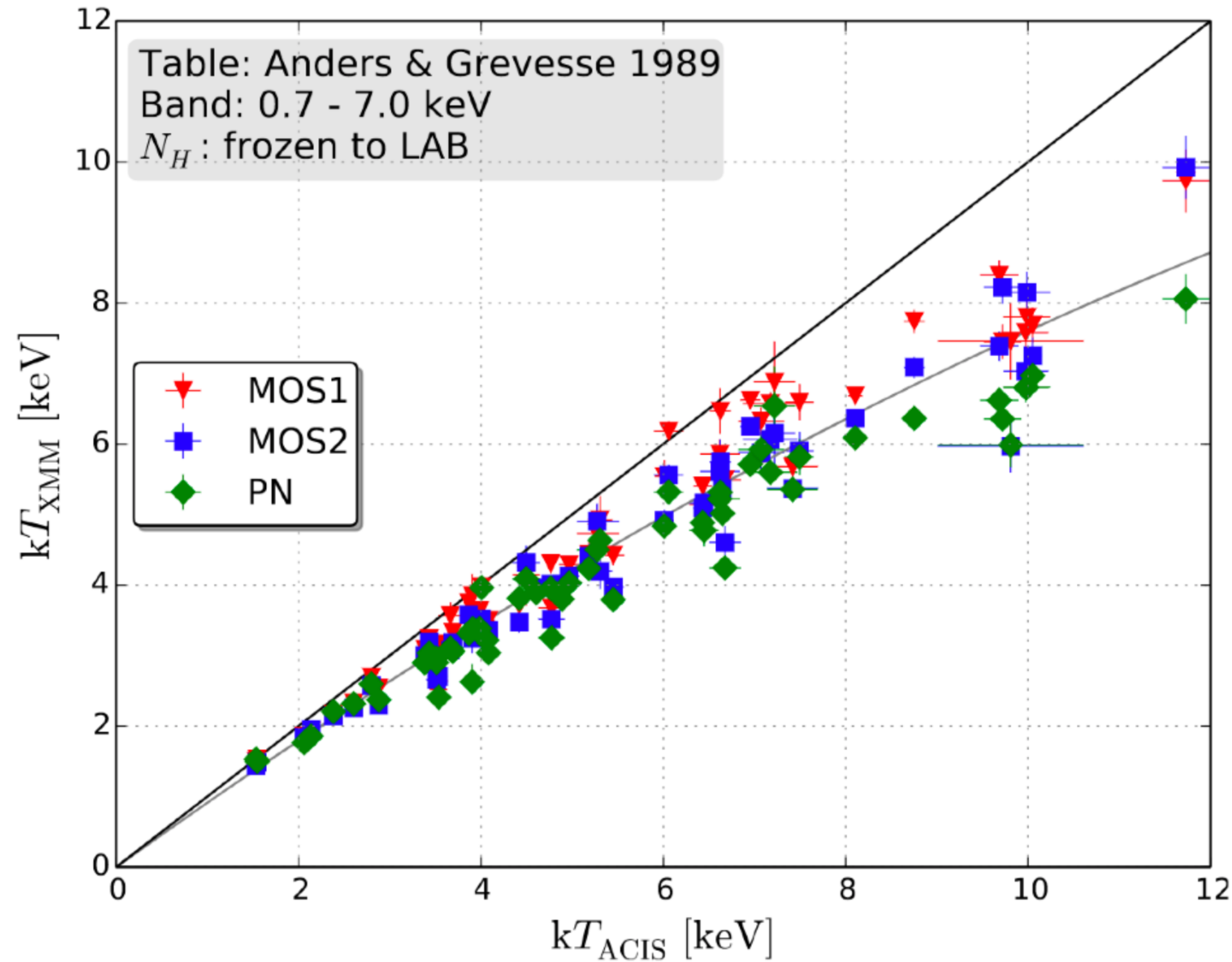
Daniel R. Wik
(University of Utah)

Based mostly on work from
Cicely Potter
(Utah)
and
Fiona Lopez
(Texas A&M)



XMM-NEWTON

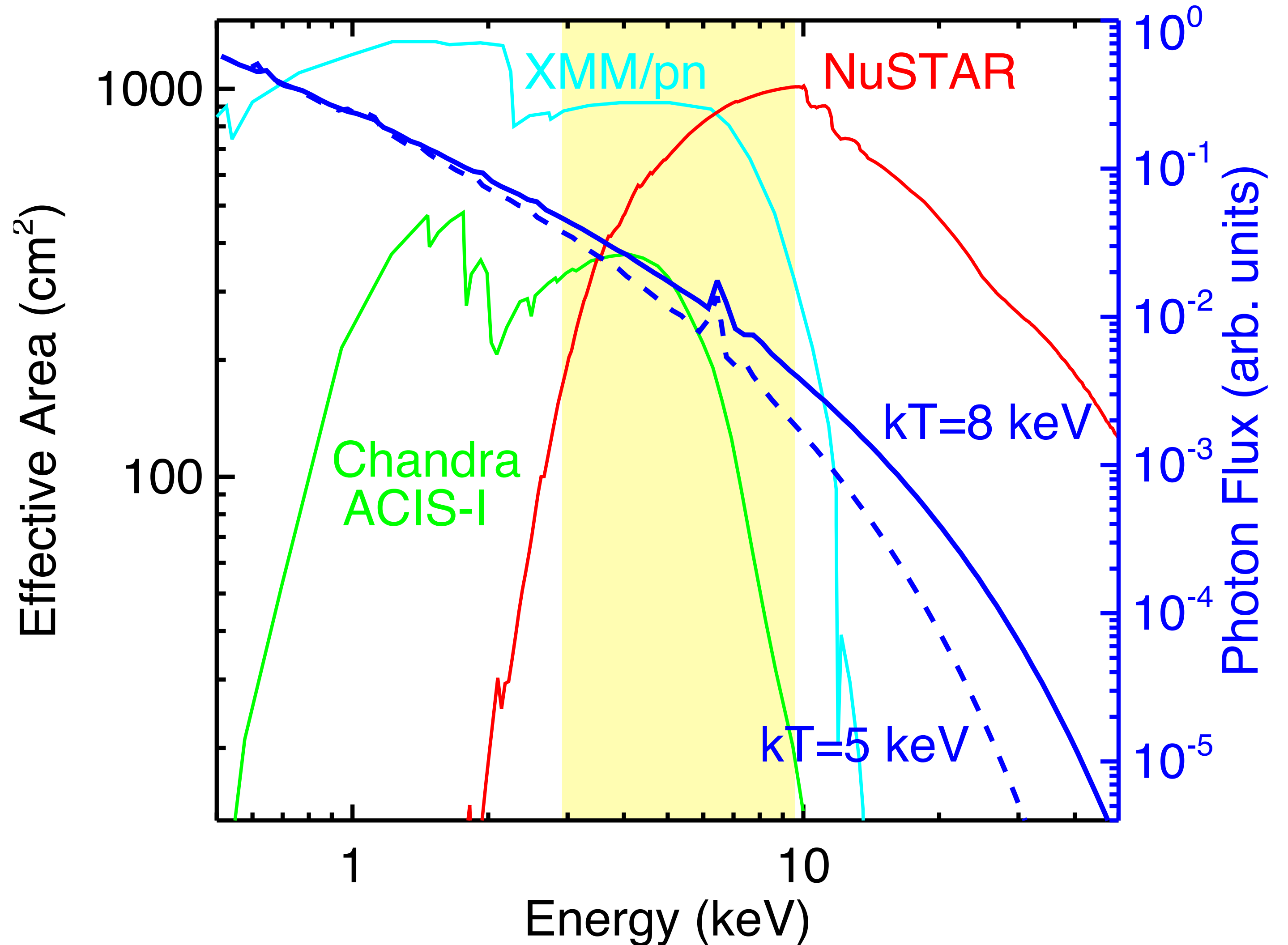
Galaxy Clusters: Temperature Discrepancy



Schellenberger+ 2015

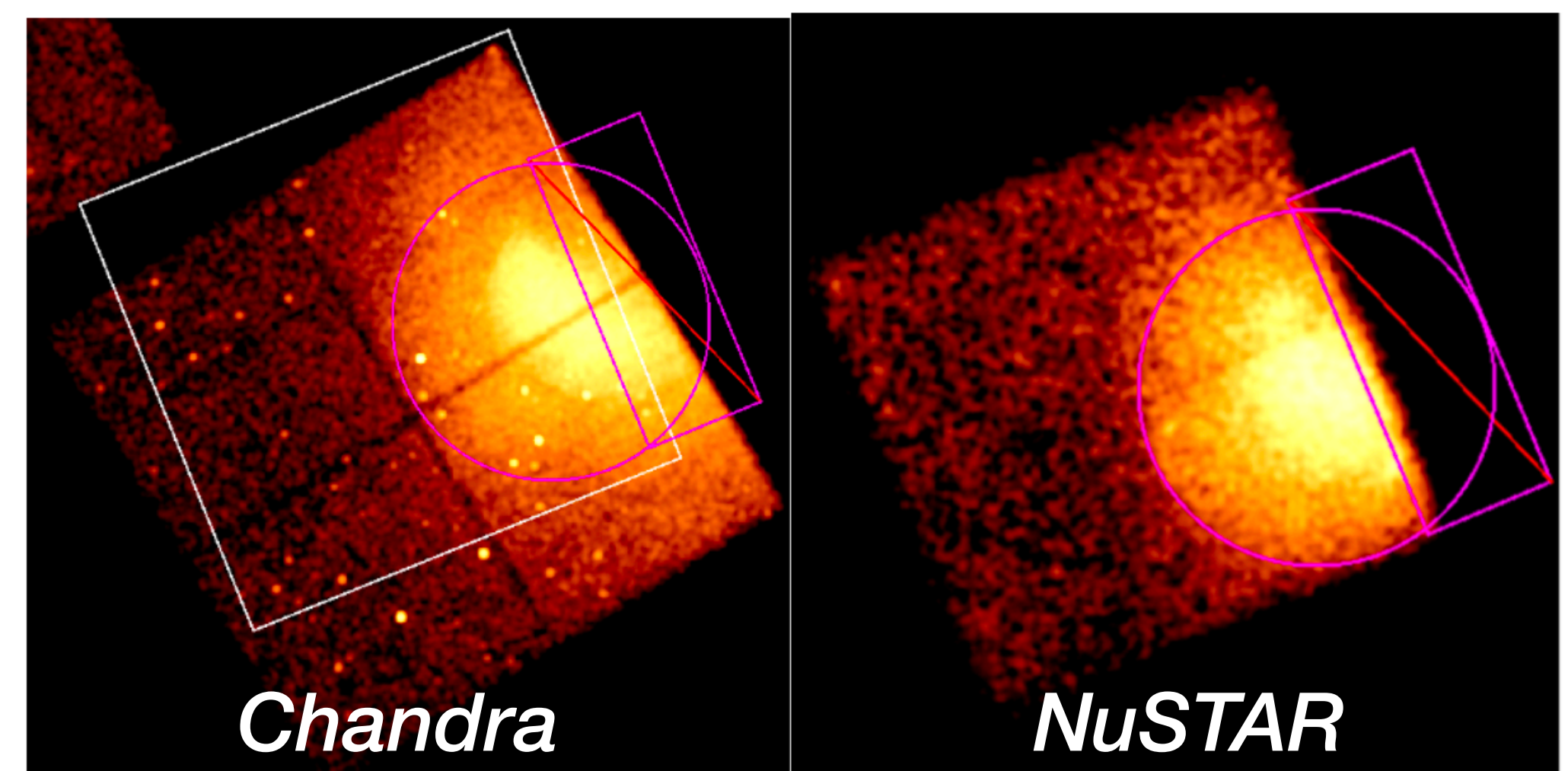
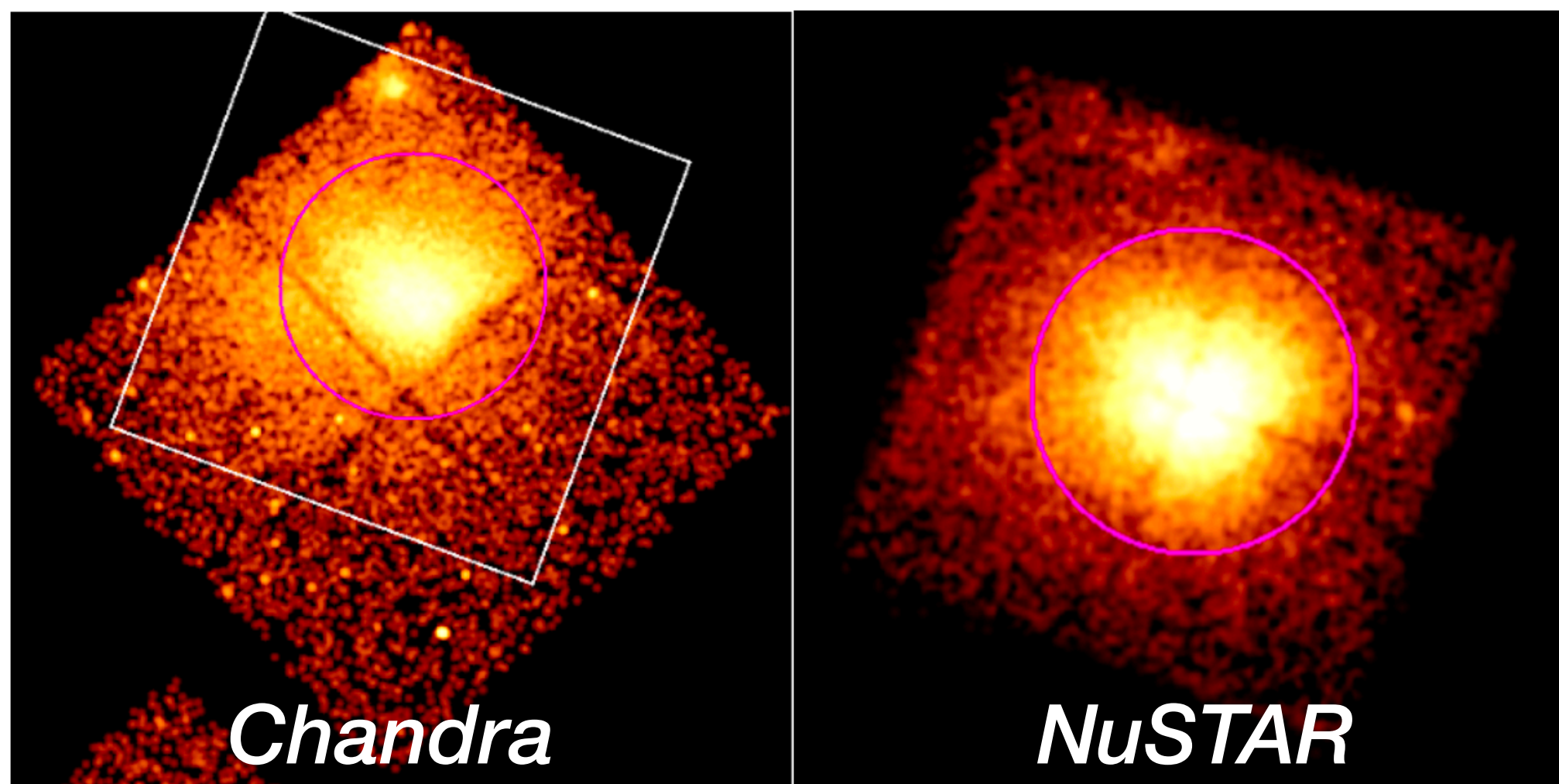
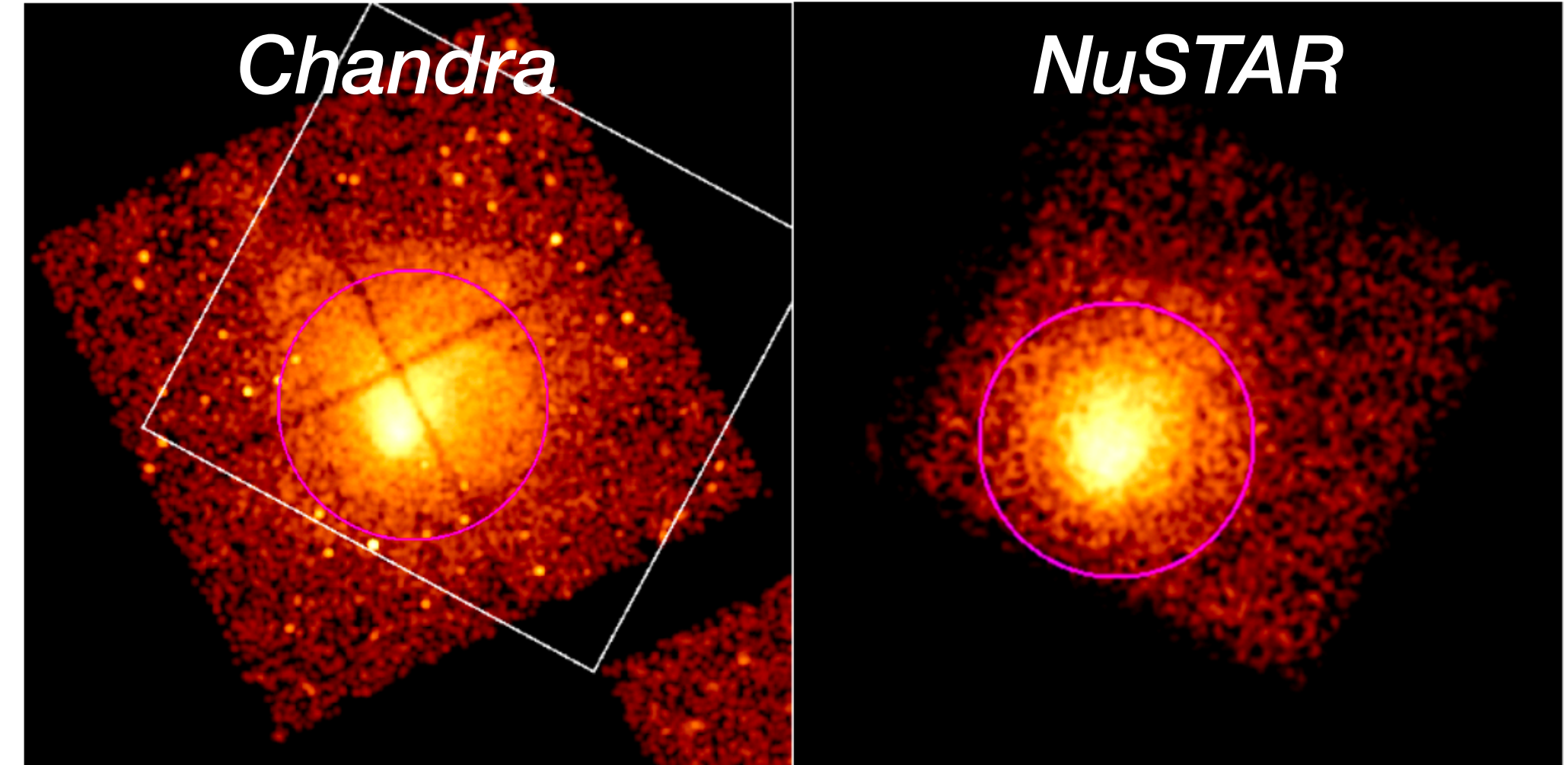
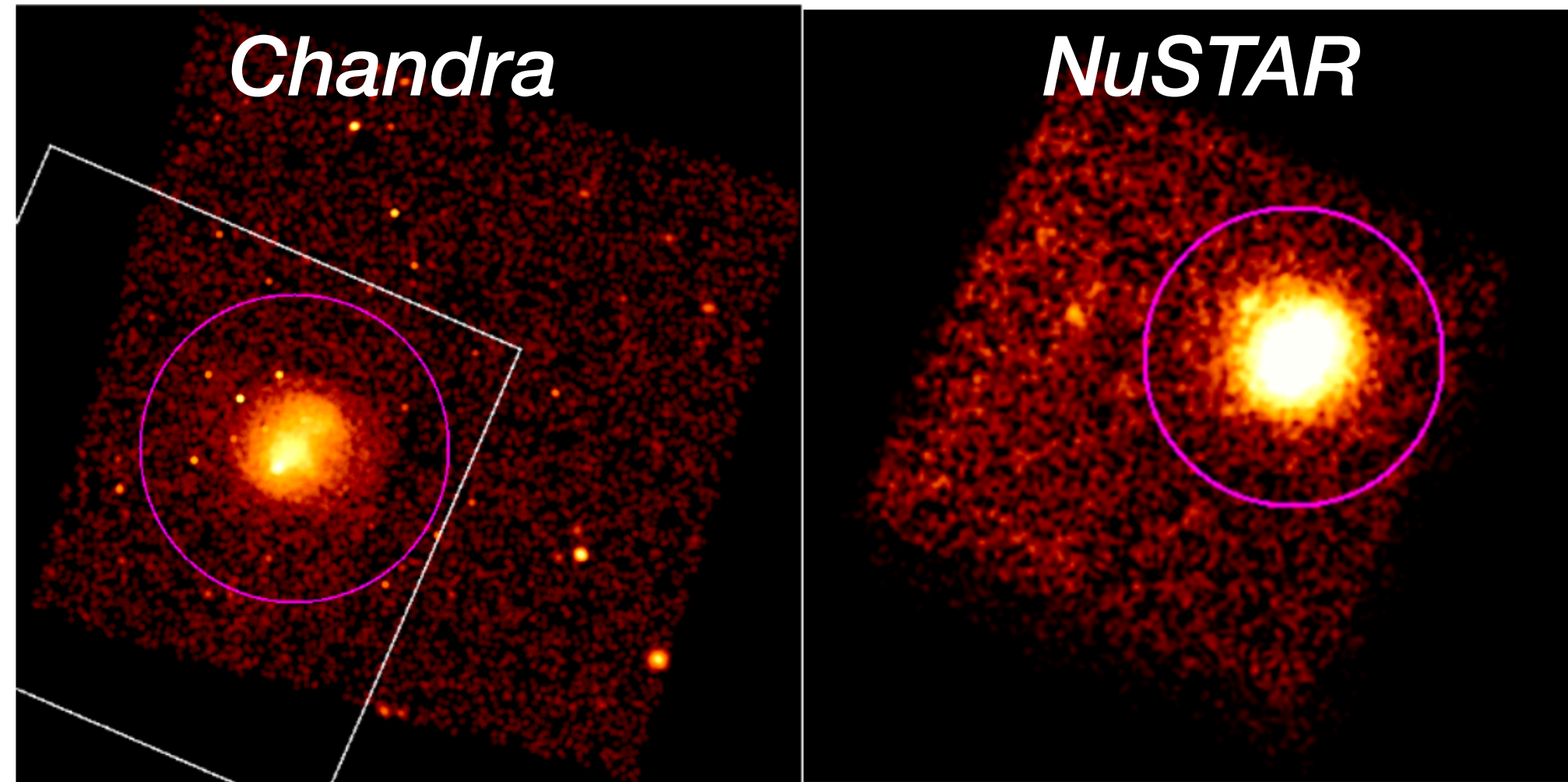
NuSTAR's Contribution

- Discrepancy is worst at the highest temperatures where *NuSTAR's* sensitivity is most useful
- Even for low kT s, *NuSTAR* has a better handle on the exponential turnover of the bremsstrahlung continuum, which drives kT estimates
- In most cases, foreground absorption becomes almost negligible and lines have less impact on the continuum

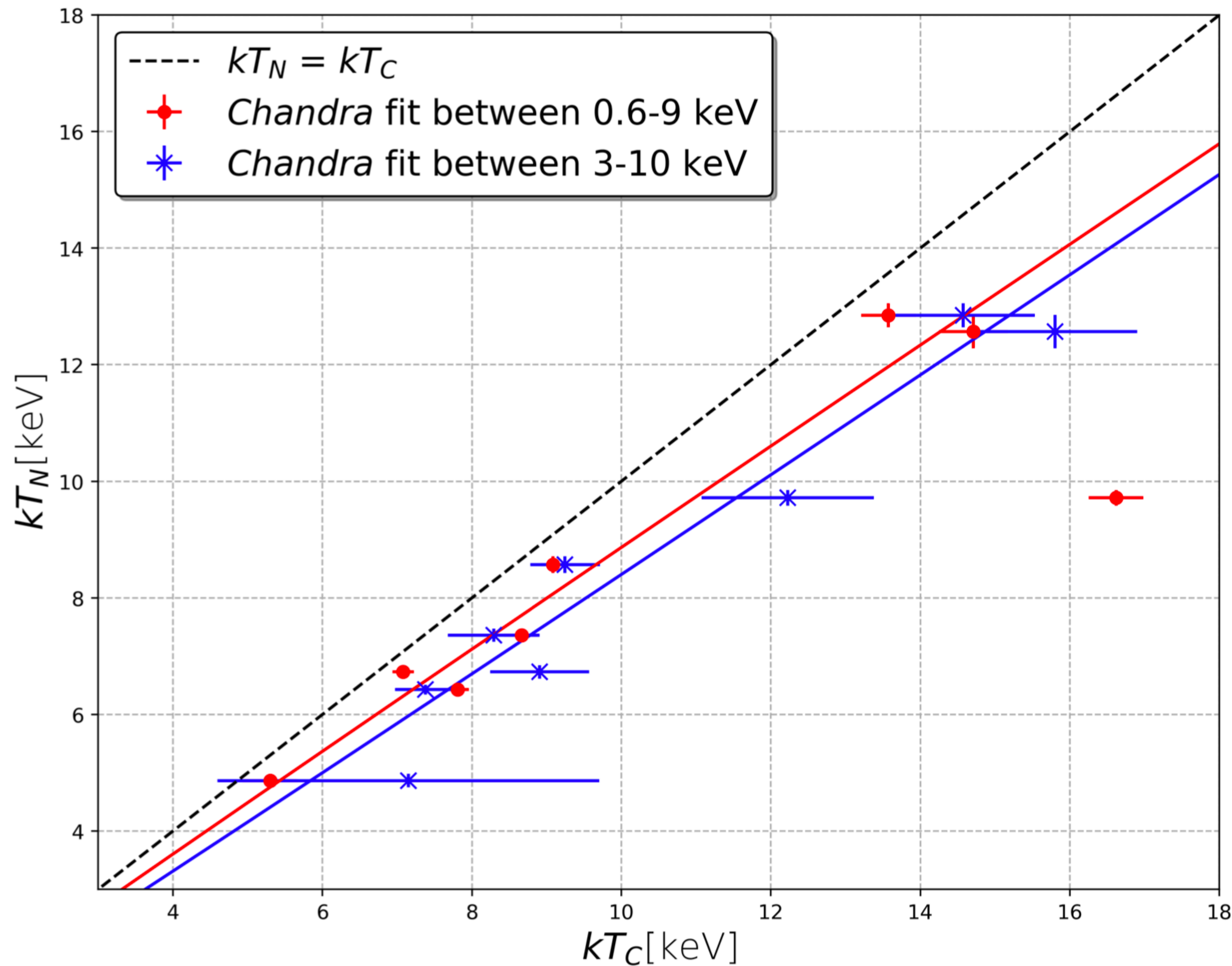


Global kT Measurements (*Chandra* vs. *NuSTAR*)

Wallbank+ 22



Global kT Measurements (*Chandra* vs. *NuSTAR*)



Cluster Name	$kT_{C,(0.6-9)}$ keV	kT_C keV	kT_N keV
Abell 2146	7.08 ± 0.14	8.9 ± 0.66	6.72 ± 0.11
Abell 2163	$16.36 \pm 0.70^\dagger$	12.23 ± 1.15	9.72 ± 0.13
Abell 2256	7.81 ± 0.15	7.38 ± 0.41	6.43 ± 0.085
Abell 523	5.30 ± 0.36	7.15 ± 2.55	4.87 ± 0.12
Abell 665	8.66 ± 0.23	8.29 ± 0.62	7.36 ± 0.11
Abell 754	9.09 ± 0.17	9.25 ± 0.47	8.57 ± 0.14
1E 0657-56	13.57 ± 0.36	14.57 ± 0.96	12.85 ± 0.20
RX J1347.5-1145	14.71 ± 0.46	15.80 ± 1.09	12.57 ± 0.29

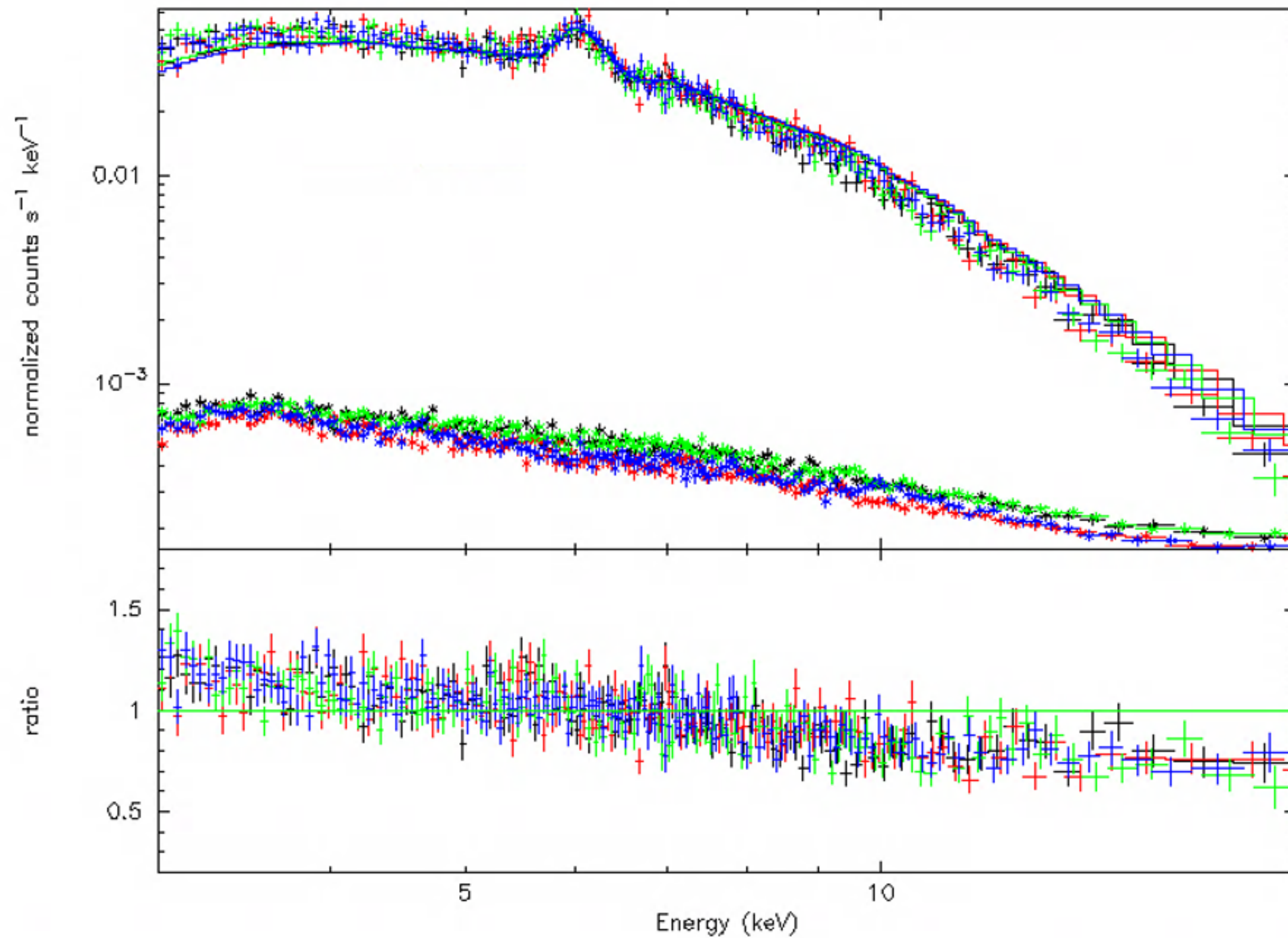
For a *Chandra* kT of 10 keV,
the *NuSTAR* kT is
11% or **16%** lower

Physically, *NuSTAR* should be
biased to *higher* kTs \rightarrow must be
due to differences in calibration

Wallbank+ 22

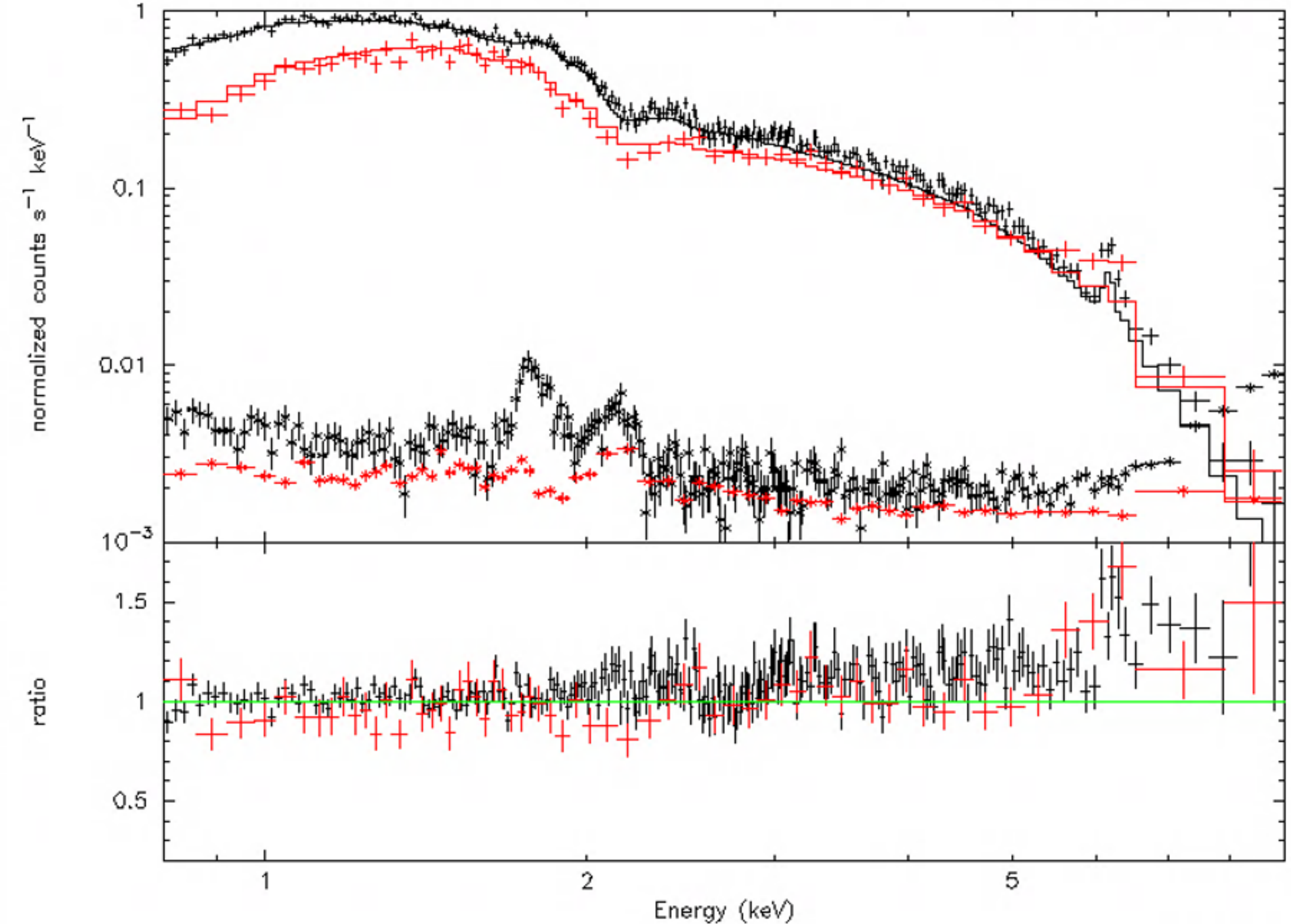
NuSTAR - Chandra Comparison

NuSTAR spec. with Chandra params (68" to 101")



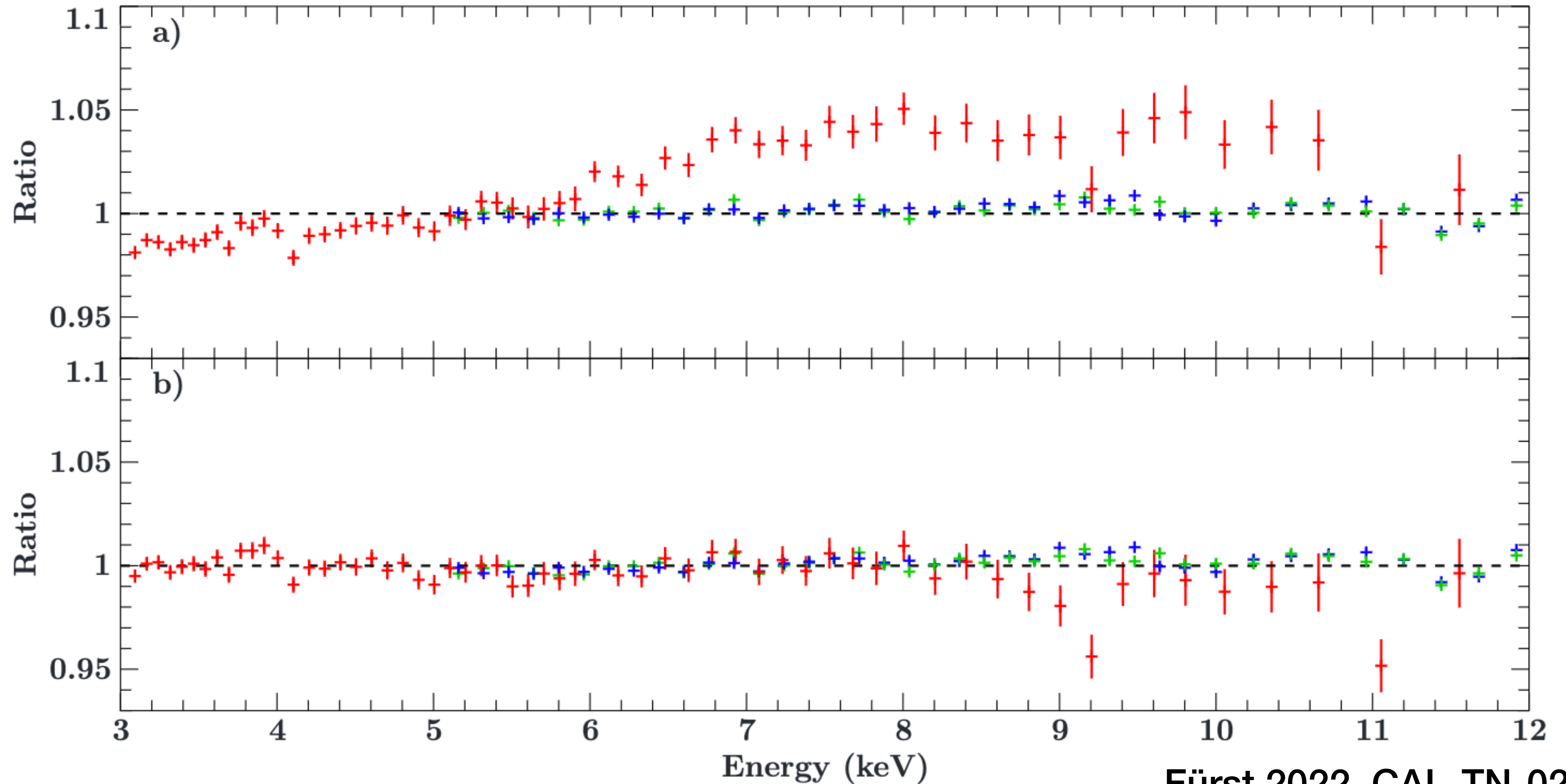
NuSTAR data with *Chandra* best-fit model
C-stat/dof: 3006/1567

Chandra spec. with NuSTAR params (68" to 101")



Chandra data with *NuSTAR* best-fit model
C-stat/dof: 1105/964

NuSTAR - *XMM-Newton* Comparison



Fürst 2022, CAL-TN-0230-1-3

Cross-calibration with Relaxed Clusters

Cicely Potter

NuSTAR Large Program
(>100 ks each)

Cluster	kT (keV)	z
Abell 2029	8.5	0.077
Abell 478	7.3	0.088
Abell 1795	6.1	0.062
Abell 2199	4.4	0.030

Reanalysis of *Chandra/XMM-Newton* data in exact same regions

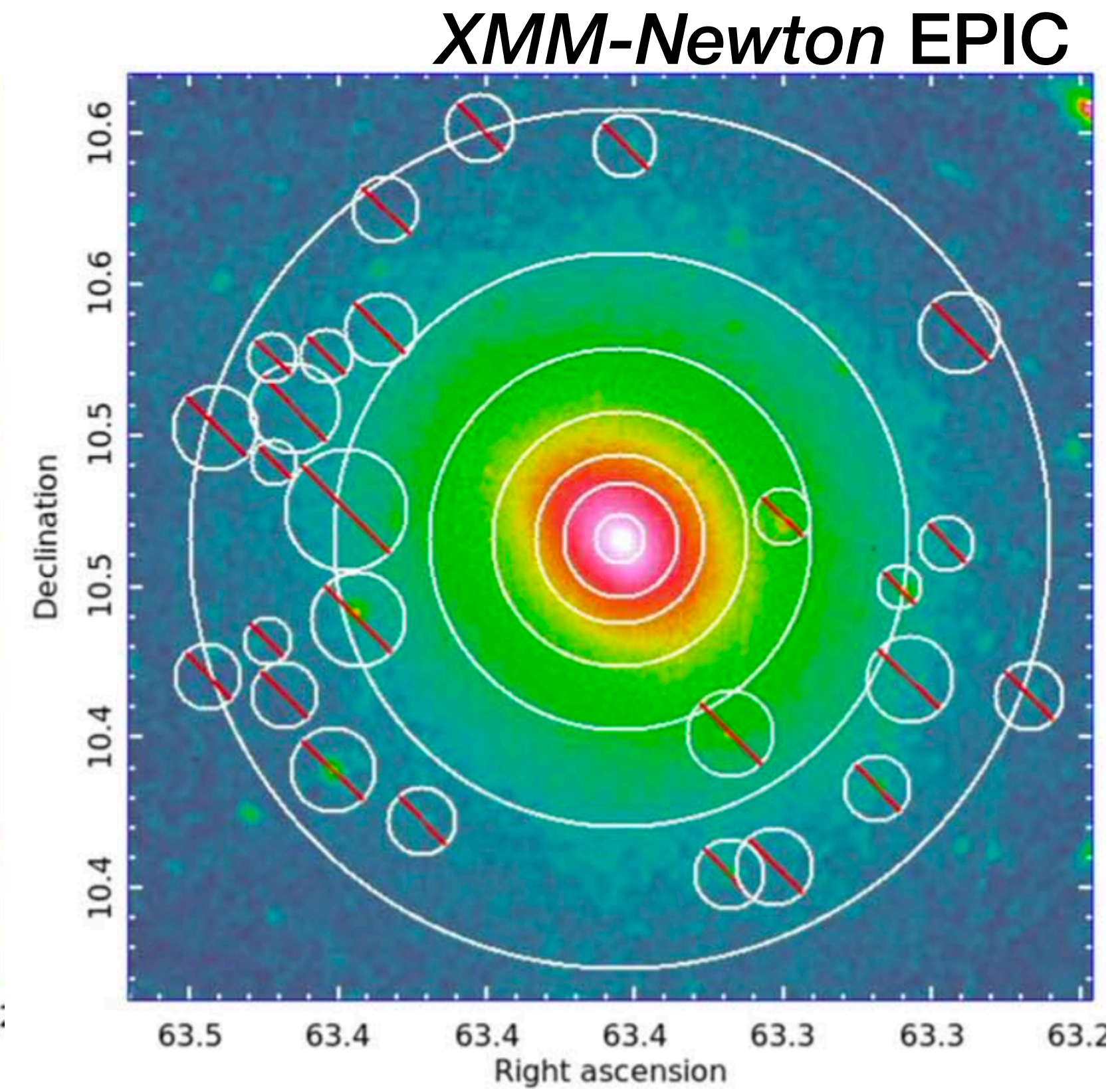
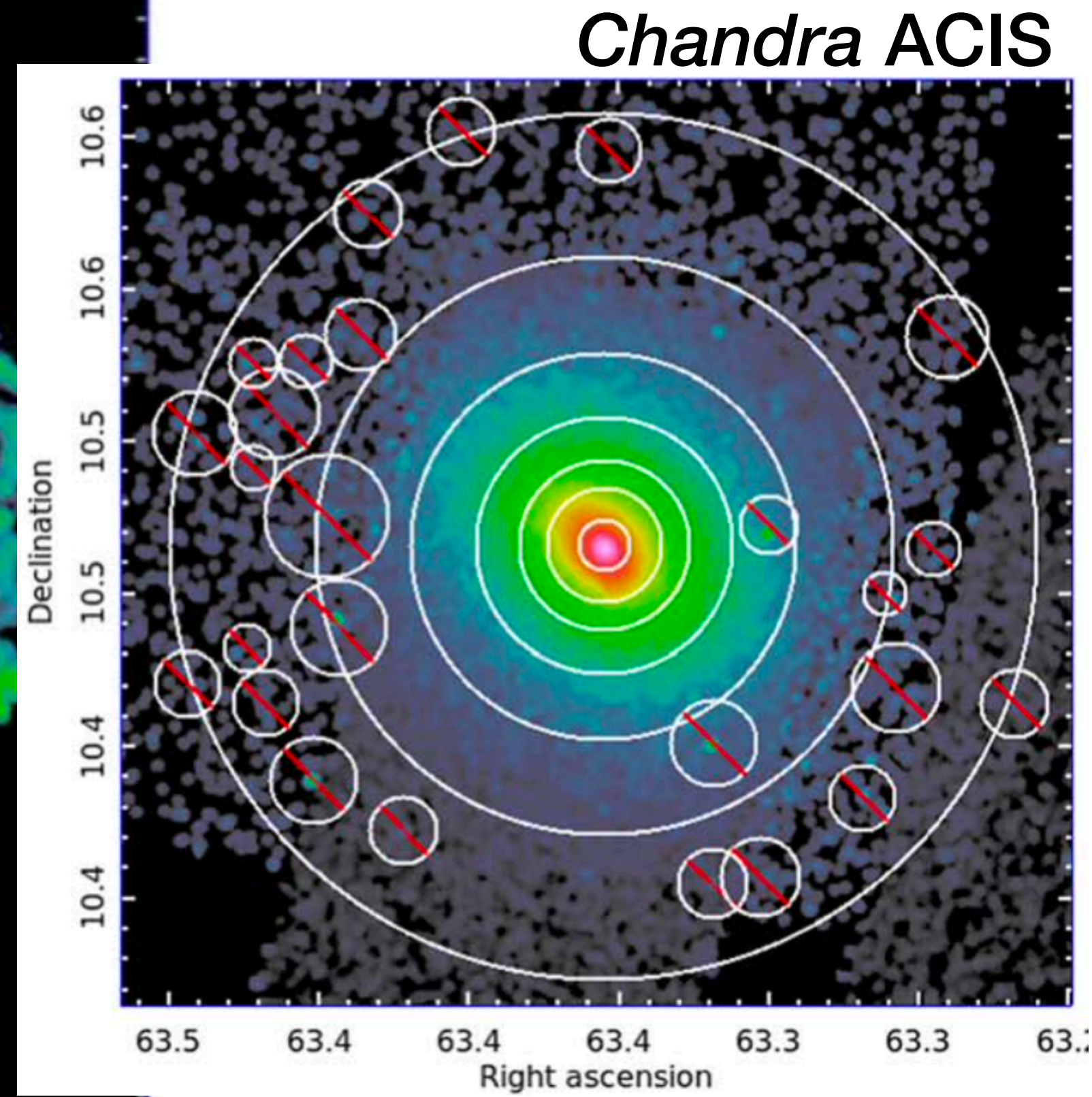
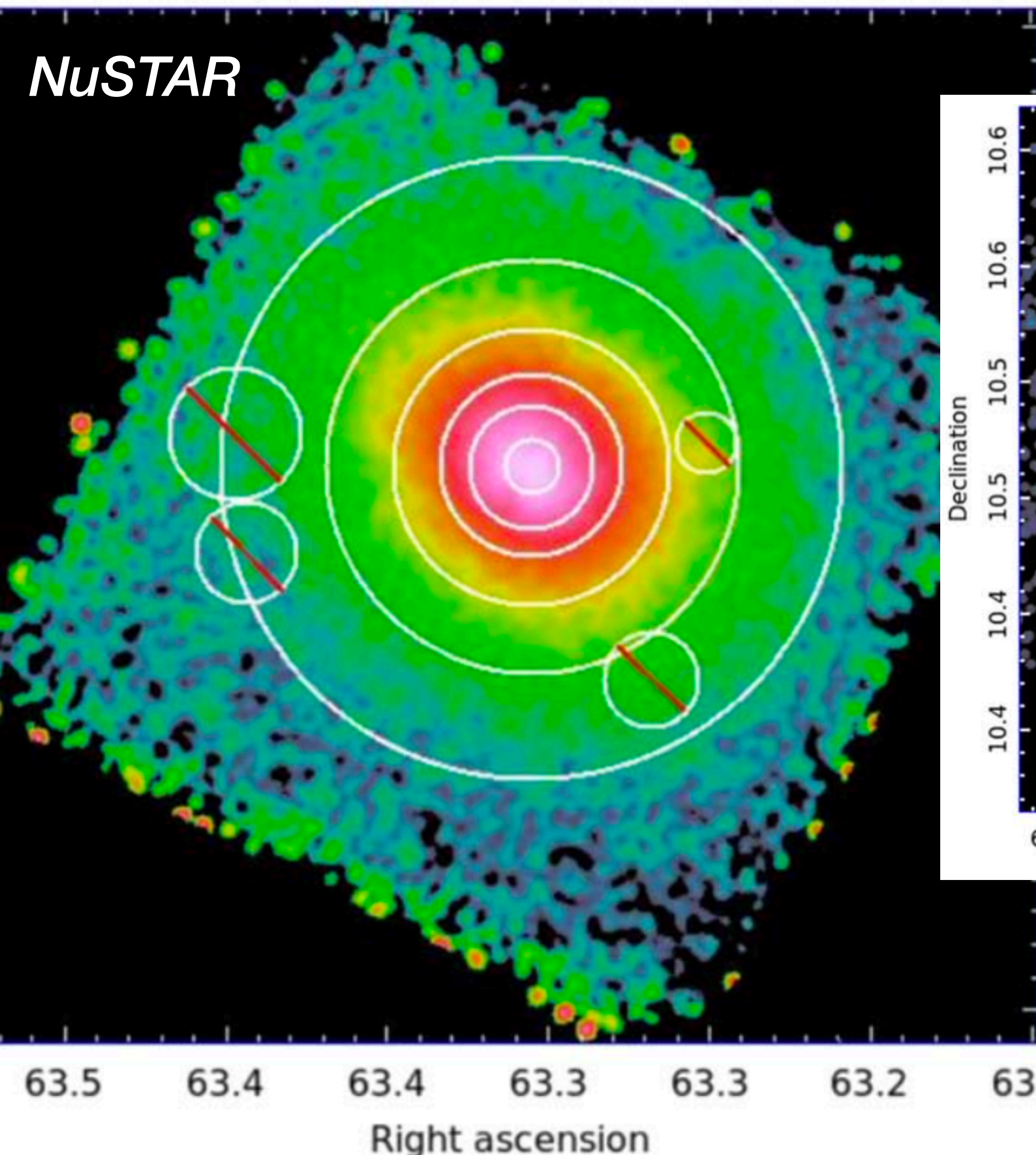
Fiona Lopez

NuSTAR Cluster Snapshot C Program
(20 ks each)

Cluster	kT_C (keV)	ΔkT_X (keV)	$\frac{T_C - T_X}{T_X}$	ΔkT_N (keV)
RXC J1504	9.8 ± 0.8	0.2	0.53	0.8
Abell 3571	8.1 ± 0.1	0.1	0.27	0.1
Abell 3558	7.4 ± 0.3	0.1	0.35	0.2
Abell 1651	7.1 ± 0.3	0.1	0.16	0.1
Abell 3391	6.6 ± 0.2	0.1	0.19	0.2
Abell 1650	6.4 ± 0.1	0.1	0.25	0.2
Abell 3158	6.0 ± 0.1	0.1	0.18	0.1
Abell 3112	5.5 ± 0.1	0.1	0.36	0.2
Abell 1644	5.3 ± 0.1	0.2	0.15	0.2
Abell 496	5.2 ± 0.1	0.1	0.18	0.2
Abell 3562	5.0 ± 0.3	0.1	0.19	0.1

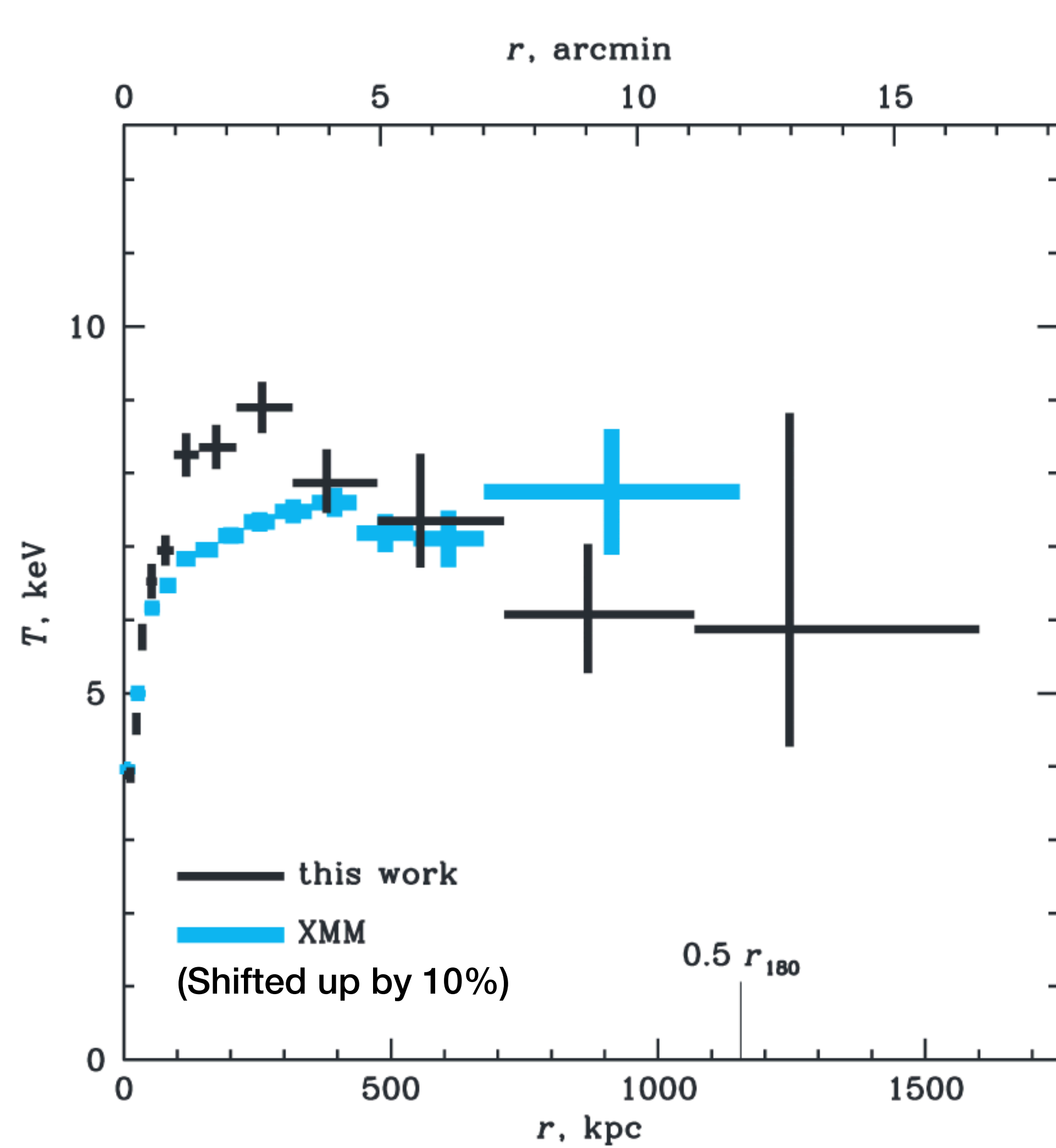
Extract same regions as in Schellenberger+ 2015
($r < 3.5'$, excising cores)

NuSTAR/Chandra/XMM-Newton of Abell 478

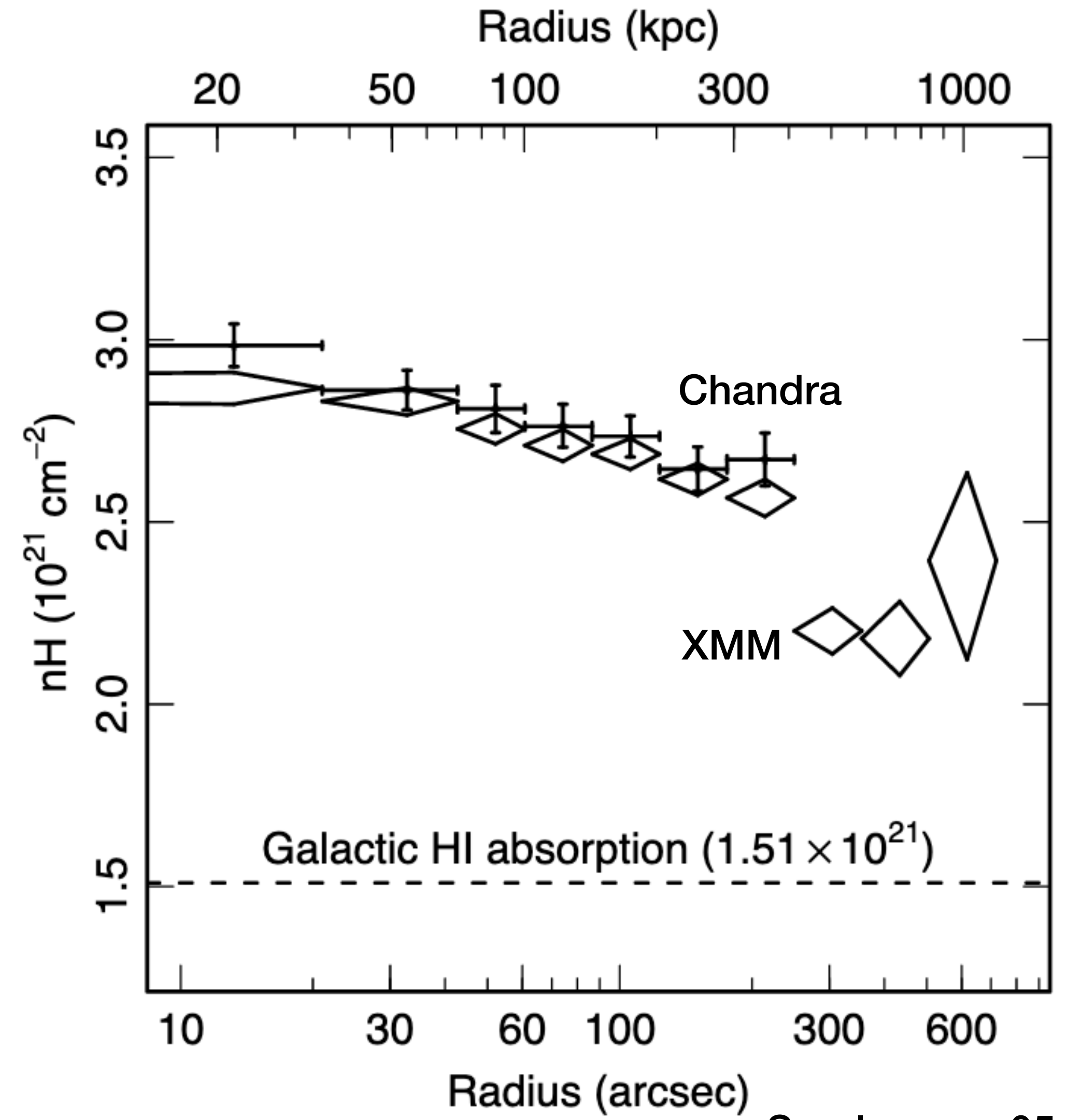


Potter+ 2023

Chandra & XMM-Newton kT Profiles

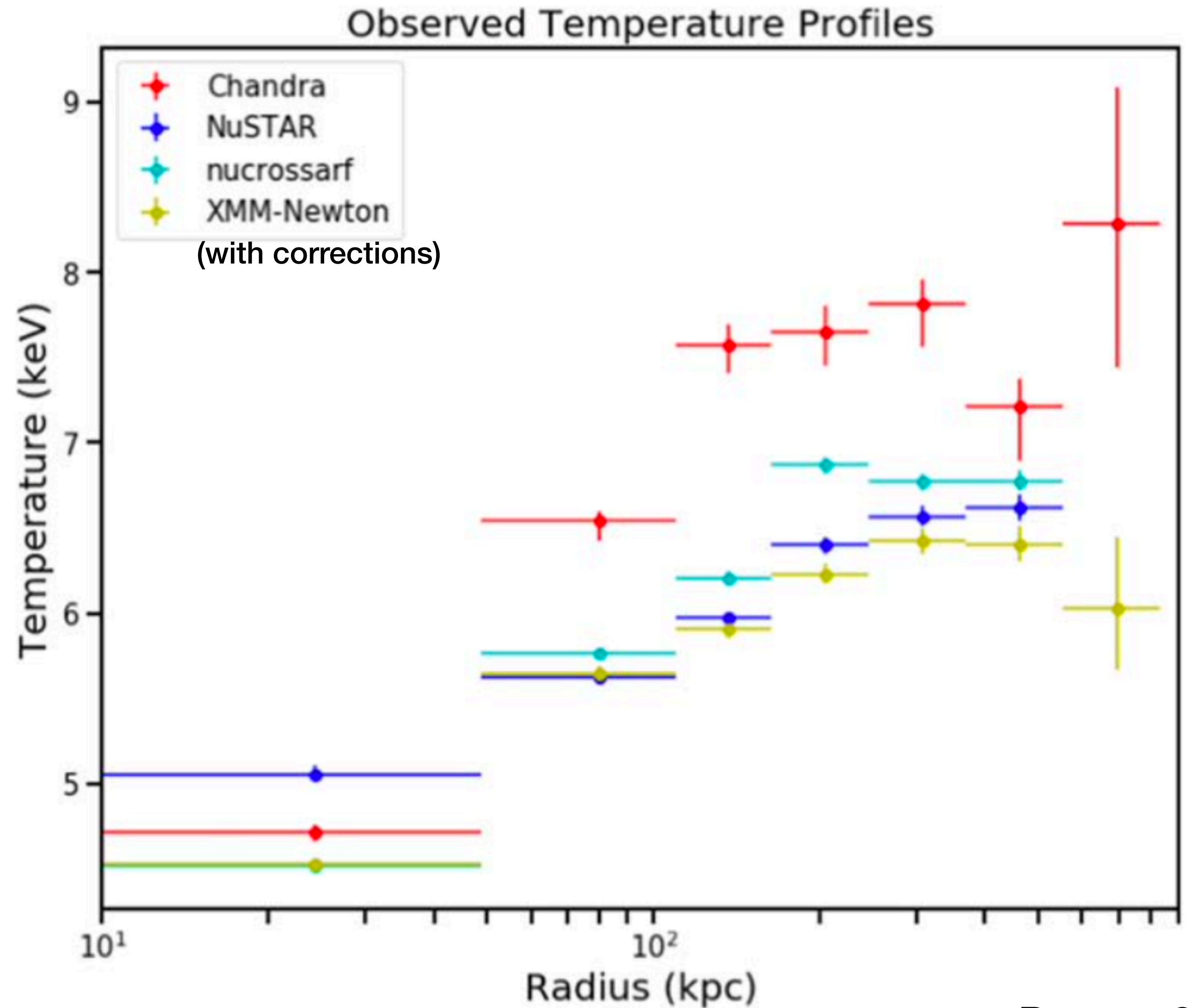


Vikhlinin+ 05, Pointecouteau+ 04



Sanderson+ 05

Abell 478: Temperature Profiles



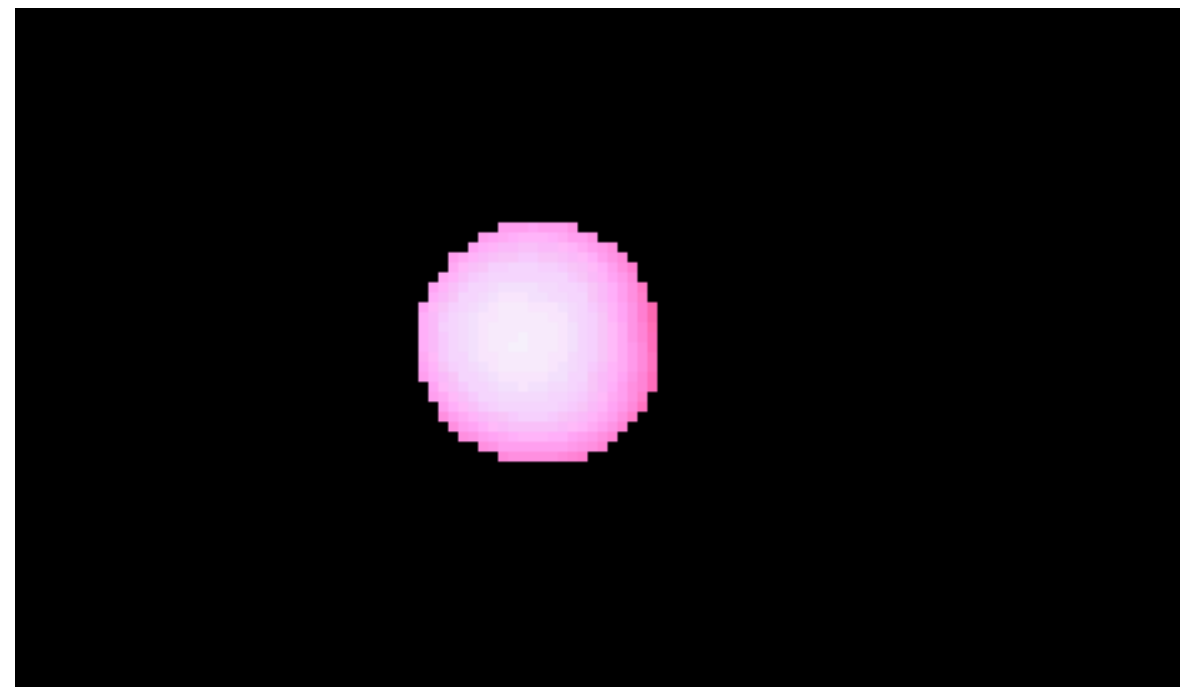
Potter+ 2023

NuSTAR PSF Correction Using “Cross-ARFs”

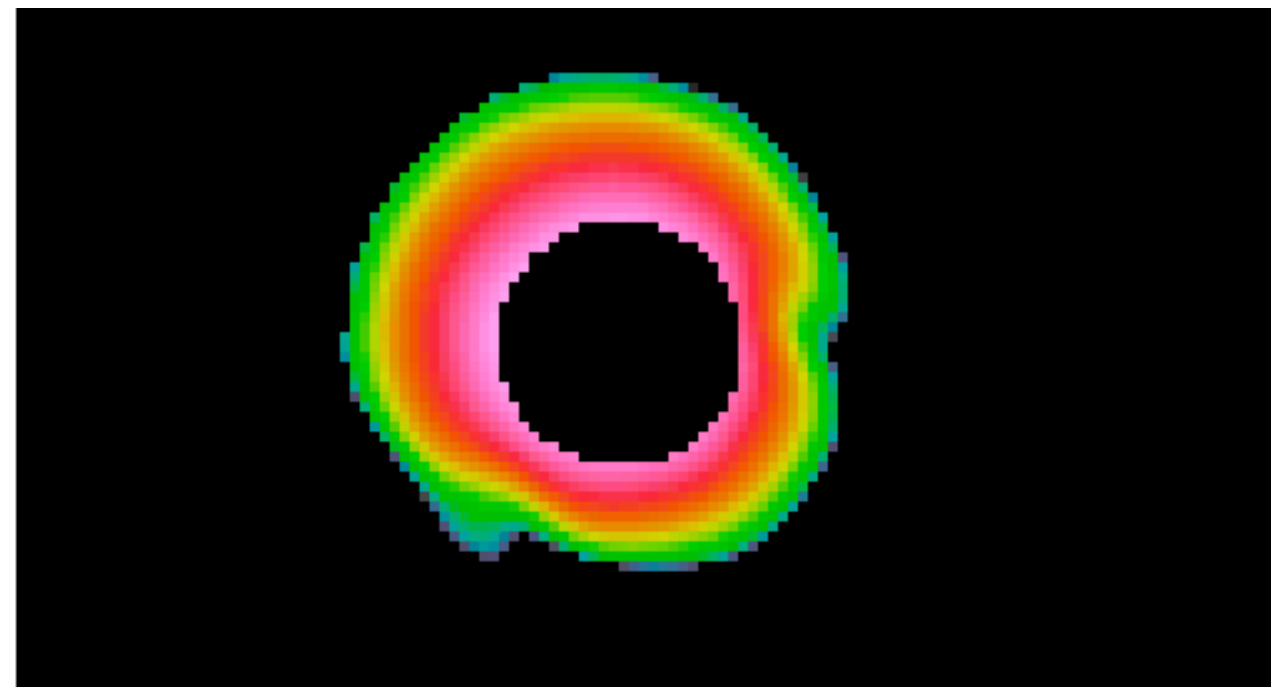
Systematic uncertainty of
point source reconstruction
is 3.4% (Creech+ 2024)



Equivalent to ARF
produced by nuproducts

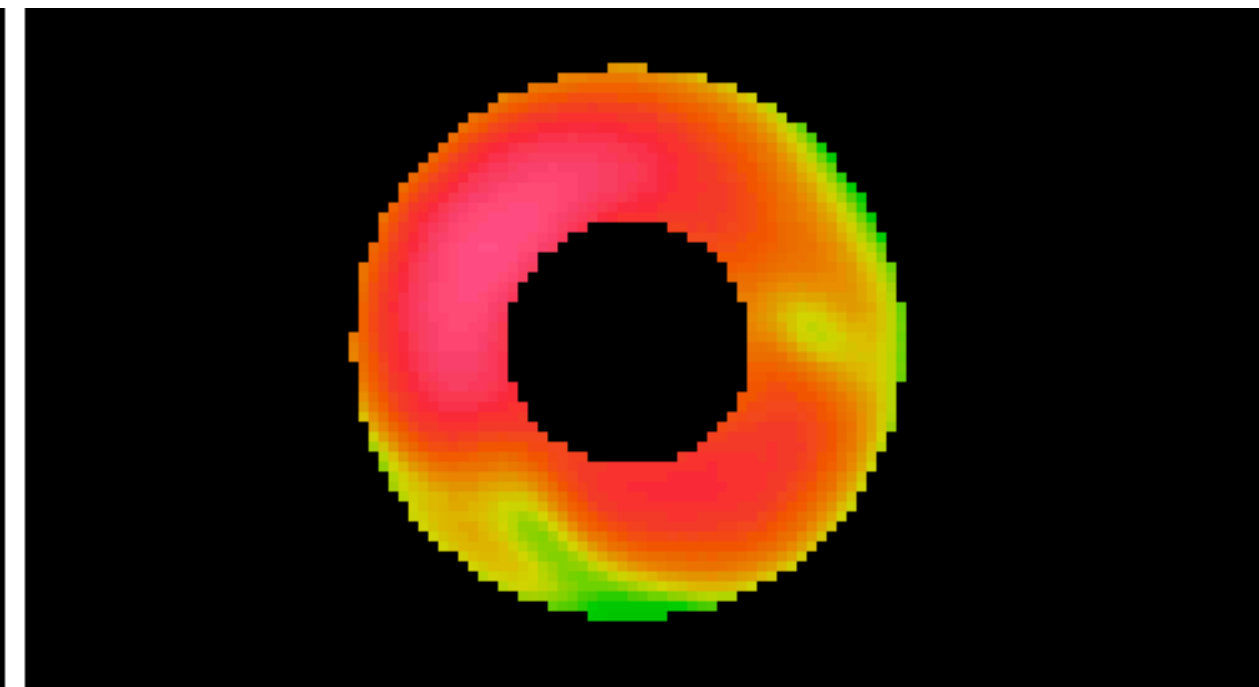


Emission inside
Annulus 1,
modulated by the
PSF, creating a
weighted ARF



Emission scattered
from Annulus 1 into
Annulus 2 by the
PSF, creating a
weighted cross-ARF

Equivalent to ARF
produced by nuproducts



Emission inside
Annulus 2,
modulated by the
PSF, creating a
weighted ARF



Emission scattered
from Annulus 2 into
Annulus 1 by the
PSF, creating a
weighted cross-ARF

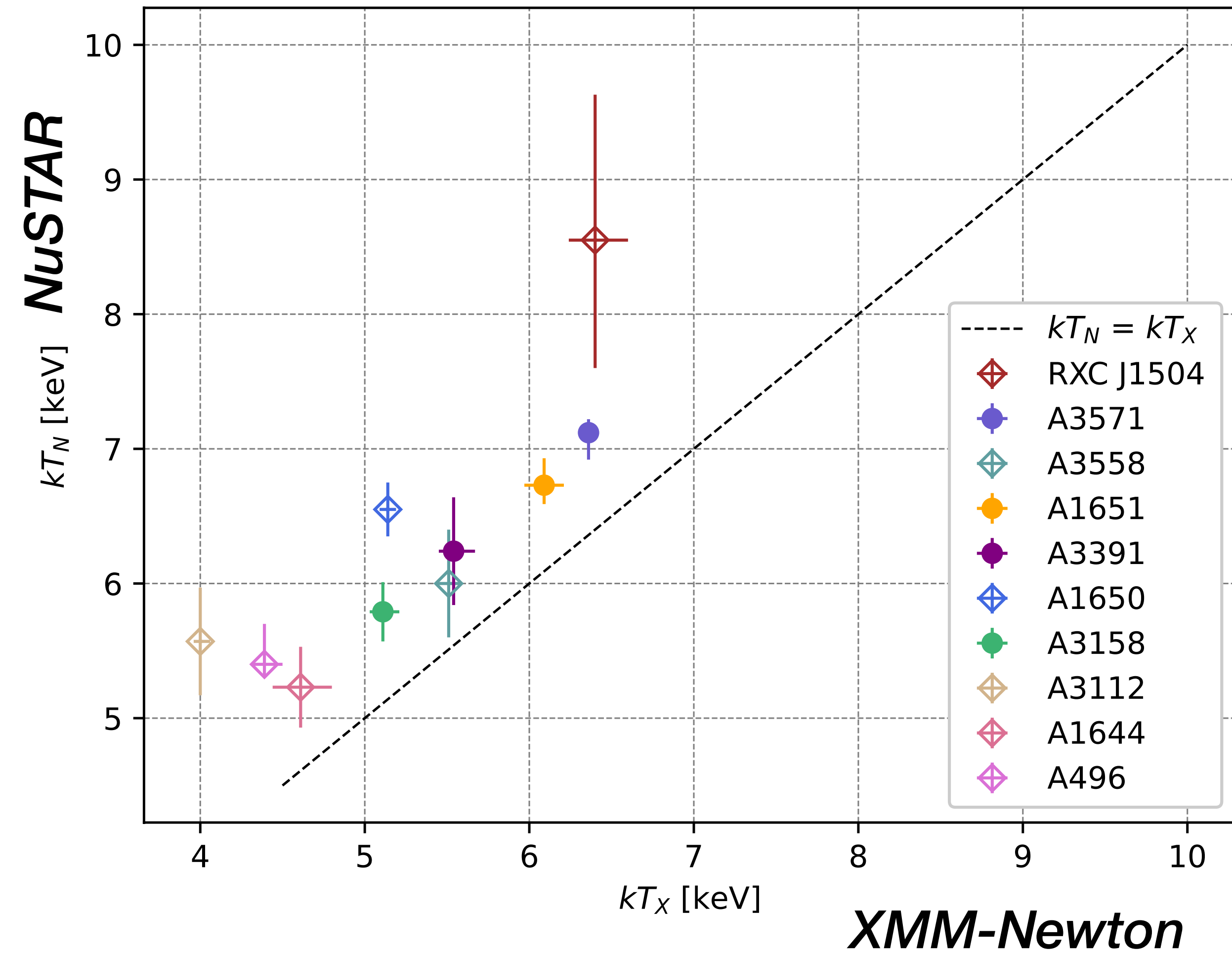
Snapshot Cluster Temperatures

Lopez+ 2024

Cluster Name	Redshift z	Gain Offset keV	kT_c keV	kT_X keV	kT_N keV	kT_{Ni} keV
RXC J1504	0.2172	-0.10 ± 0.04	$9.81^{+0.80}_{-0.79}$	$6.40^{+0.20}_{-0.16}$	$8.55^{+1.09}_{-0.95}$	$5.93^{+0.18}_{-0.33}$
Abell 3571	0.0390	-0.09 ± 0.02	$8.10^{+0.08}_{-0.08}$	$6.36^{+0.06}_{-0.03}$	$7.12^{+0.10}_{-0.20}$	
Abell 3558	0.0484	-0.05 ± 0.03	$7.42^{+0.27}_{-0.28}$	$5.51^{+0.08}_{-0.08}$	$6.00^{+0.40}_{-0.40}$	$6.23^{+0.30}_{-0.30}$
Abell 1651	0.0850	-0.09 ± 0.04	$7.07^{+0.25}_{-0.25}$	$6.09^{+0.12}_{-0.12}$	$6.73^{+0.20}_{-0.14}$	
Abell 3391	0.0561	-0.10 ± 0.07	$6.62^{+0.22}_{-0.22}$	$5.54^{+0.13}_{-0.09}$	$6.24^{+0.40}_{-0.40}$	
Abell 1650	0.0838	-0.10 ± 0.04	$6.43^{+0.10}_{-0.10}$	$5.14^{+0.05}_{-0.05}$	$6.55^{+0.20}_{-0.20}$	$5.88^{+0.90}_{-0.30}$
Abell 3158	0.0592	-0.05 ± 0.05	$6.01^{+0.10}_{-0.10}$	$5.11^{+0.10}_{-0.08}$	$5.79^{+0.22}_{-0.22}$	
Abell 3112	0.0753	-0.10 ± 0.03	$5.45^{+0.12}_{-0.09}$	$4.00^{+0.06}_{-0.04}$	$5.57^{+0.40}_{-0.40}$	$4.59^{+0.20}_{-0.20}$
Abell 1644	0.0474	-0.06 ± 0.05	$5.31^{+0.14}_{-0.13}$	$4.61^{+0.19}_{-0.17}$	$5.23^{+0.30}_{-0.30}$	$5.24^{+0.20}_{-0.20}$
Abell 496	0.0331	-0.07 ± 0.03	$5.18^{+0.07}_{-0.07}$	$4.39^{+0.11}_{-0.08}$	$5.40^{+0.30}_{-0.10}$	$3.82^{+0.10}_{-0.03}$

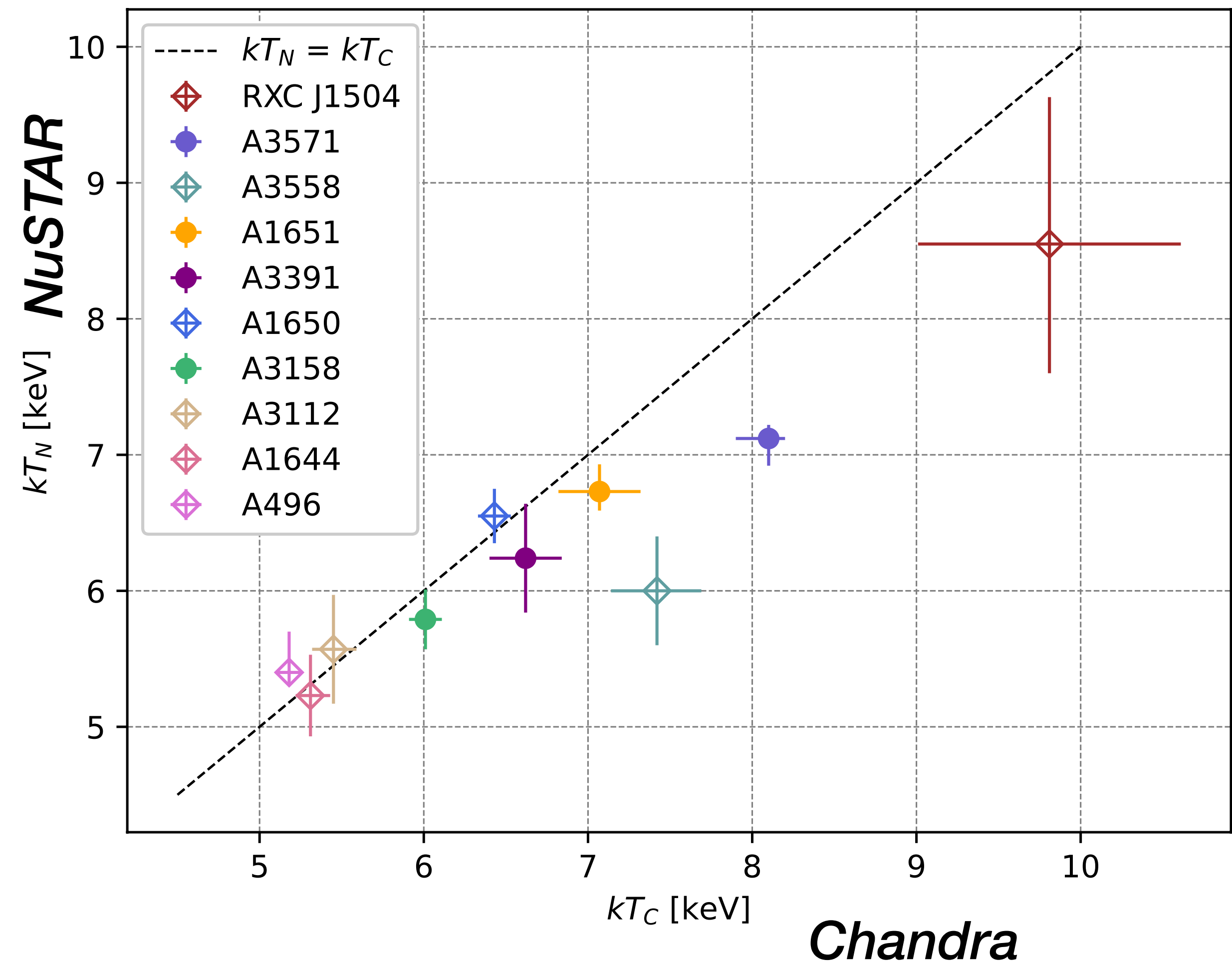
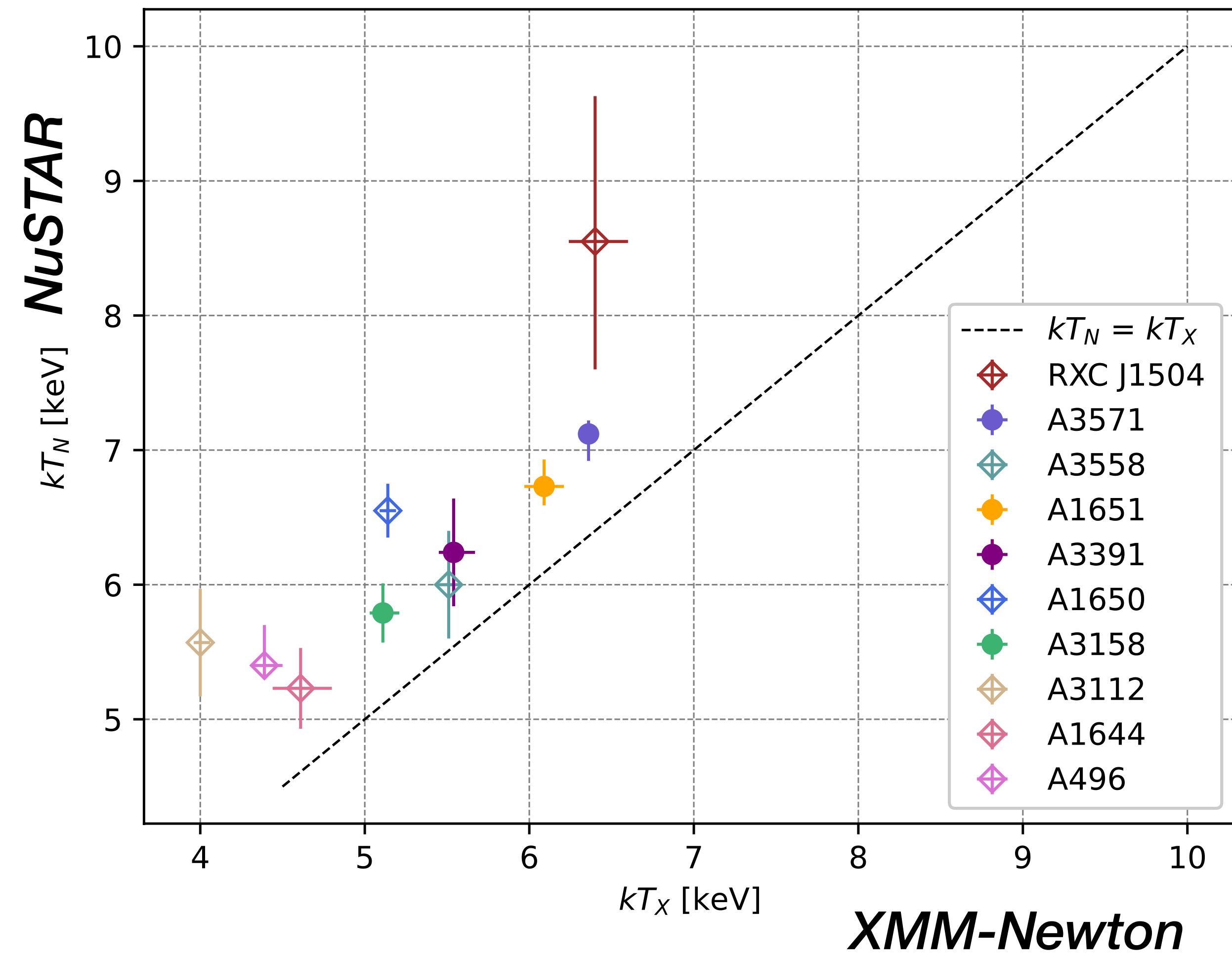
\uparrow \uparrow
 Schellenberger+ 2015

Snapshot Cluster Temperatures



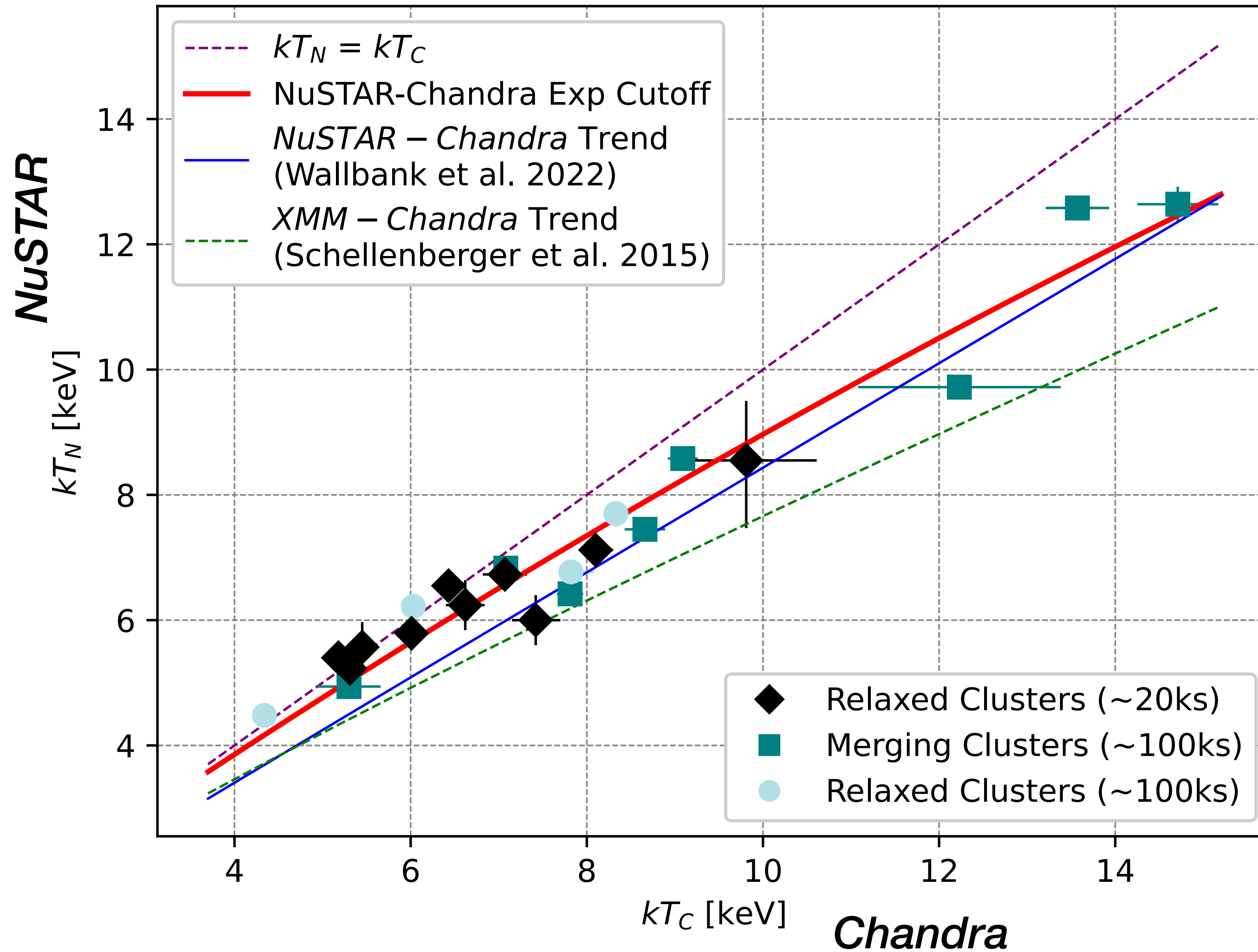
Lopez+ 2024 (*Chandra/XMM-Newton* kT s from Schellenberger+ 2015)

Snapshot Cluster Temperatures



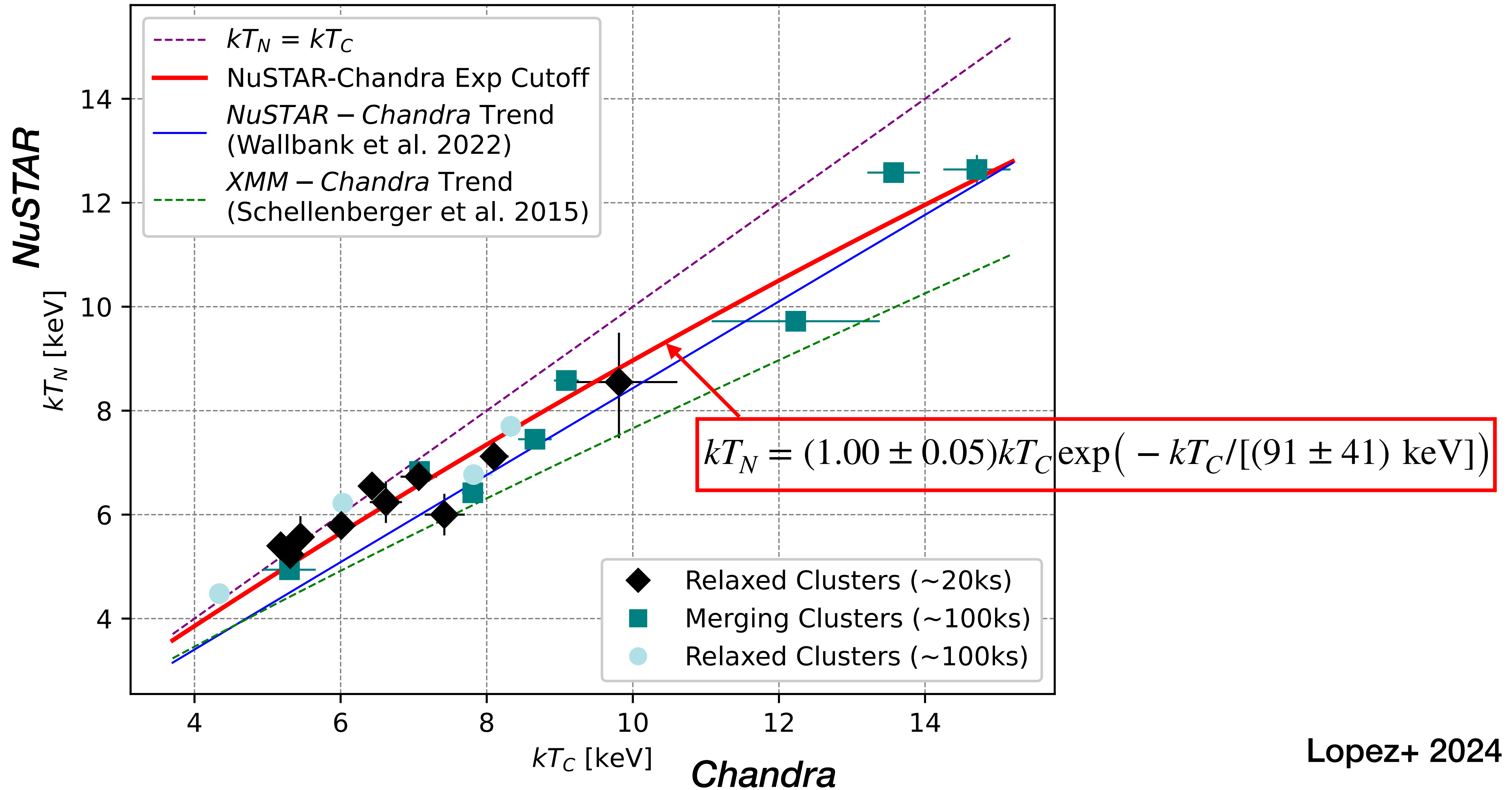
Lopez+ 2024 (*Chandra/XMM-Newton* kTs from Schellenberger+ 2015)

Snapshot Cluster Temperatures



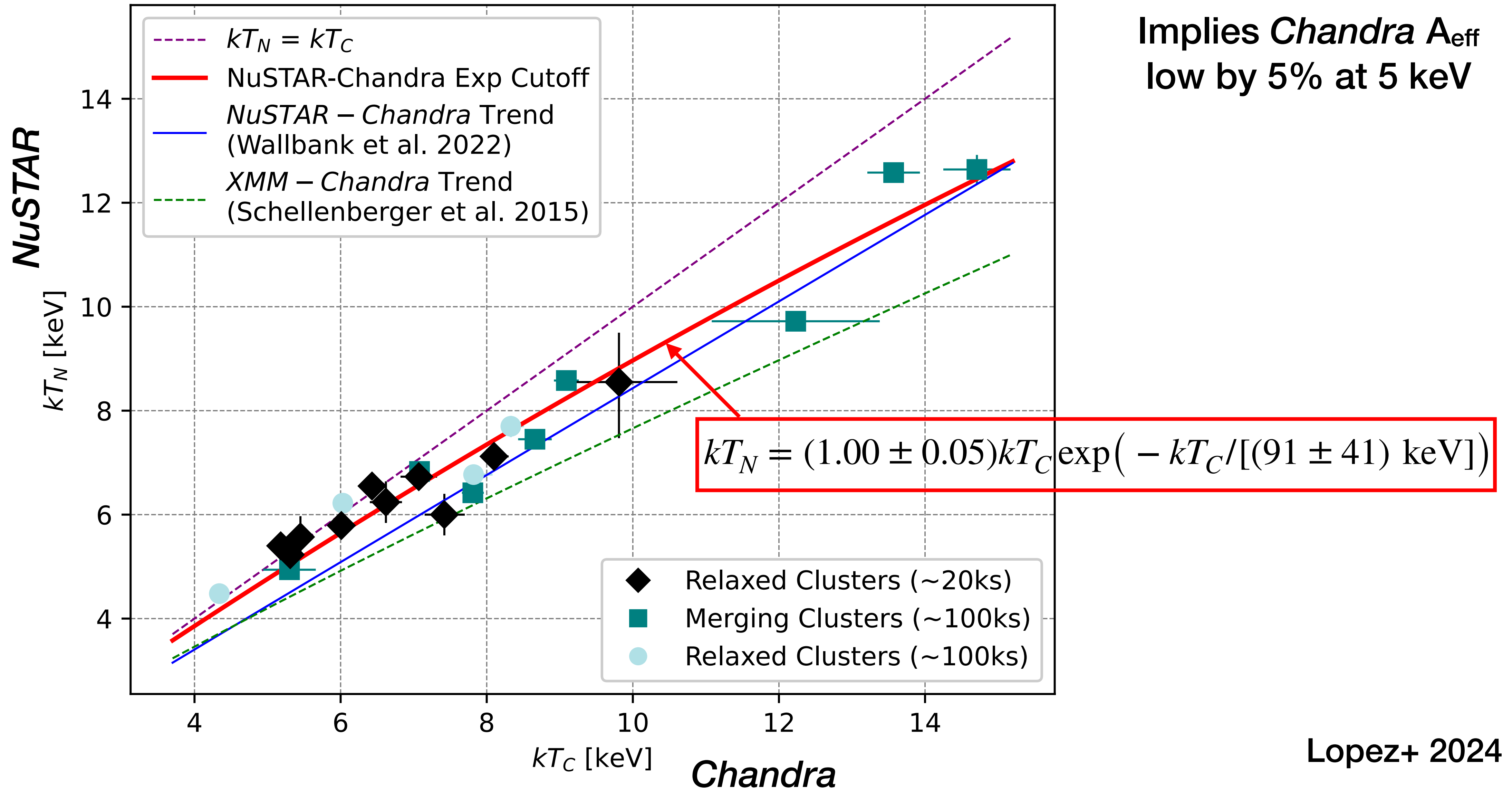
Lopez+ 2024

Snapshot Cluster Temperatures

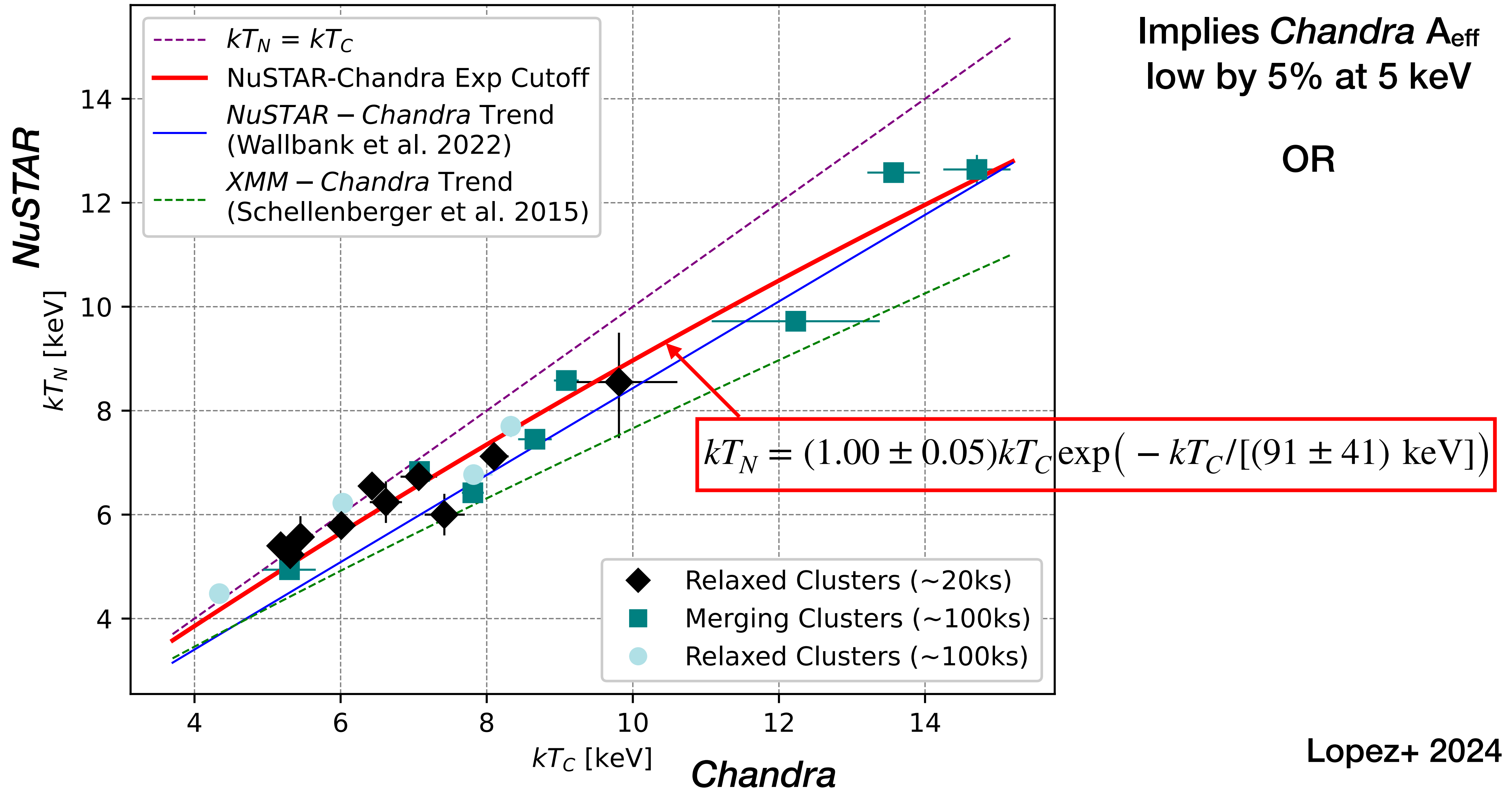


Lopez+ 2024

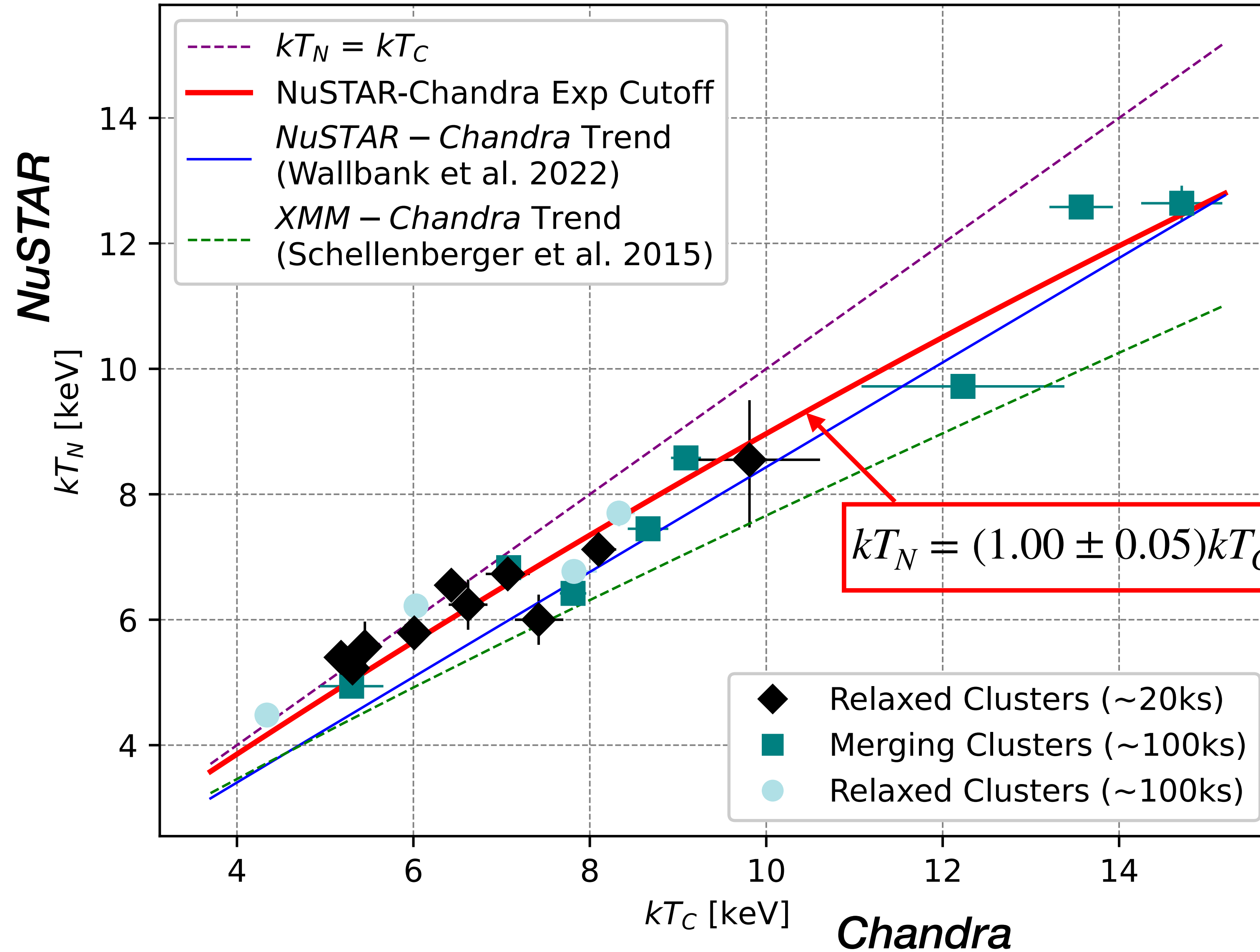
Snapshot Cluster Temperatures



Snapshot Cluster Temperatures



Snapshot Cluster Temperatures



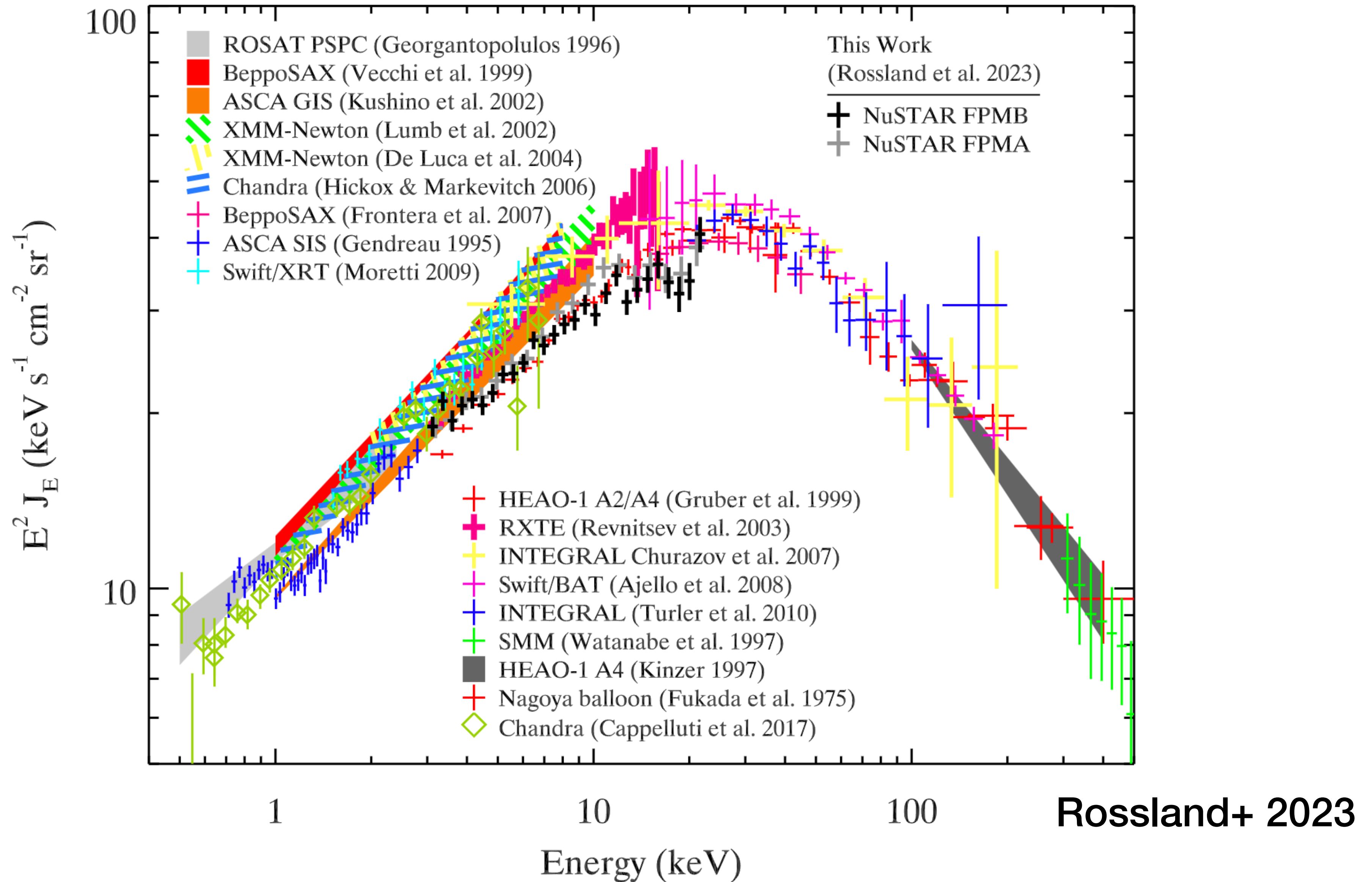
Implies *Chandra* A_{eff} low by 5% at 5 keV

OR

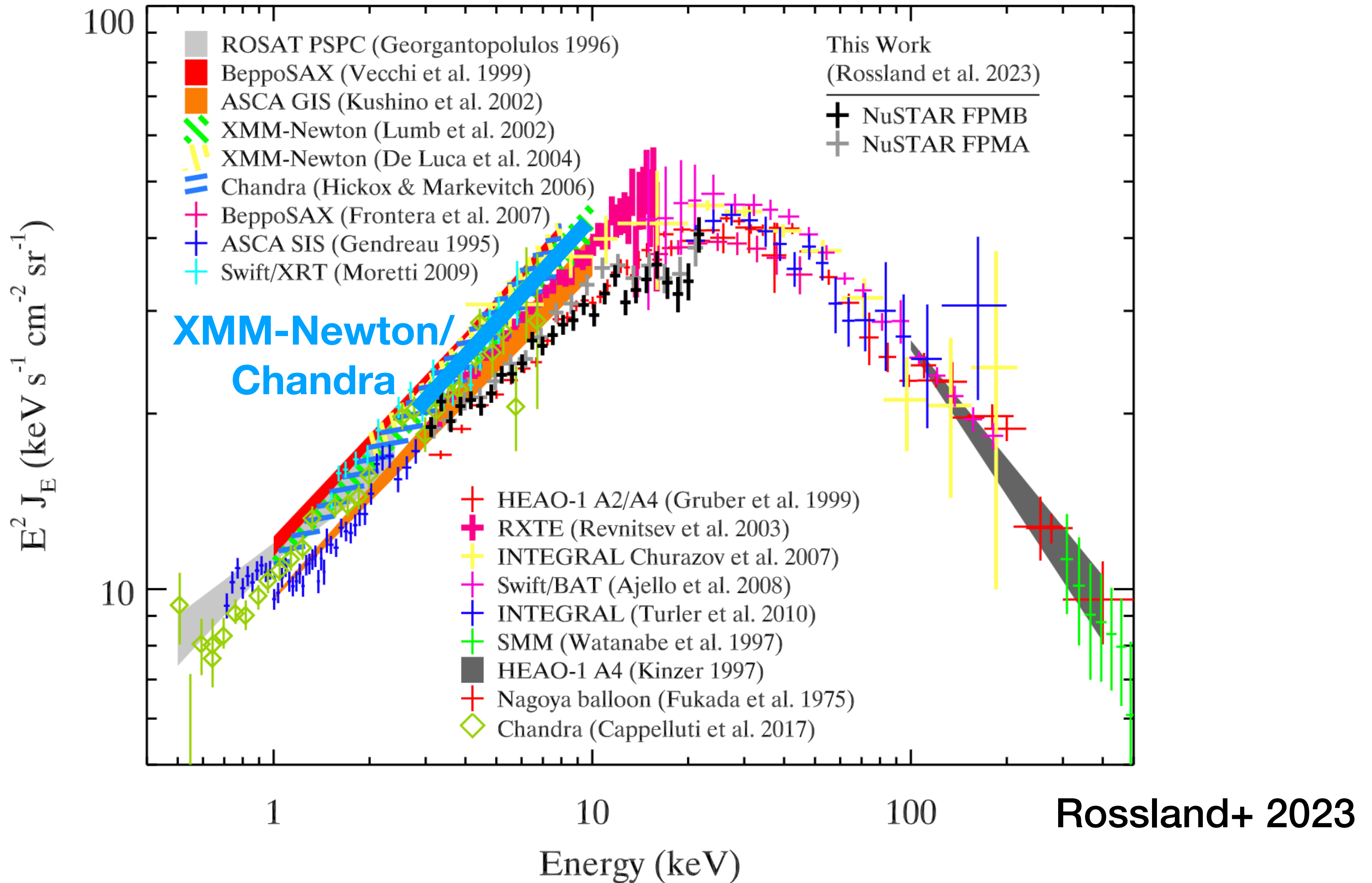
Implies *NuSTAR* A_{eff} low by 25%/13%/6% at 3/5/10 keV

Lopez+ 2024

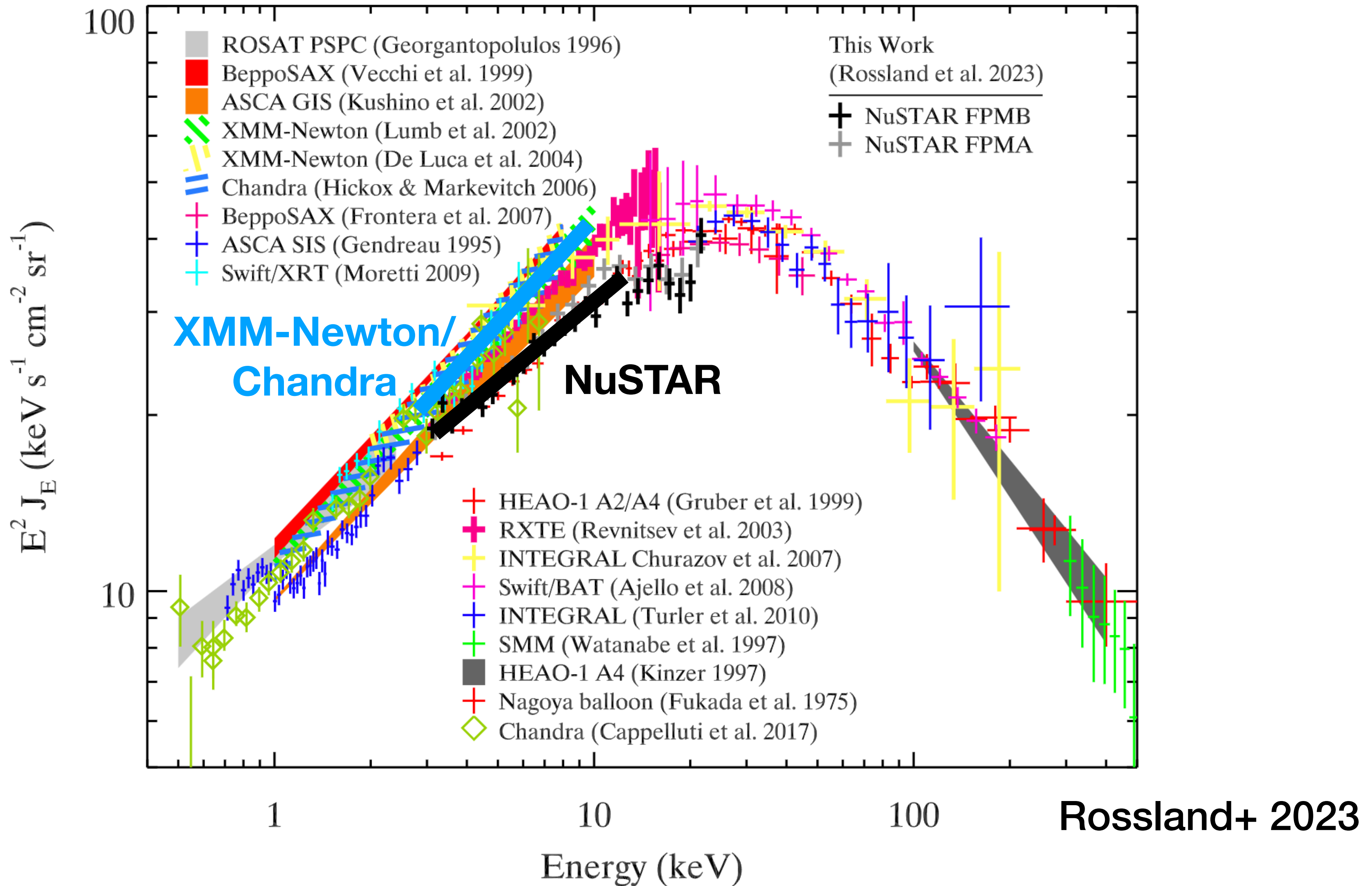
CXB Measurement Consistent

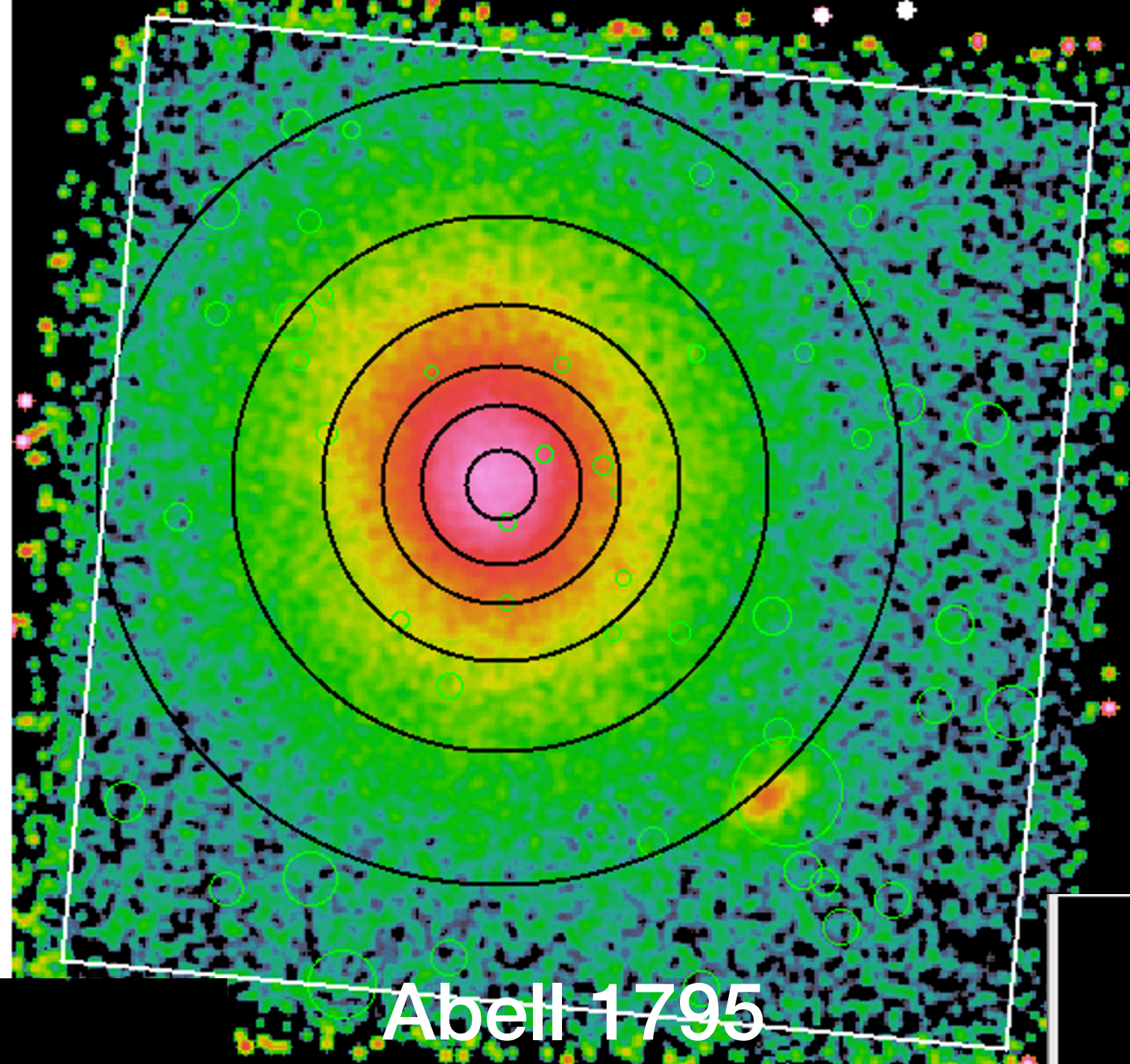
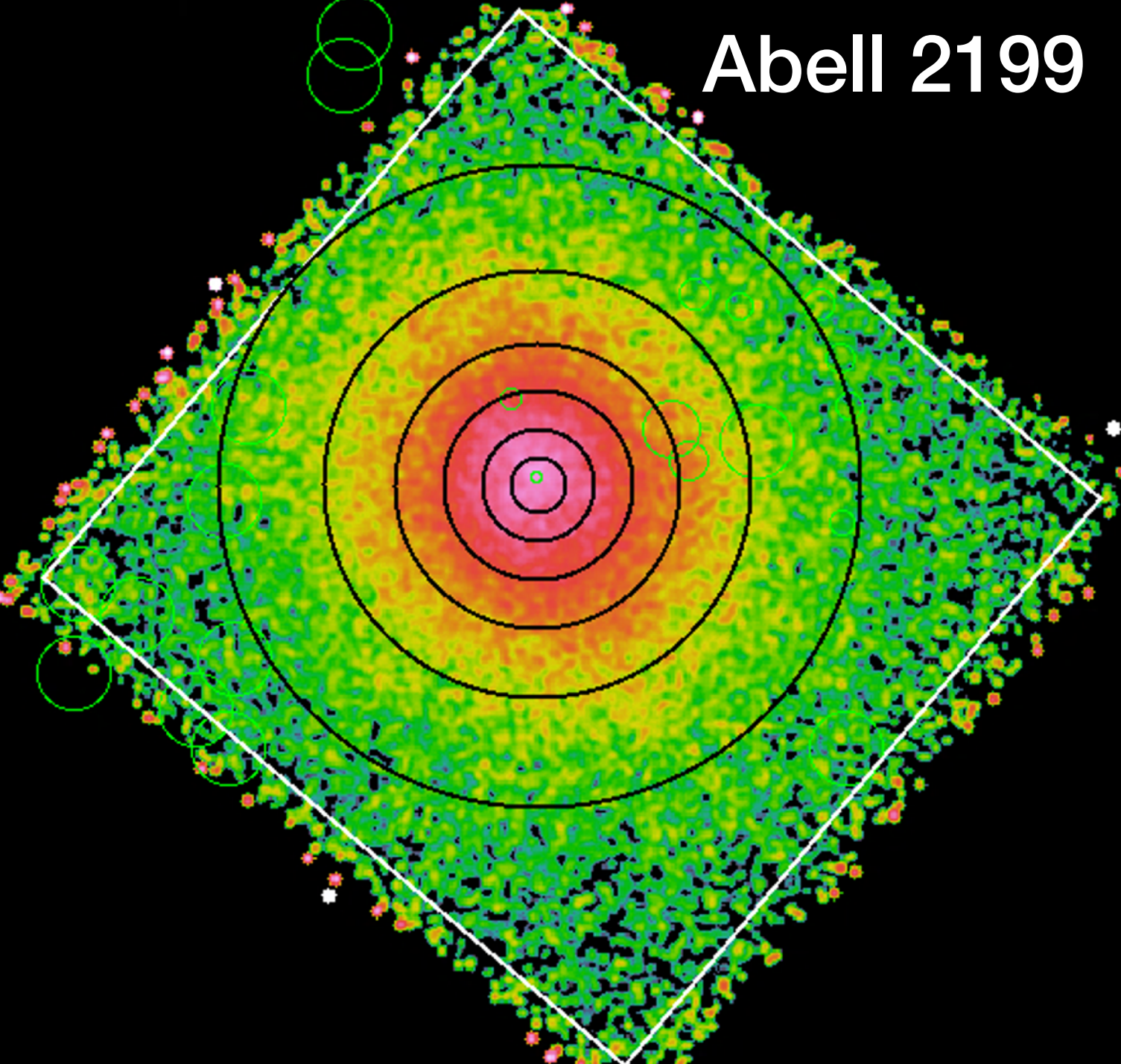


CXB Measurement Consistent



CXB Measurement Consistent

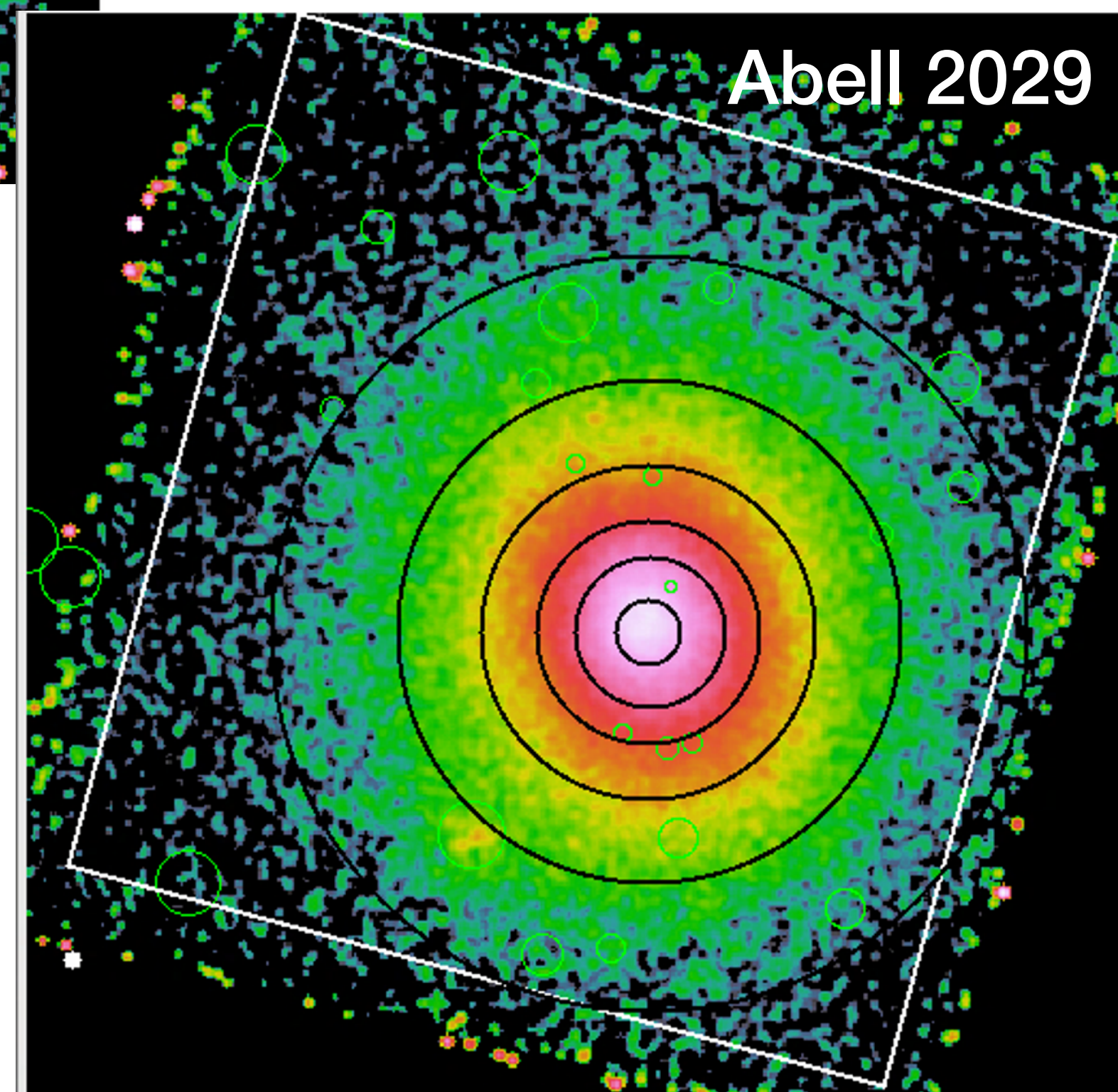
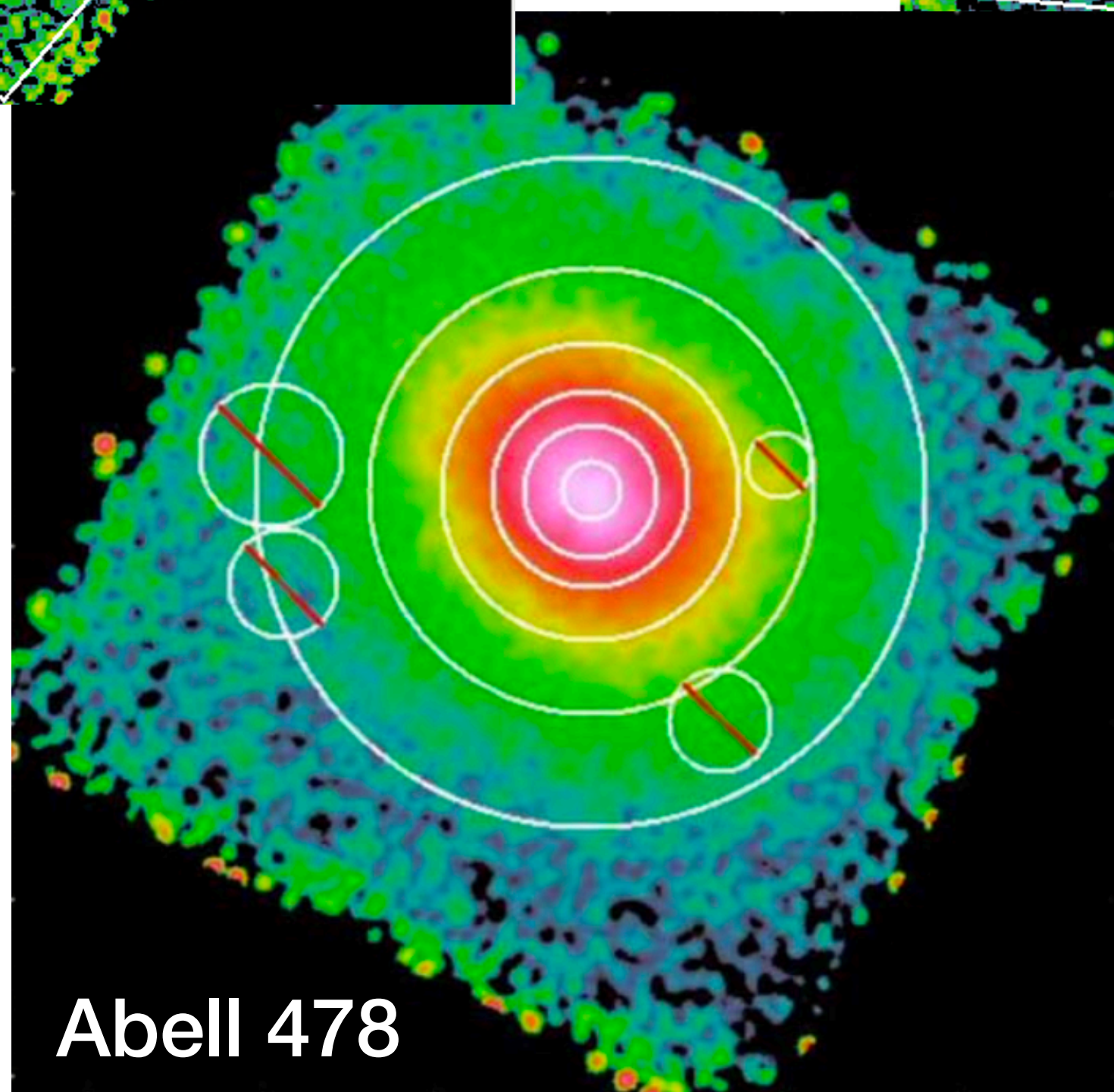




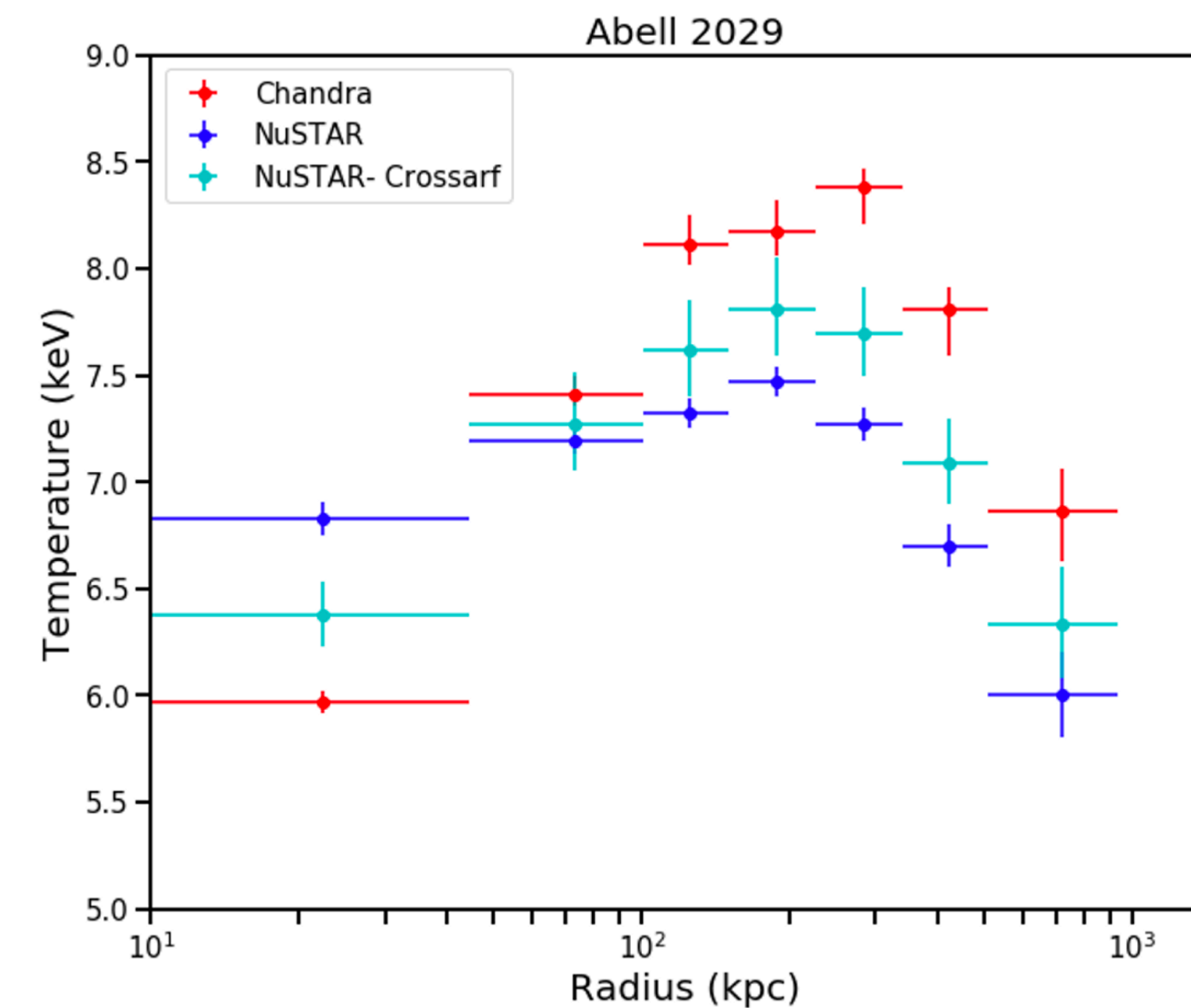
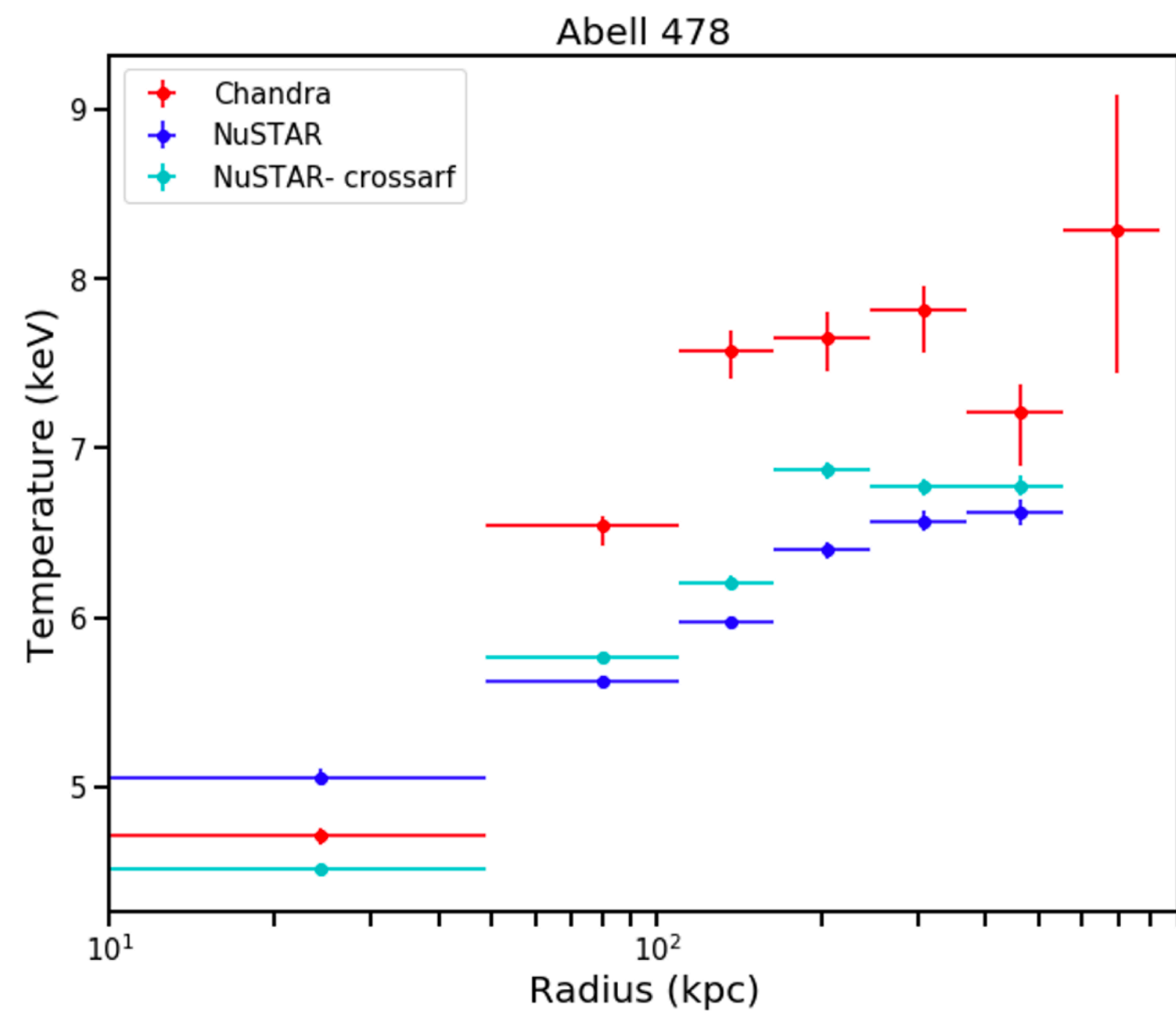
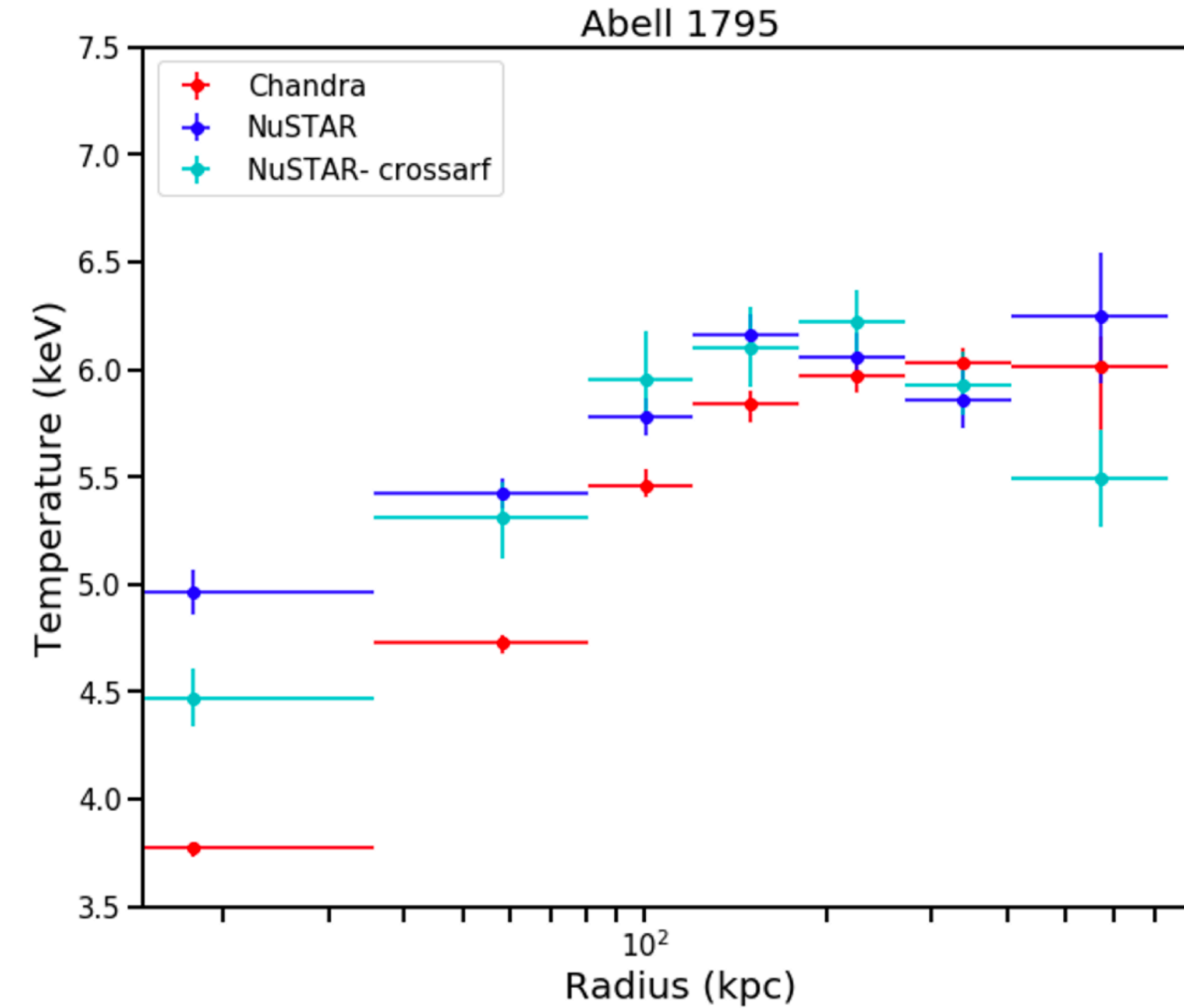
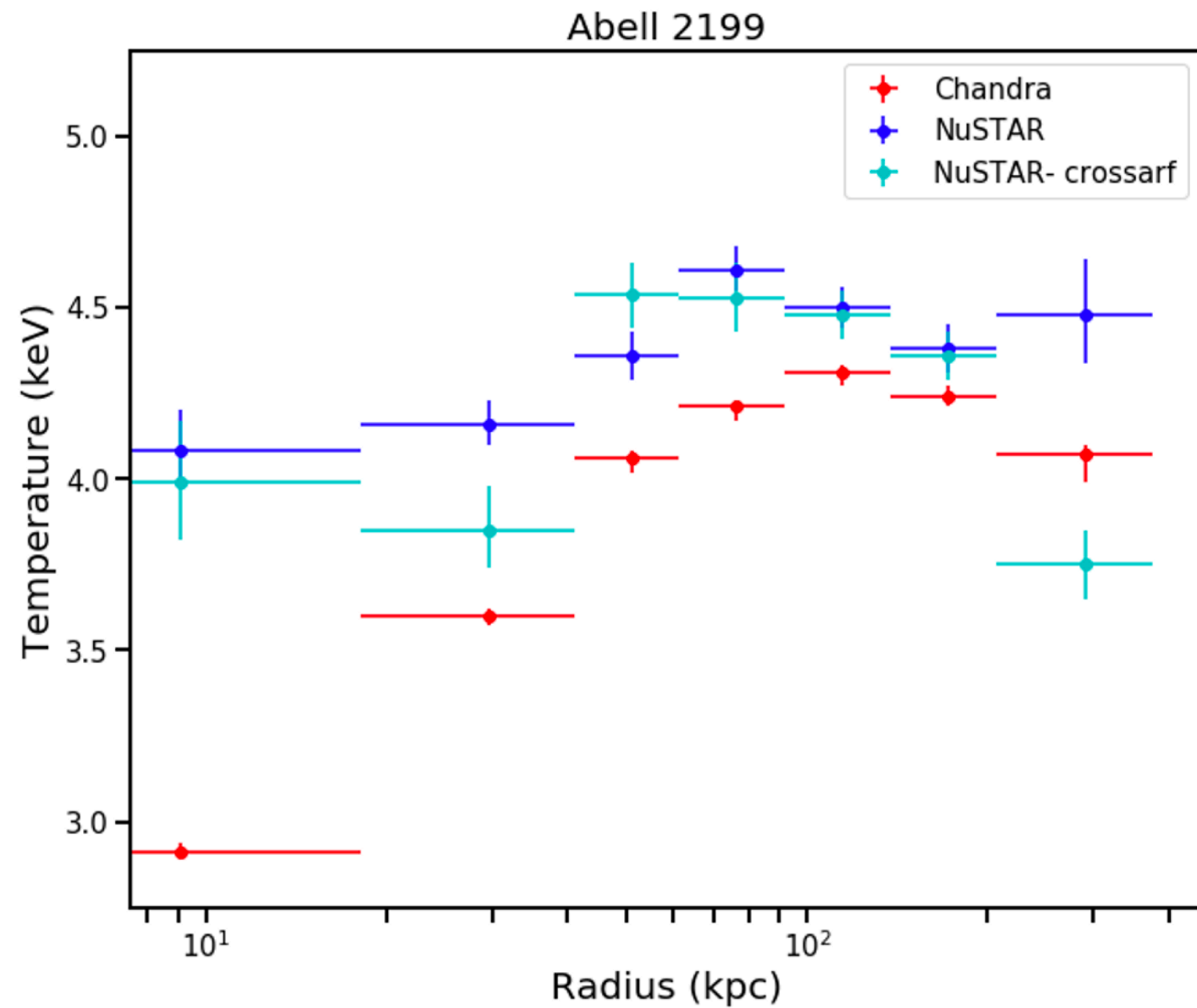
NuSTAR FPMA+B combined
(Bgd-sub, exp-corrected)

4-25 keV

Potter+ in prep

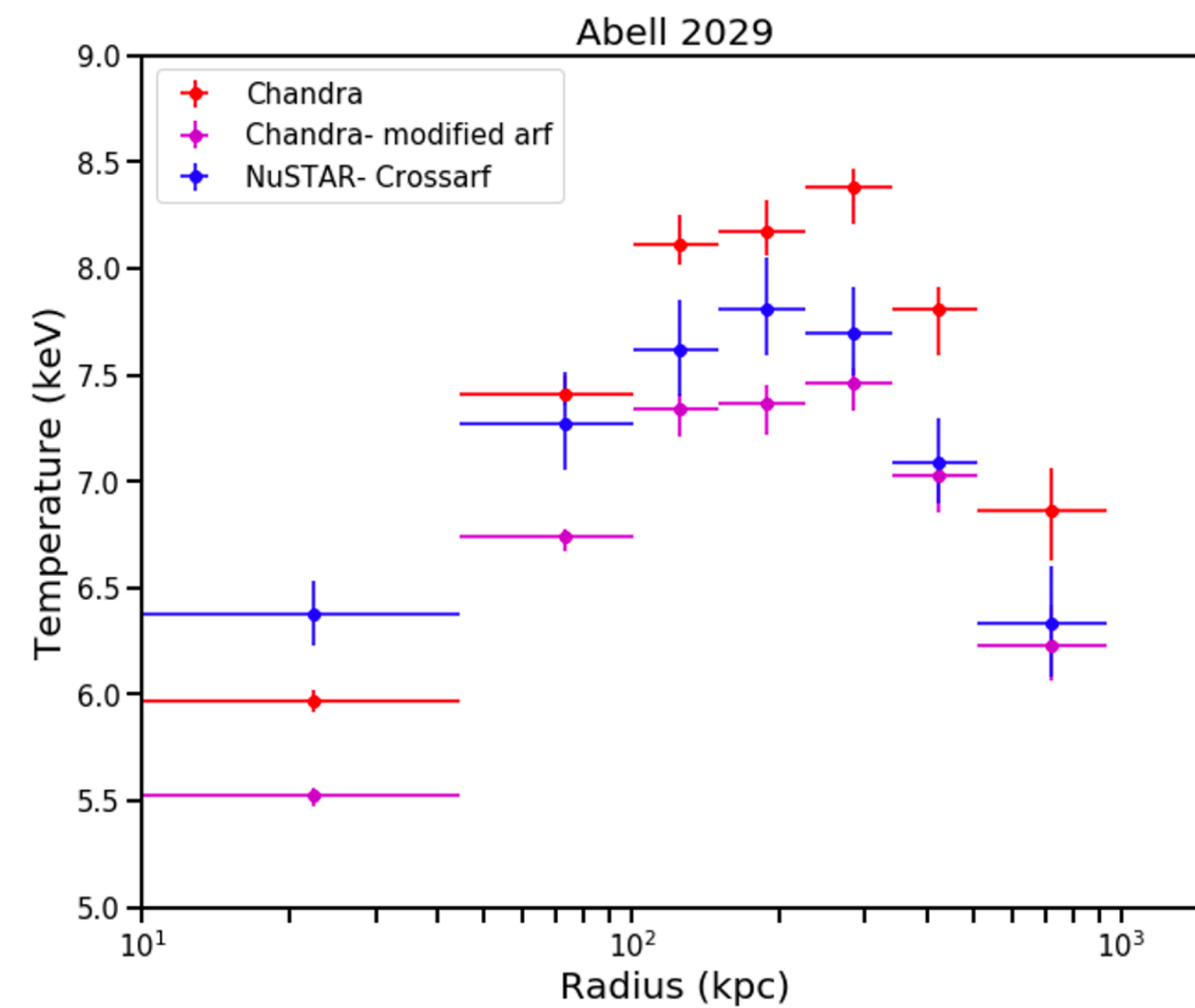
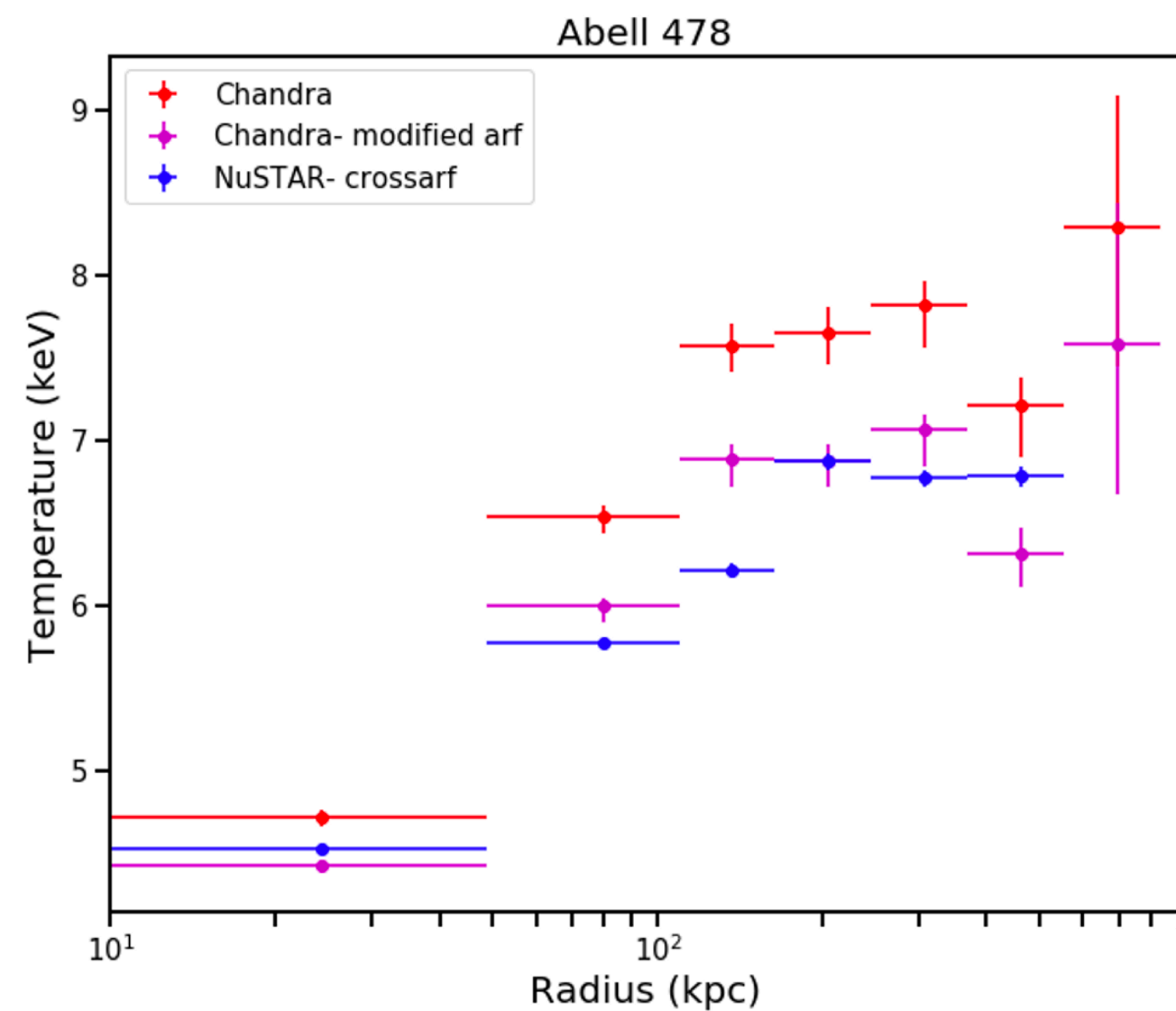
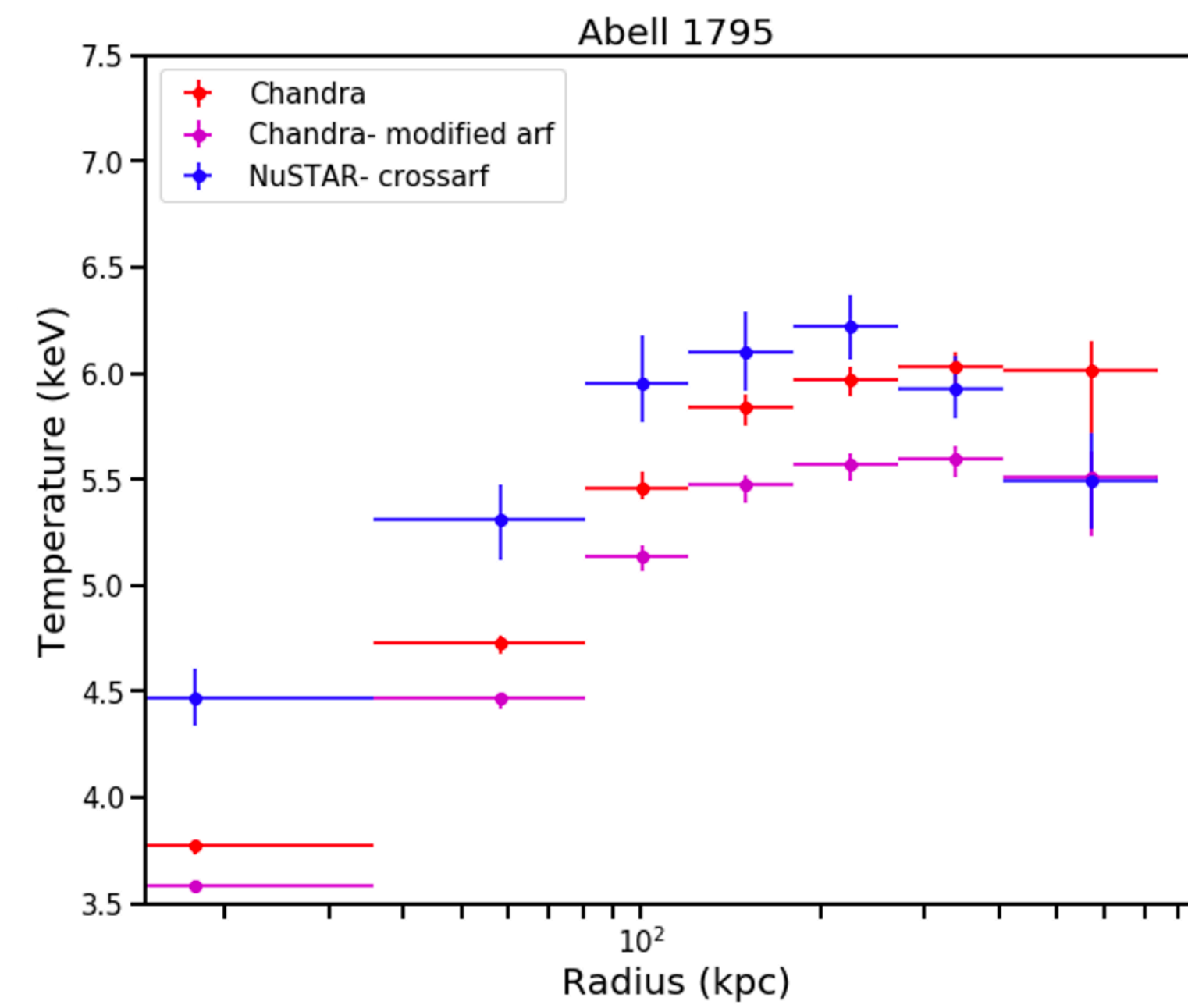
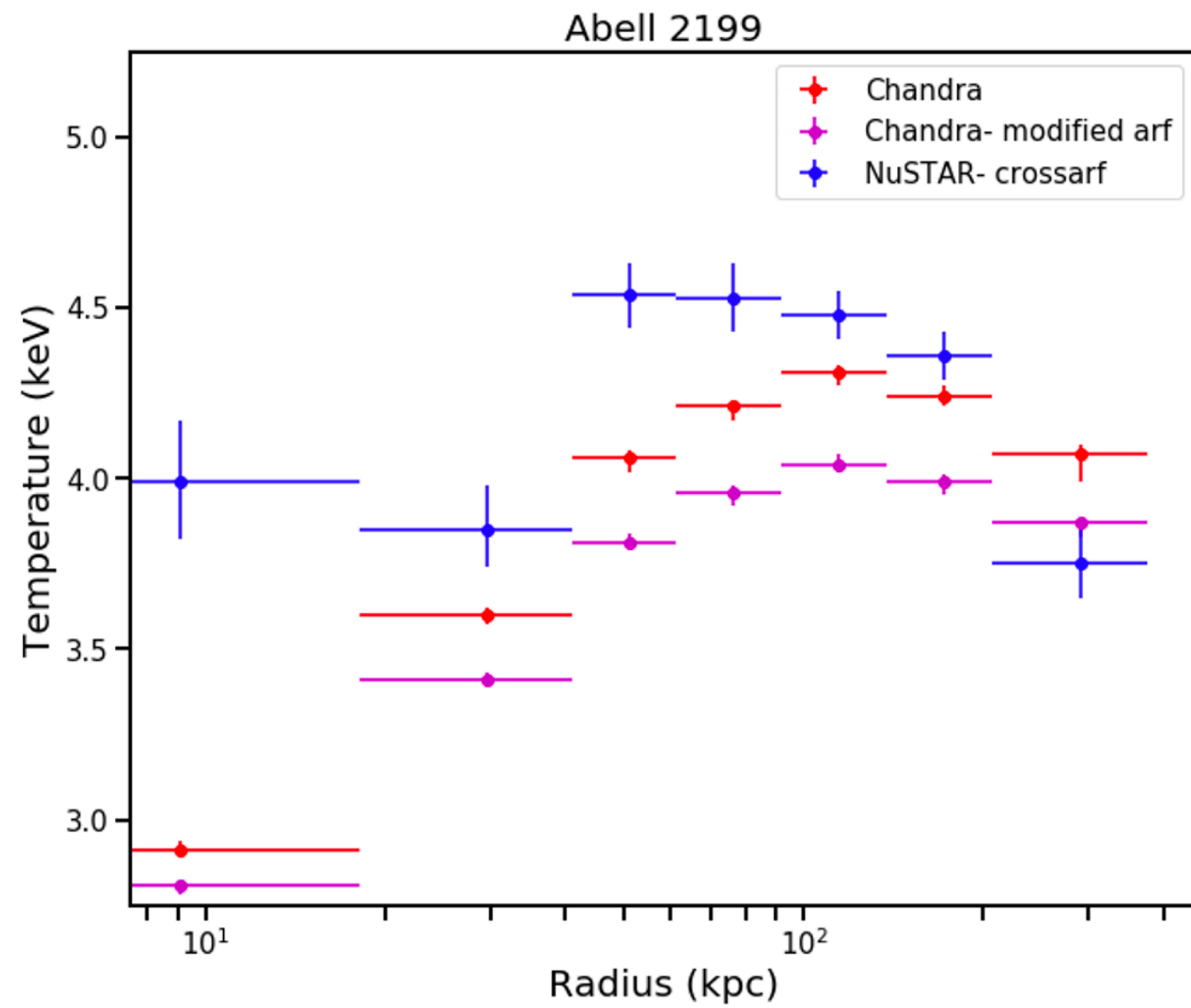


Deep observations of relaxed clusters
Nominal Chandra ARFs



Potter+ in prep

Deep observations of relaxed clusters
Modified Chandra ARFs

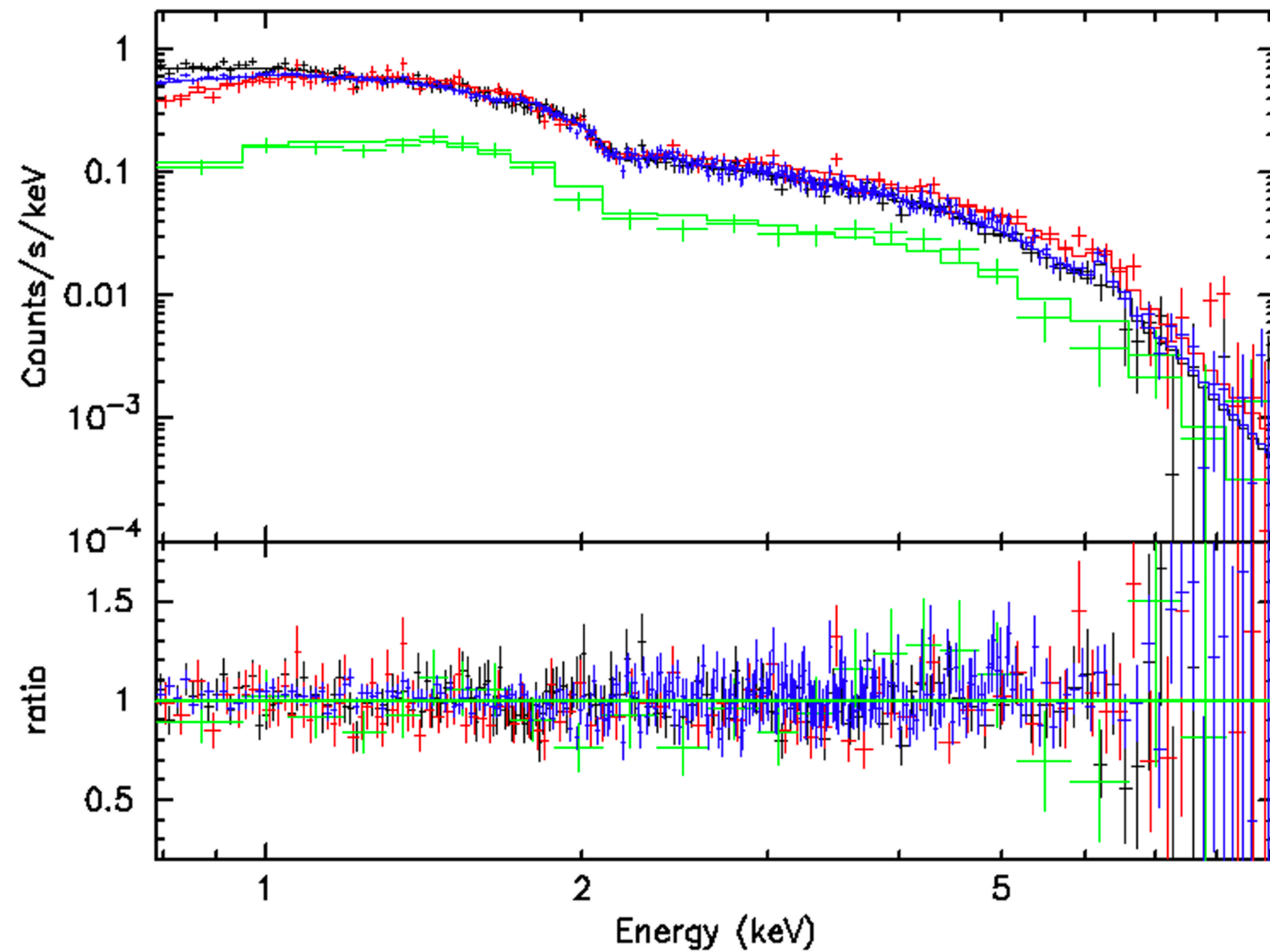


Potter+ in prep

Abell 2029, 5th Annulus

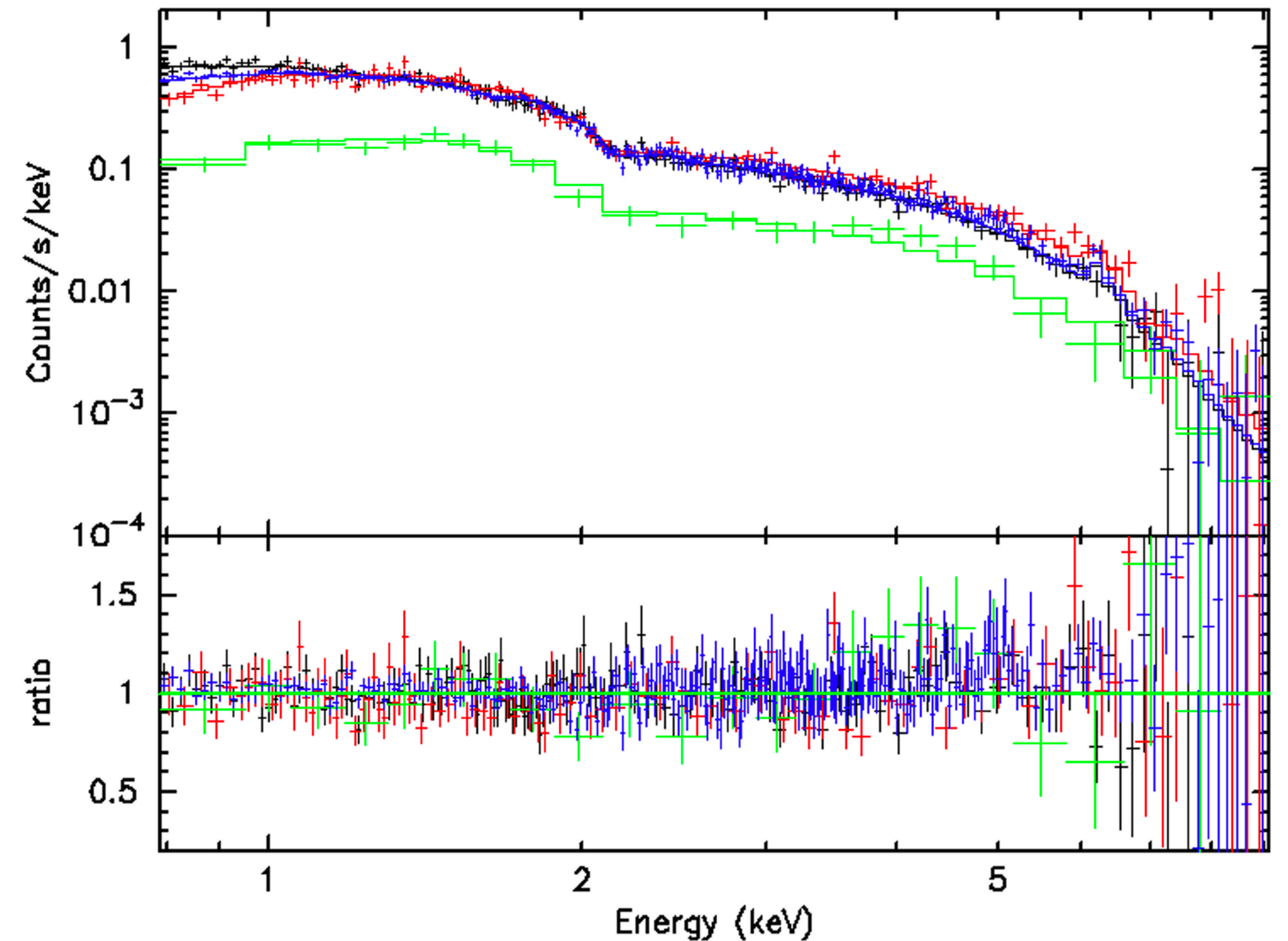
Nominal Chandra ARF

A2029 228–342": Nominal ARF Fit



Modified Chandra ARF

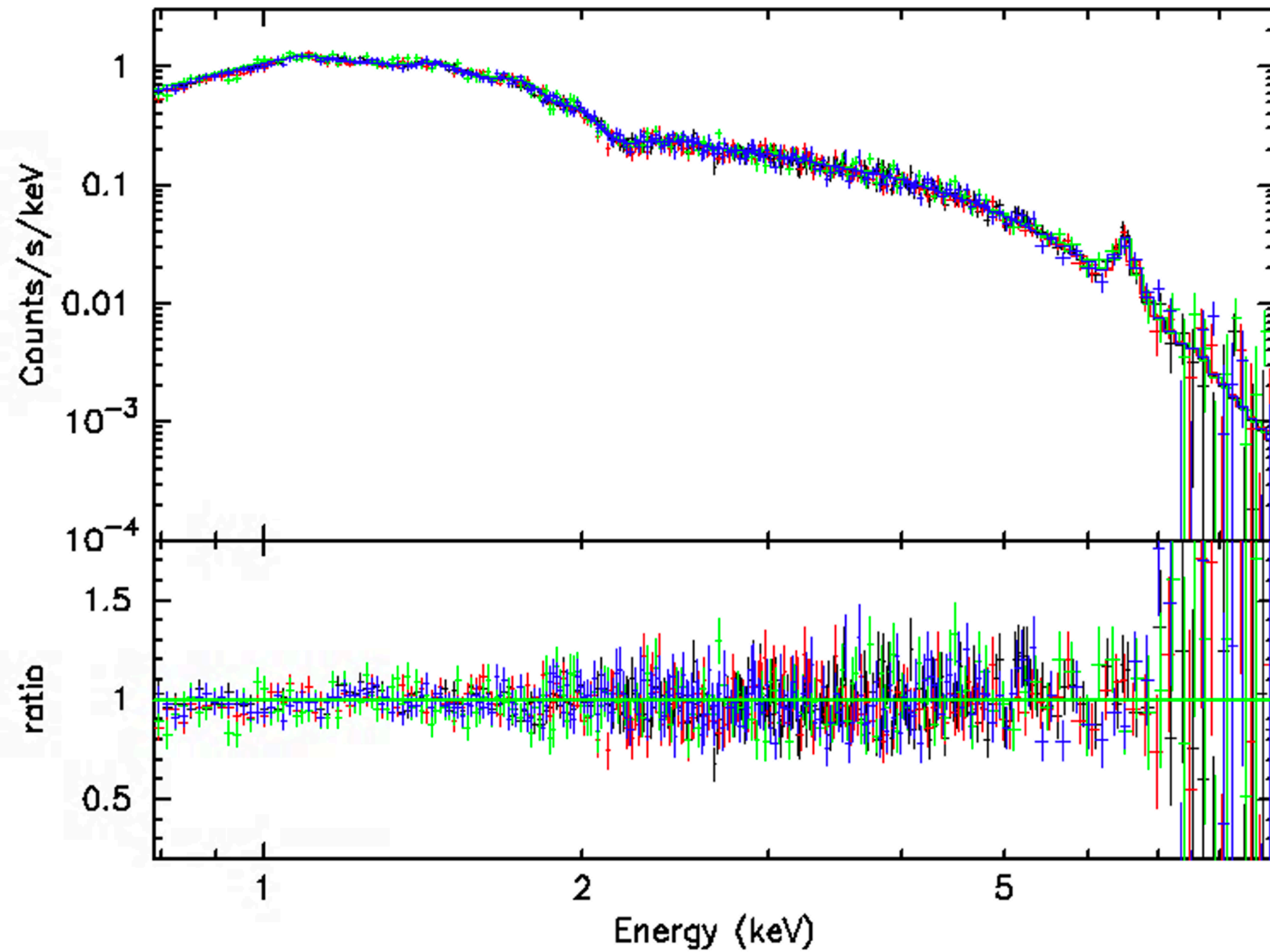
A2029 228–342": Modified ARF Fit



Abell 2199, 5th Annulus

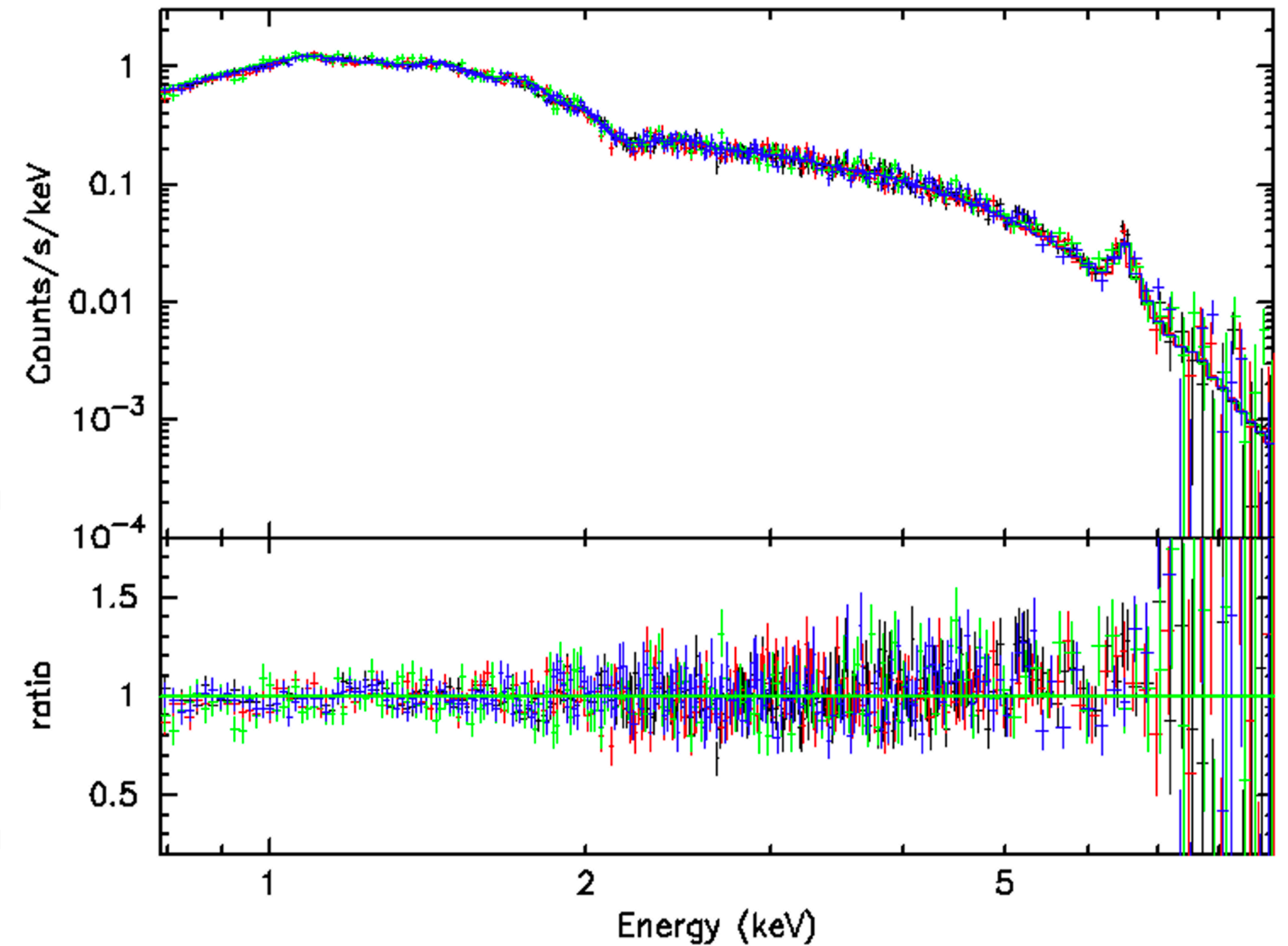
Nominal Chandra ARF

A2199 228–342": Nominal ARF Fit

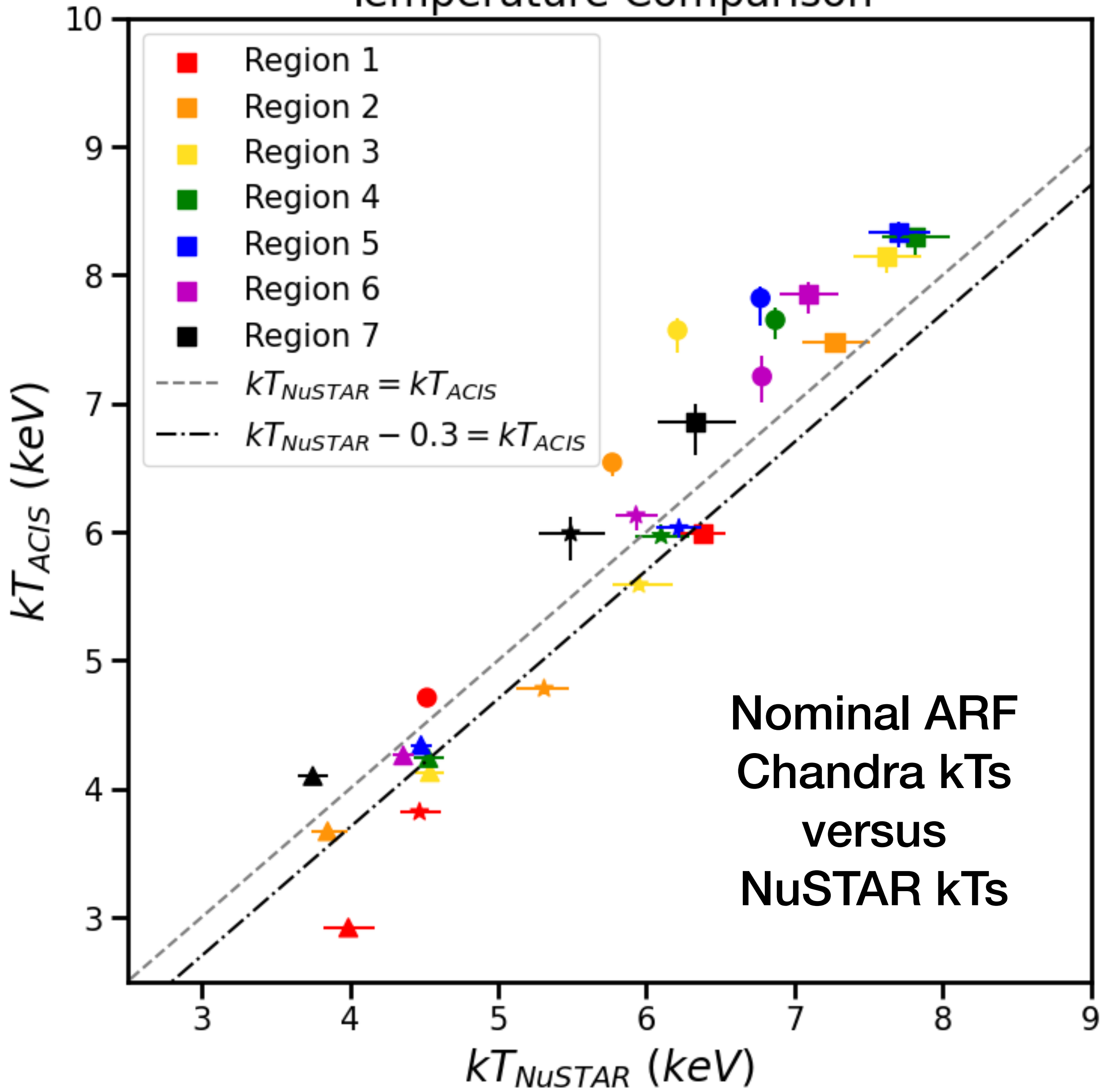


Modified Chandra ARF

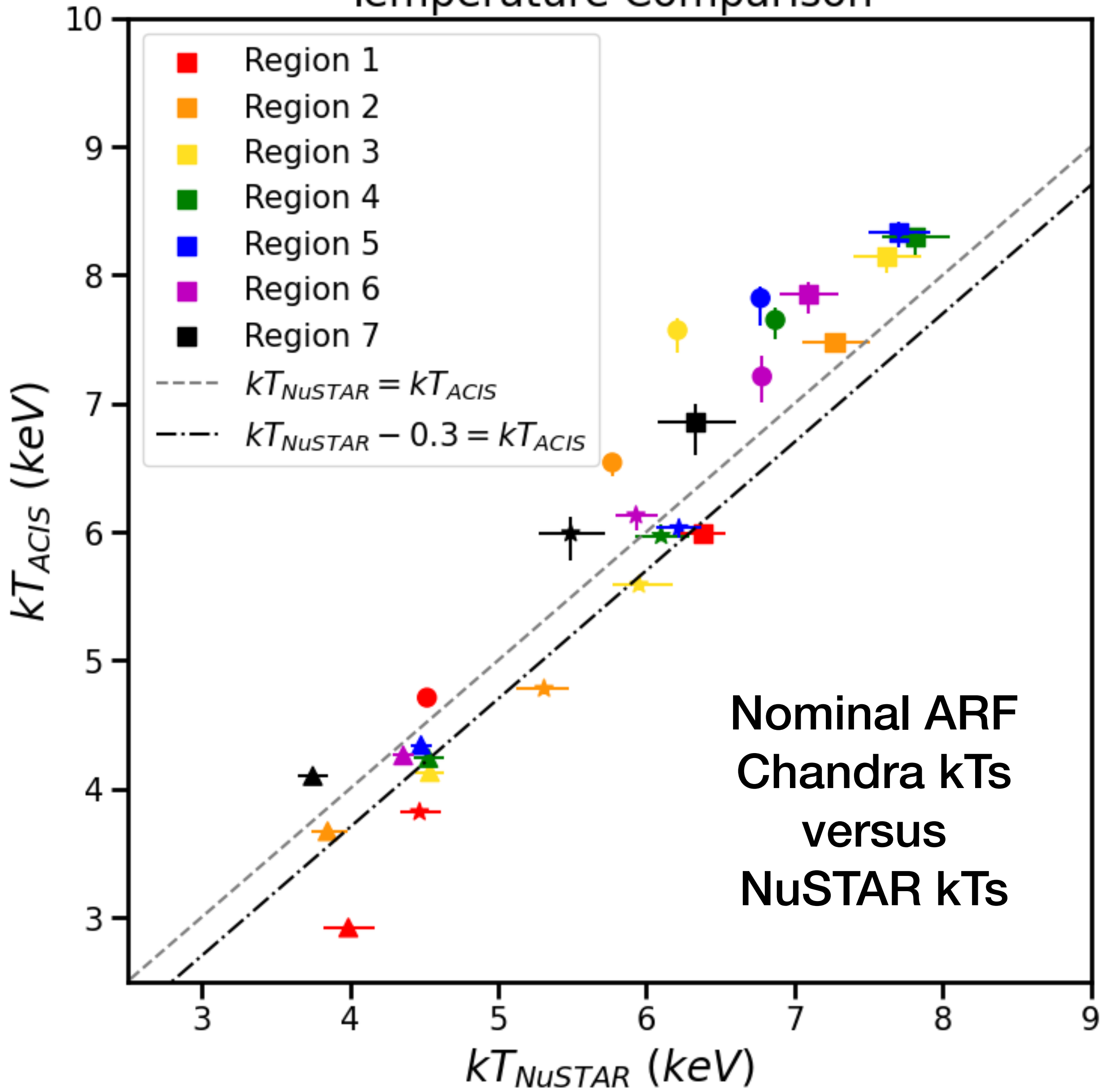
A2199 228–342": Modified ARF Fit



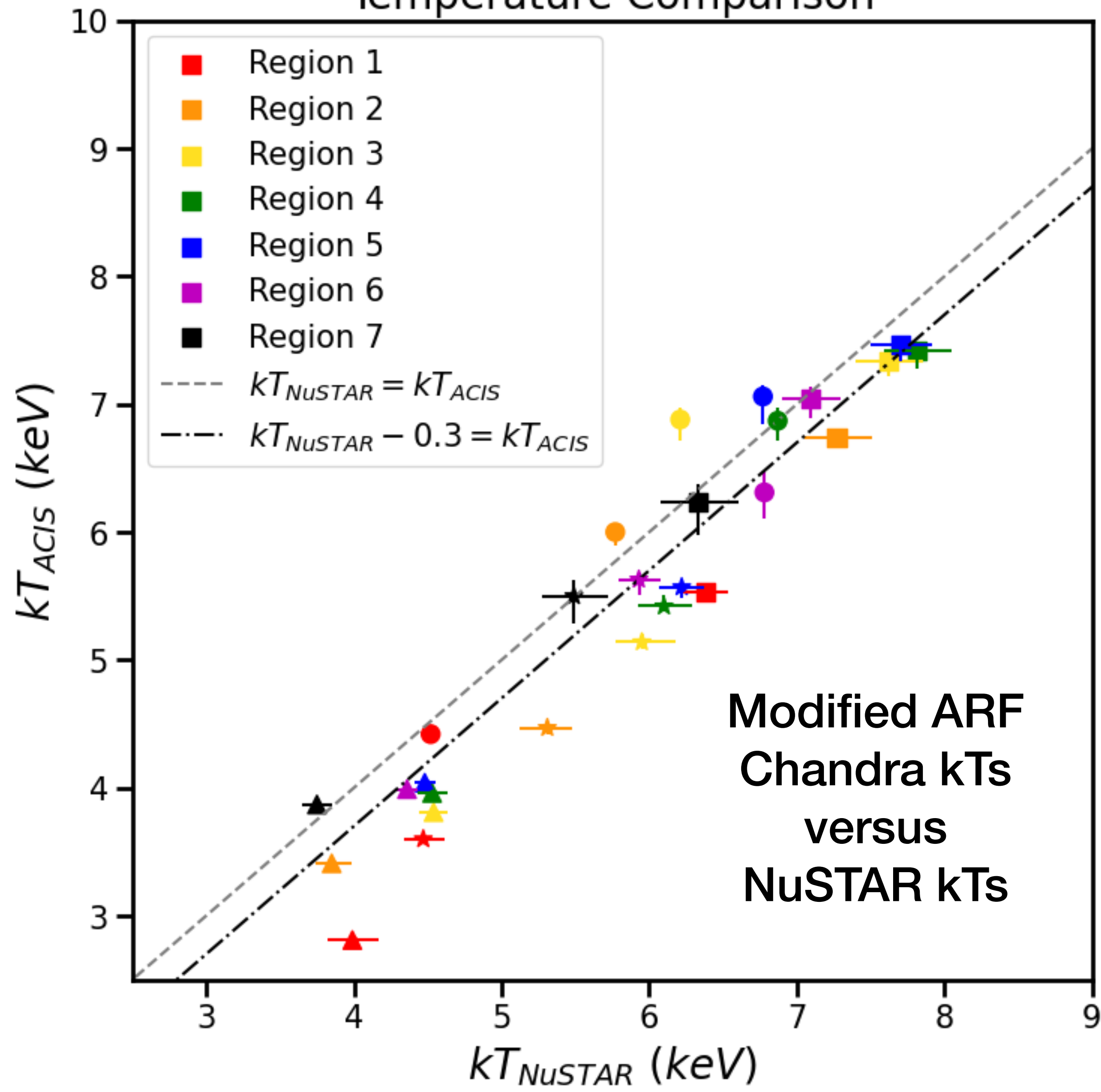
Temperature Comparison



Temperature Comparison

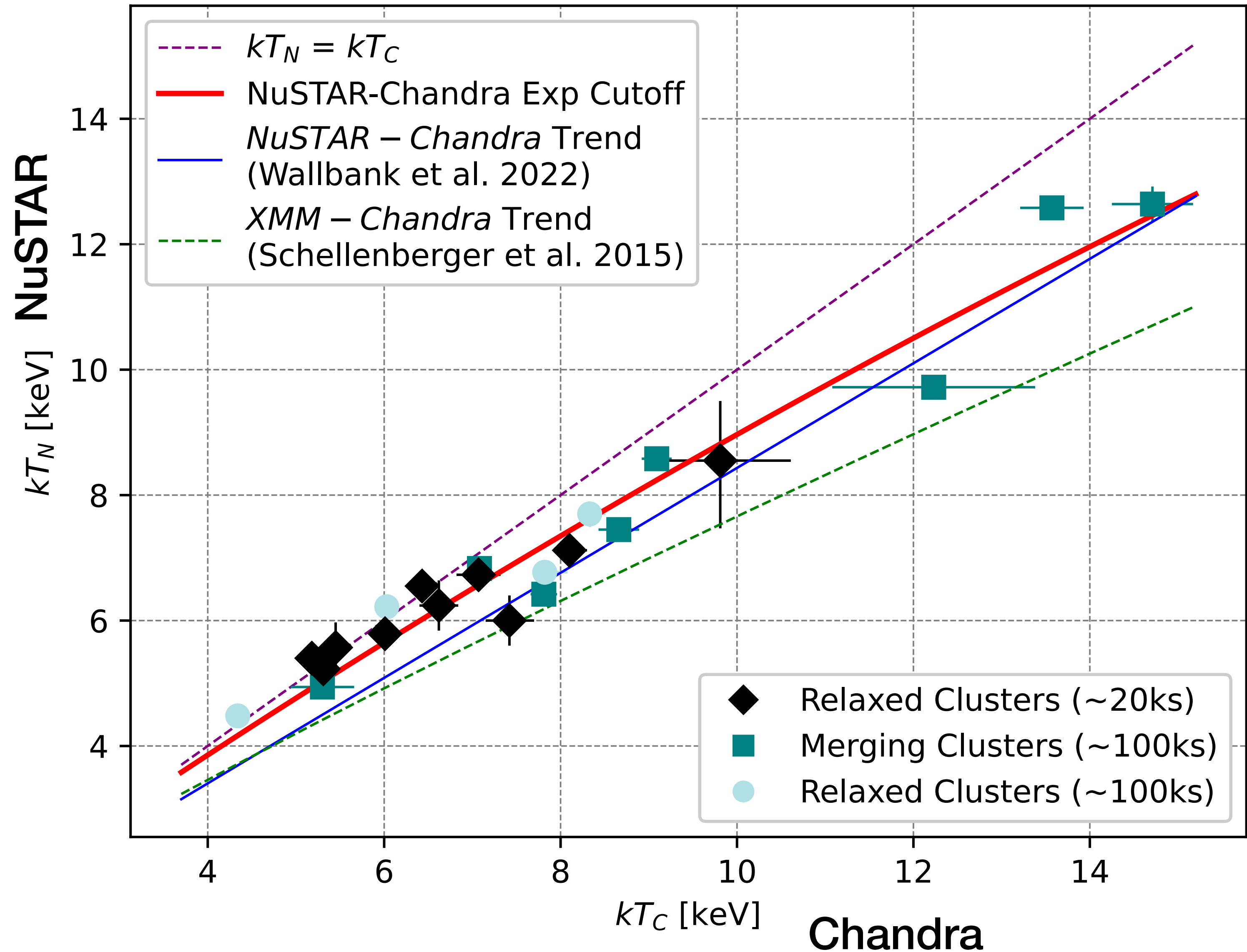


Temperature Comparison

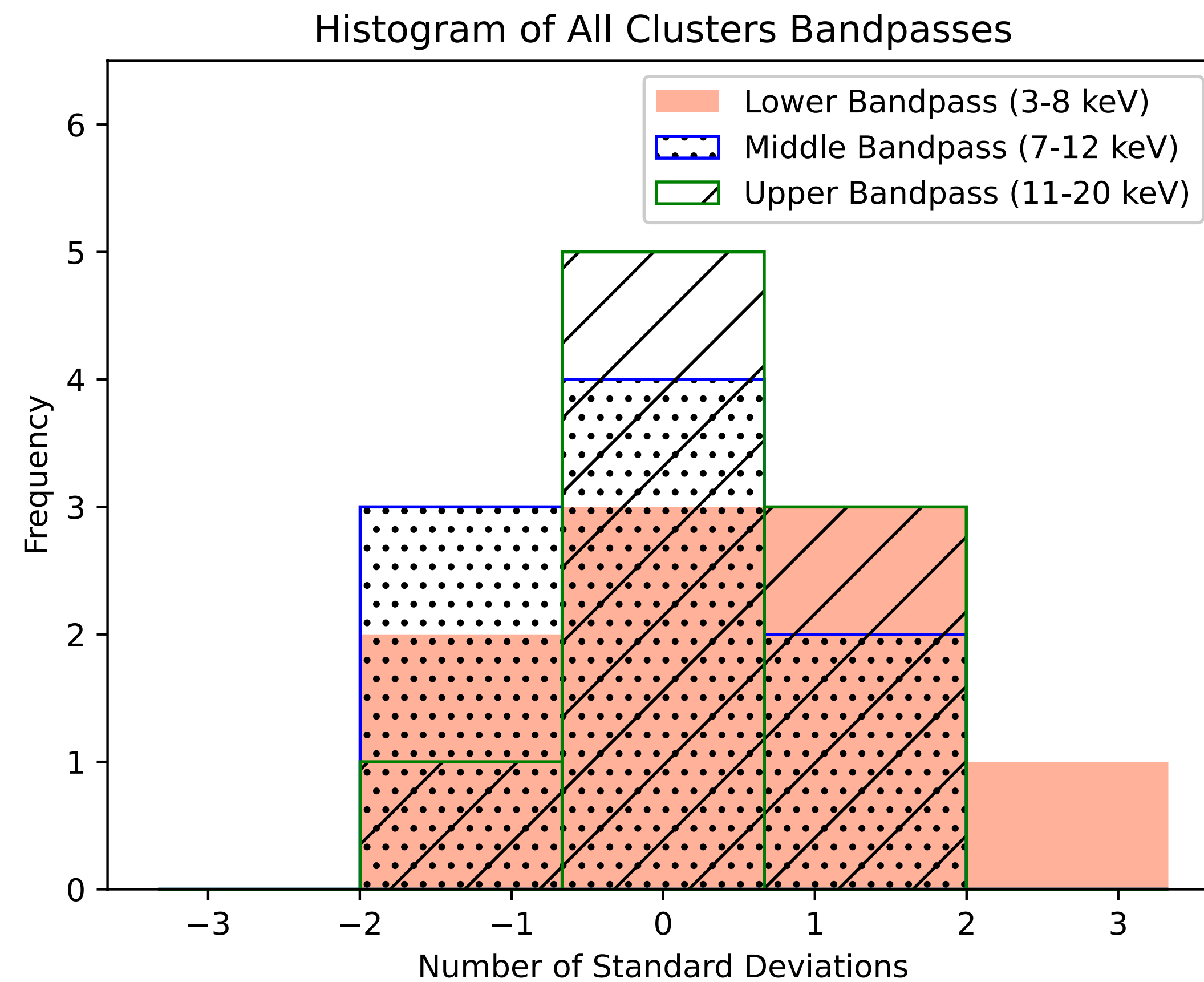
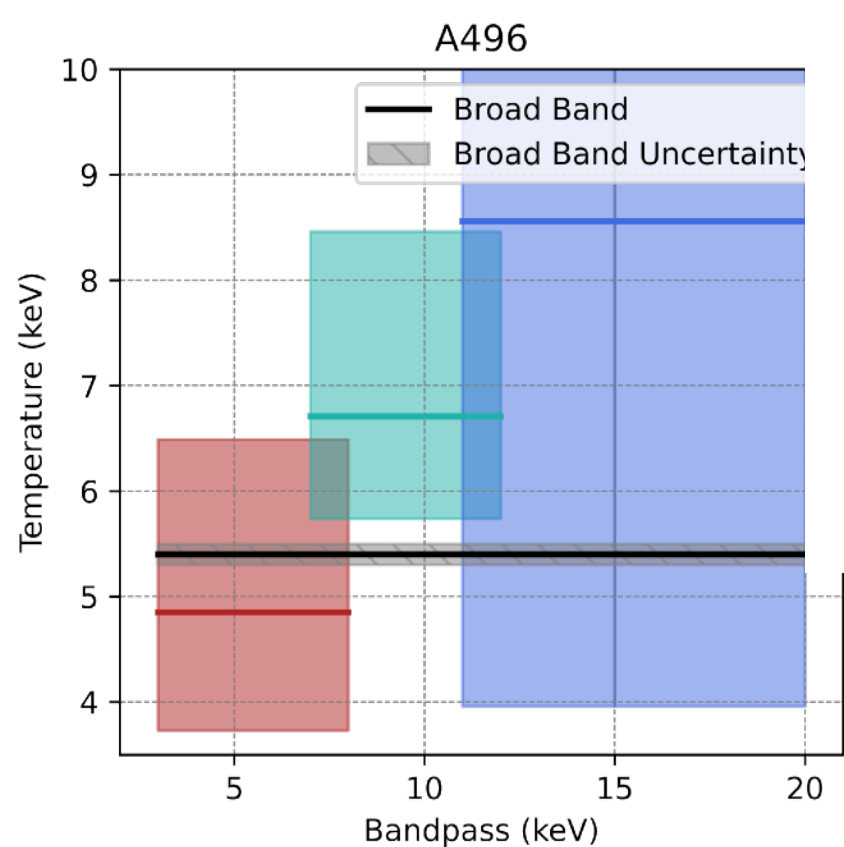
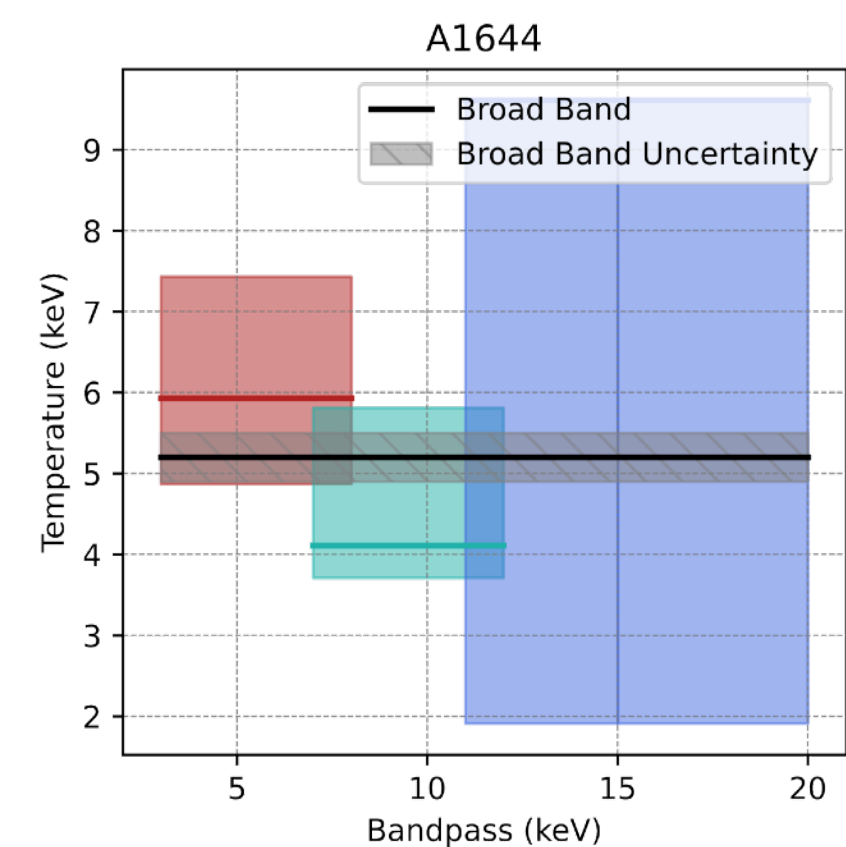
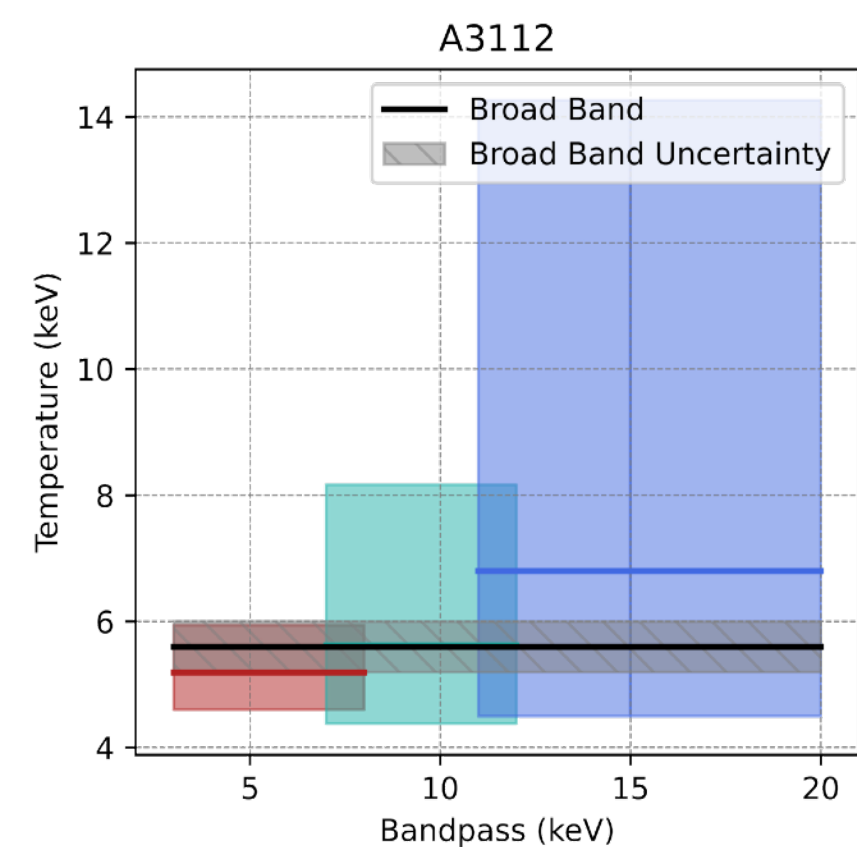
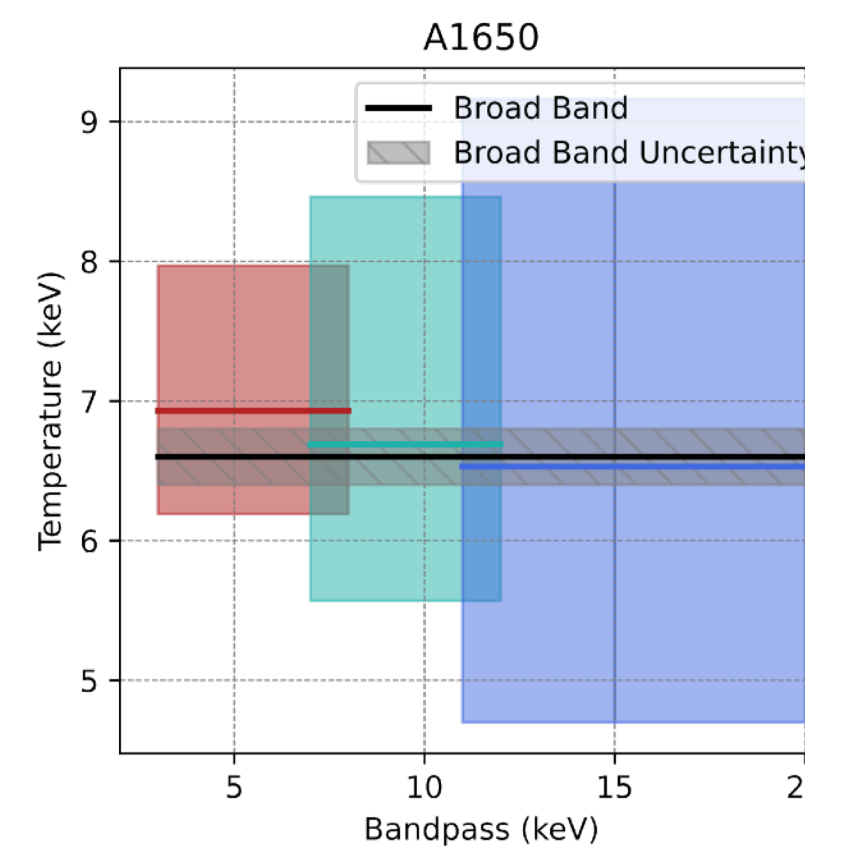
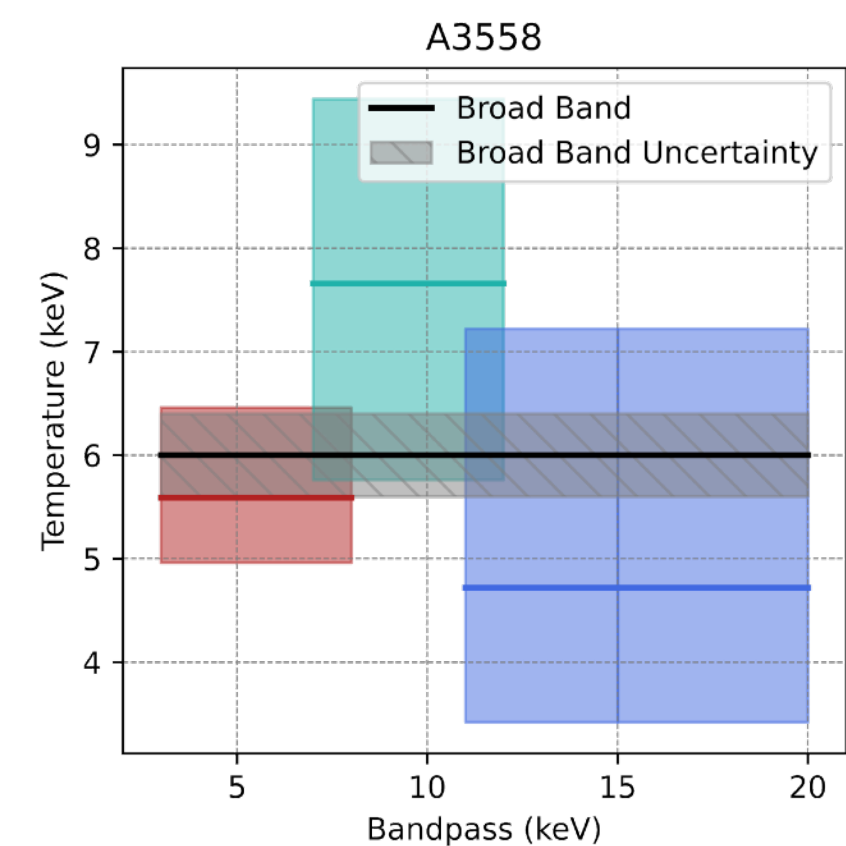
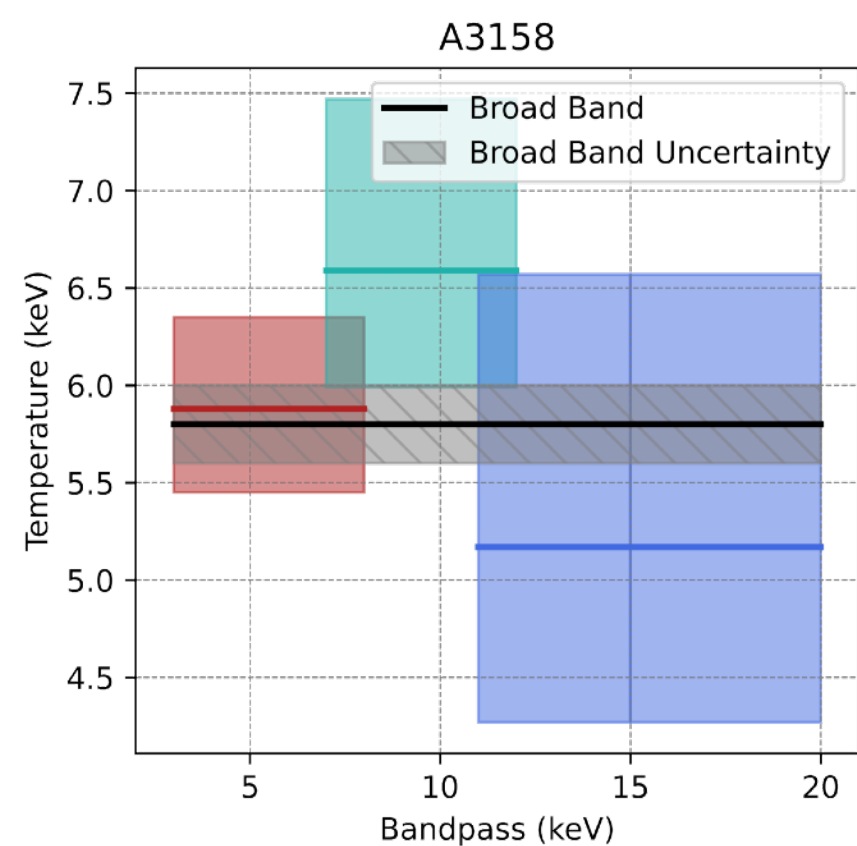
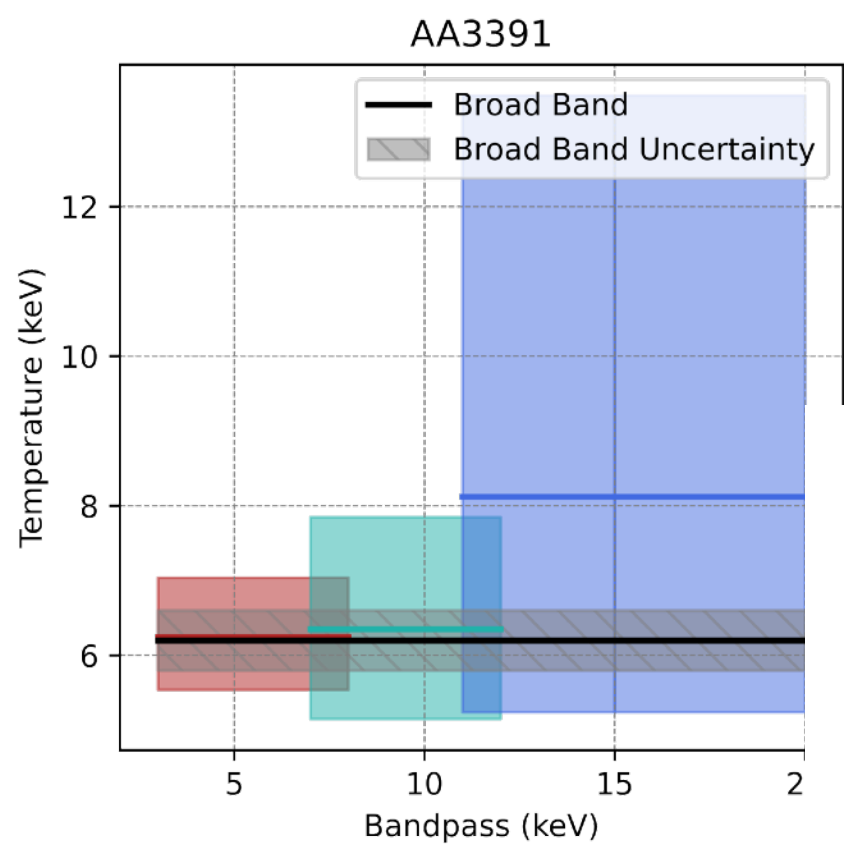
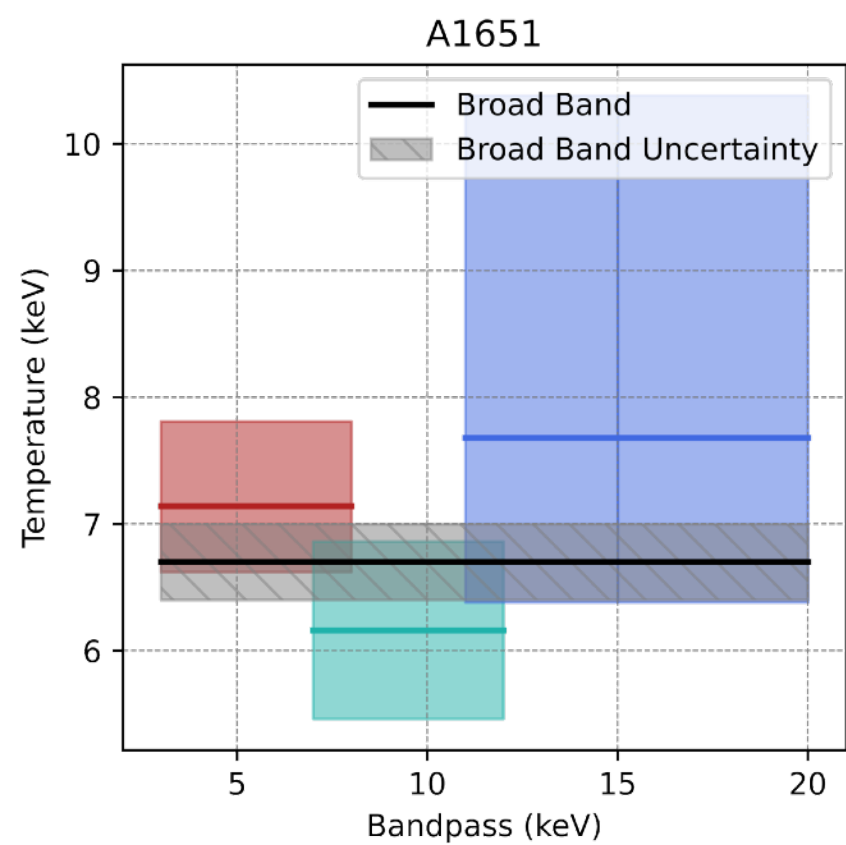
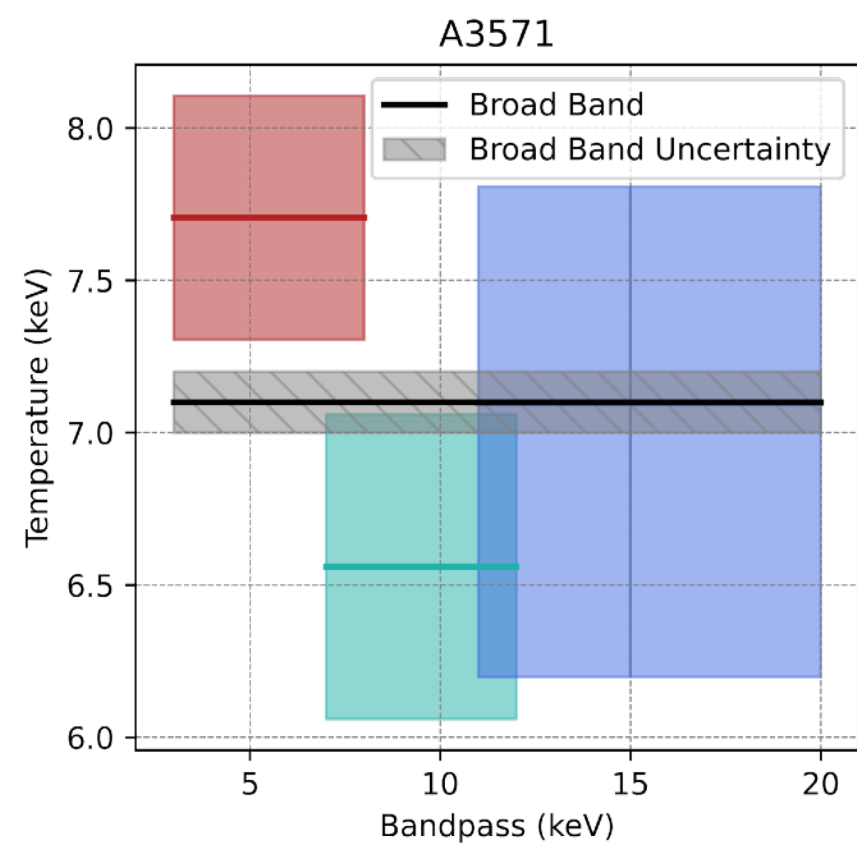


In Summary

- *NuSTAR* kT s are systematically LOWER than *Chandra* kT s, which physically shouldn't happen
- *NuSTAR* kT s are systematically HIGHER than *XMM-Newton* kT s and comparable to *Chandra* kT s for cooler clusters
- Trend not sensitive to dynamical state, only overall temperature matters
- A correction to *Chandra*'s hard band effective area similar to *XMM-Newton*'s achieves better agreement with *NuSTAR*, although it's not perfect
- The *XMM-Newton* effective area correction may exacerbate disagreement with *NuSTAR*, but physical explanation plausible

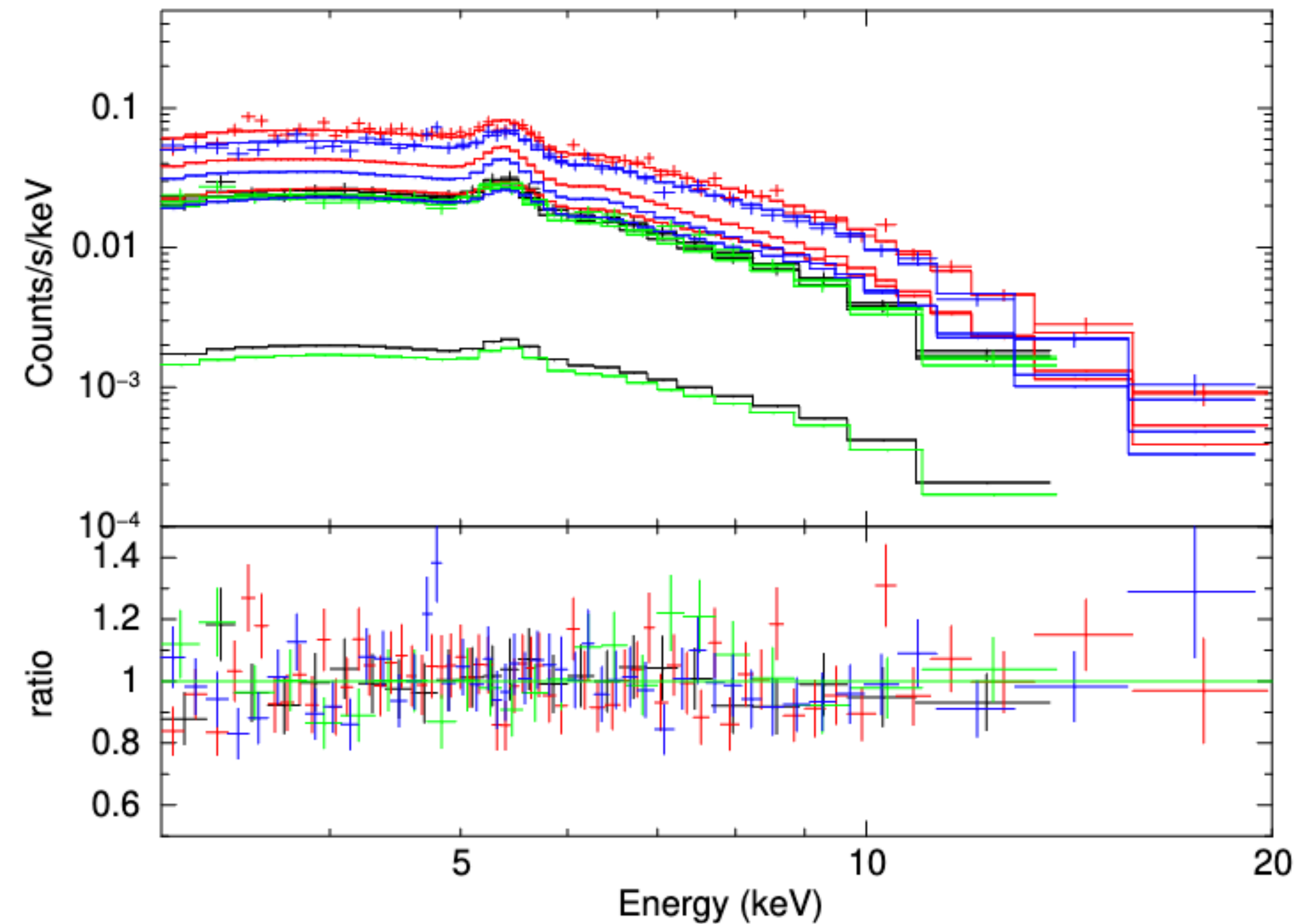


Backup Slides

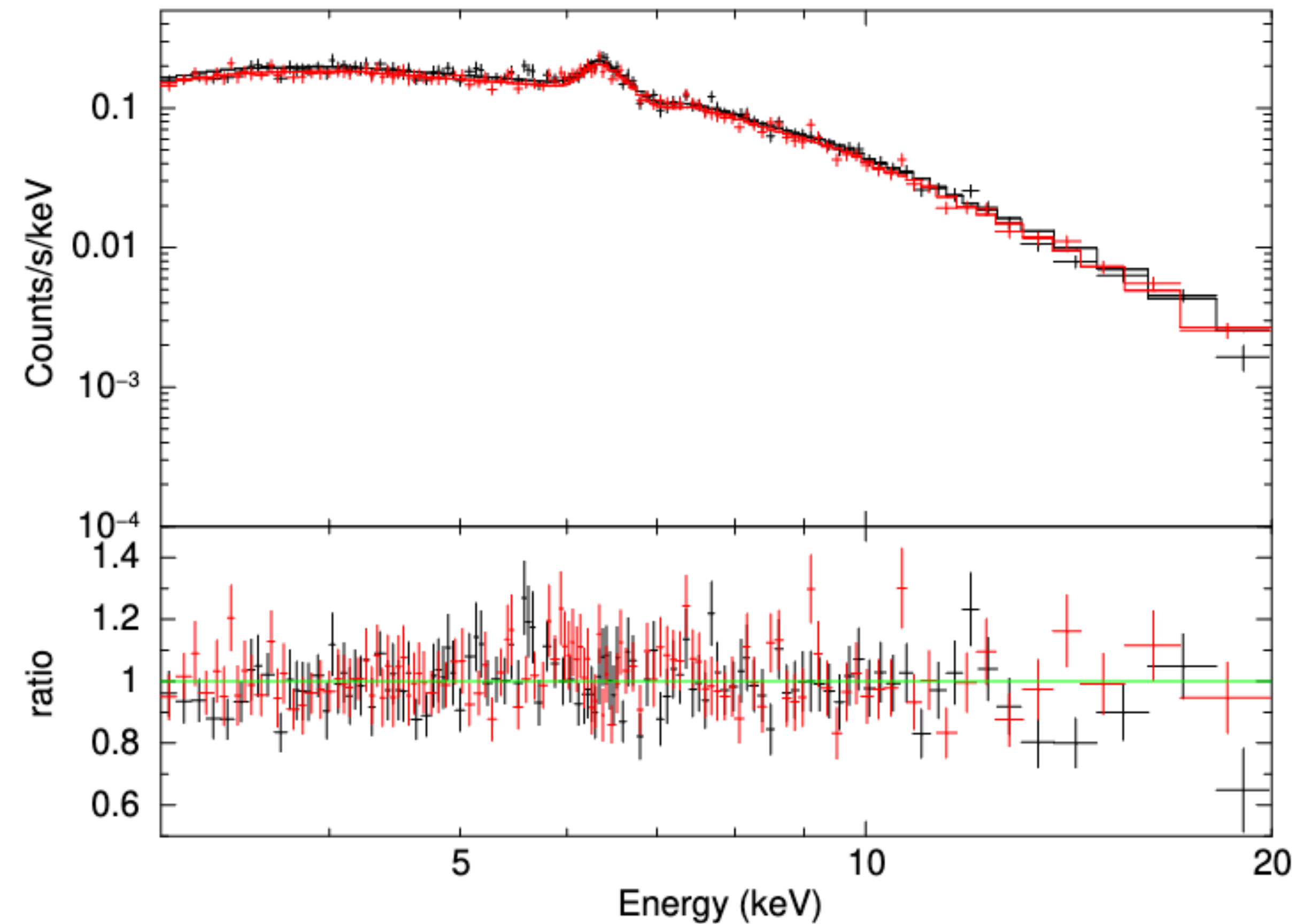


Snapshot Spectral Fits

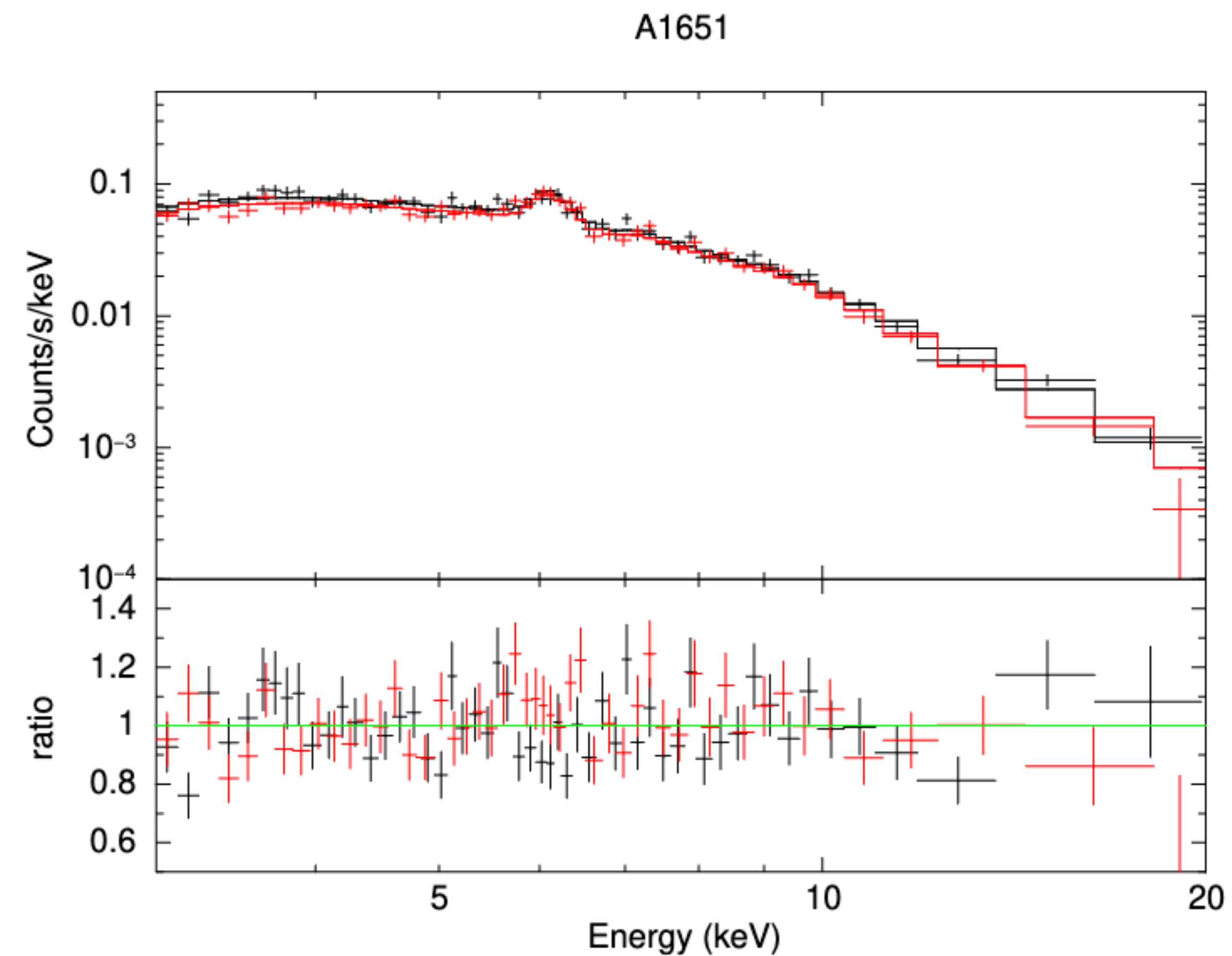
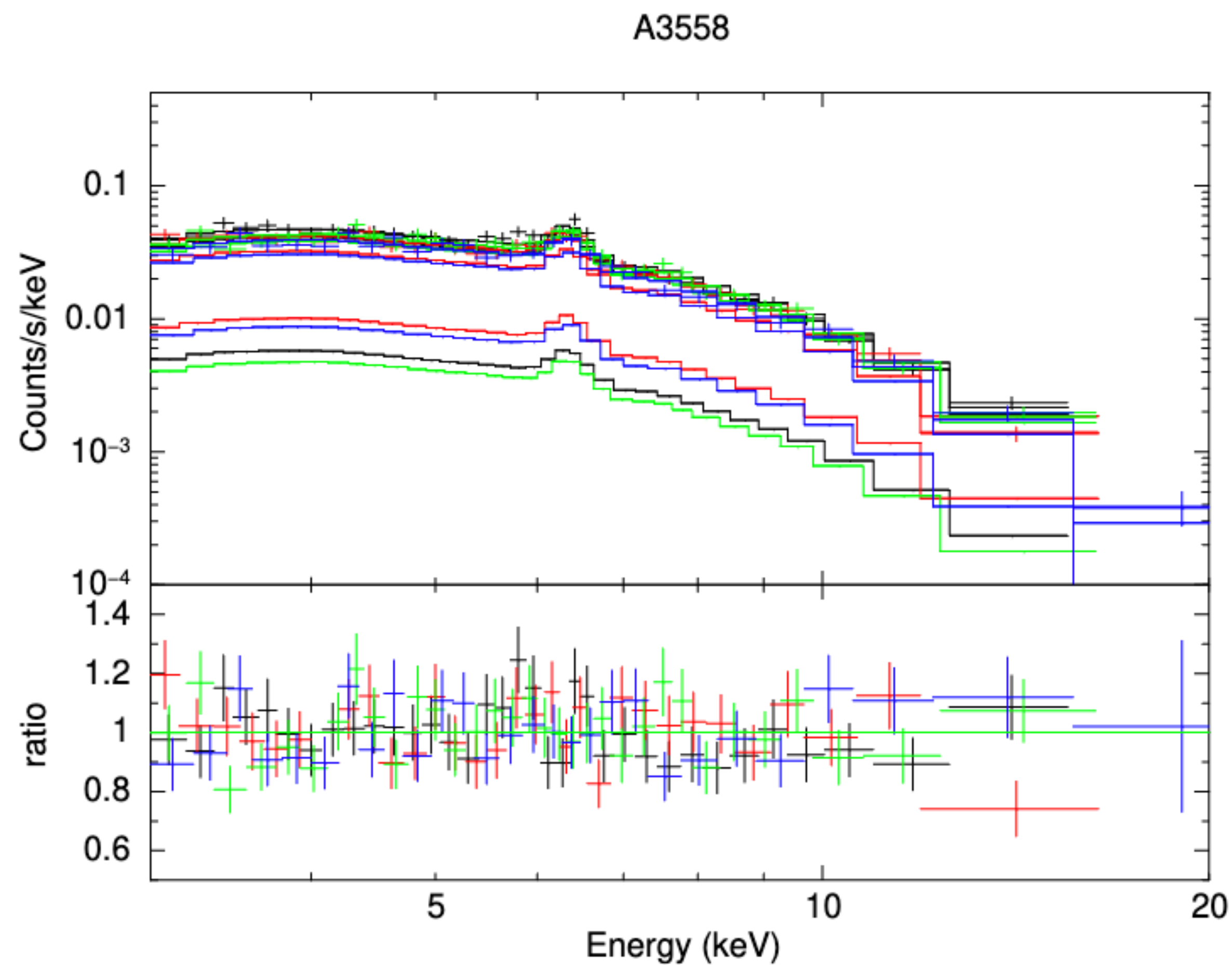
RXC-J1504



A3571

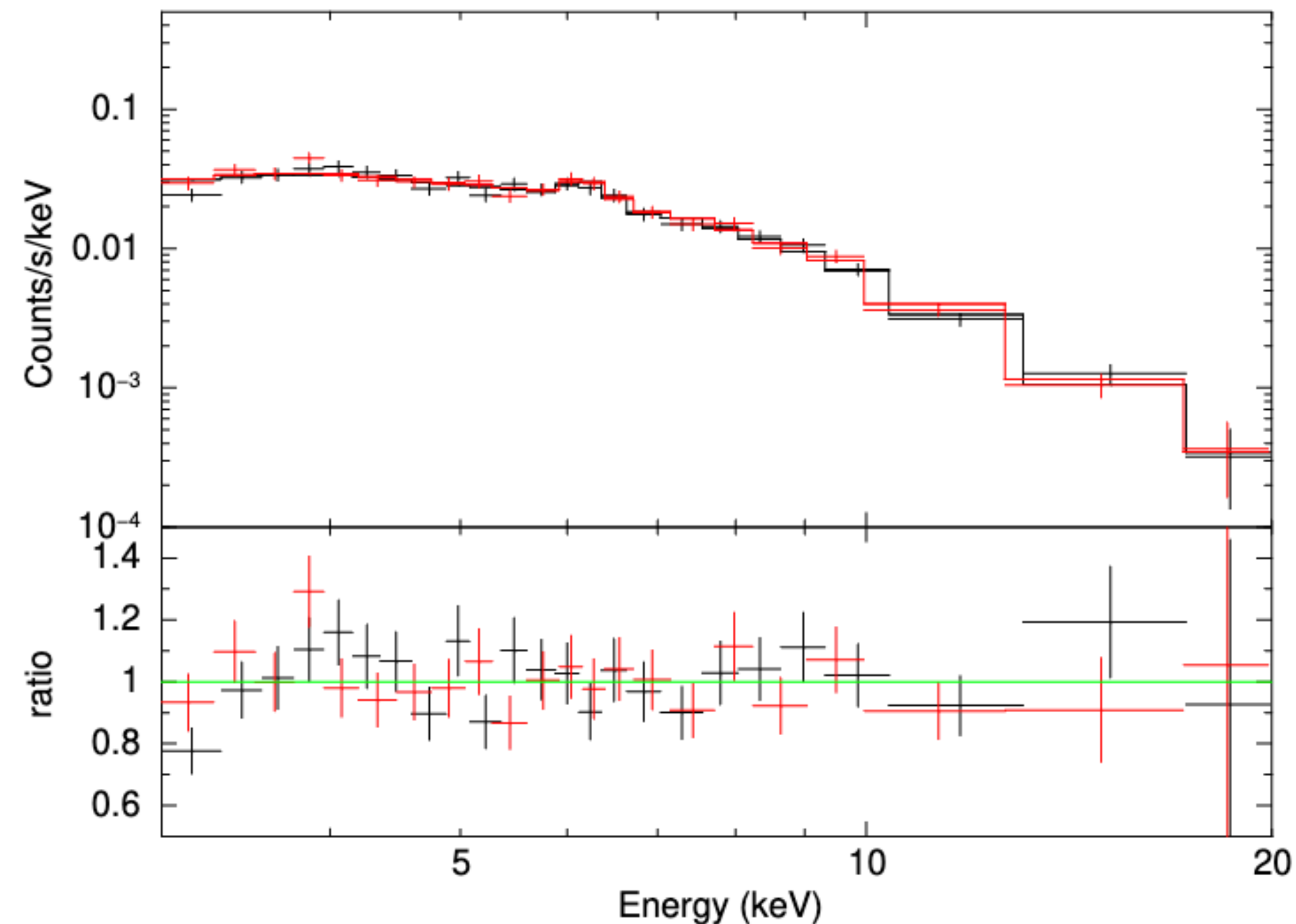


Snapshot Spectral Fits

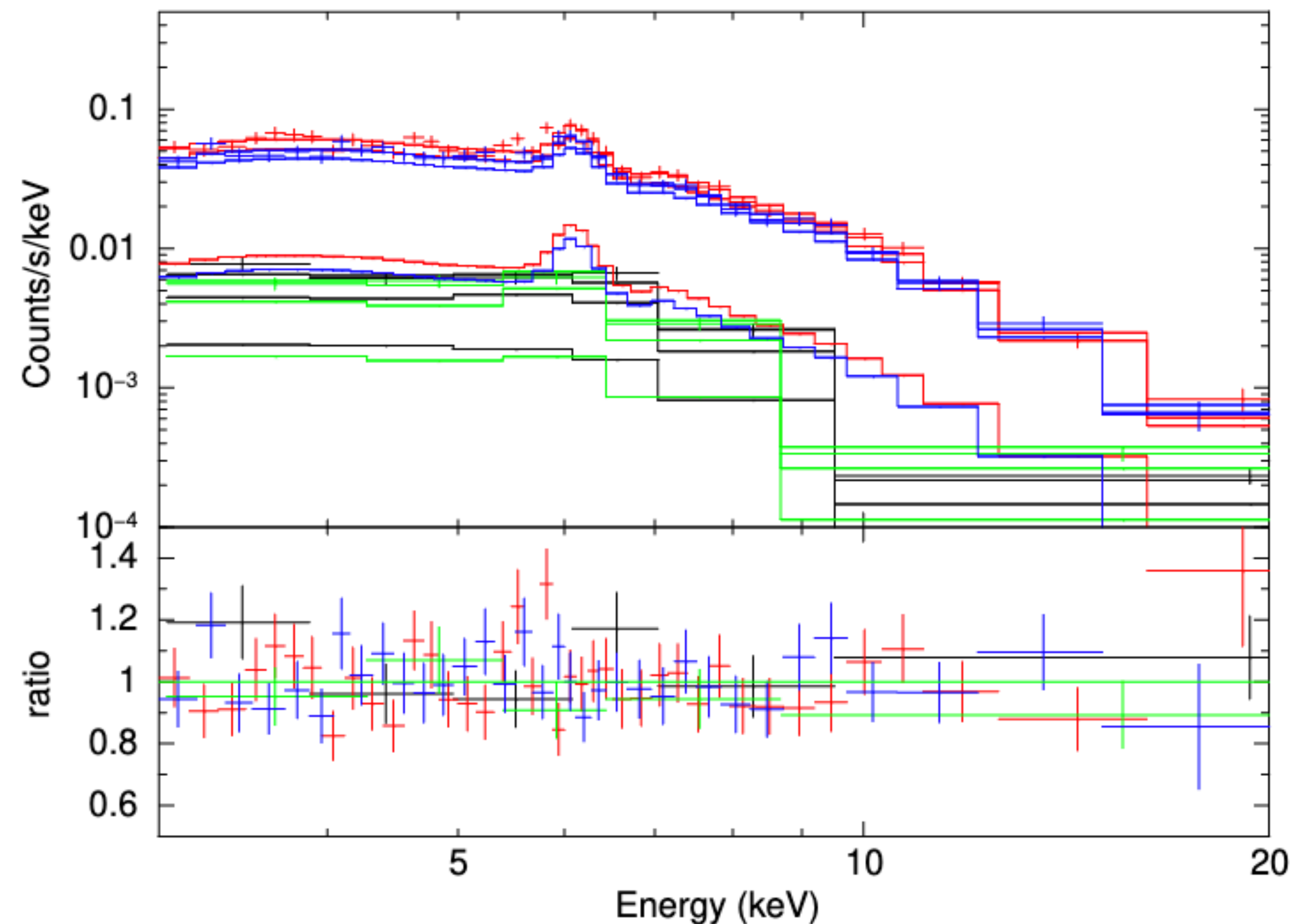


Snapshot Spectral Fits

A3391

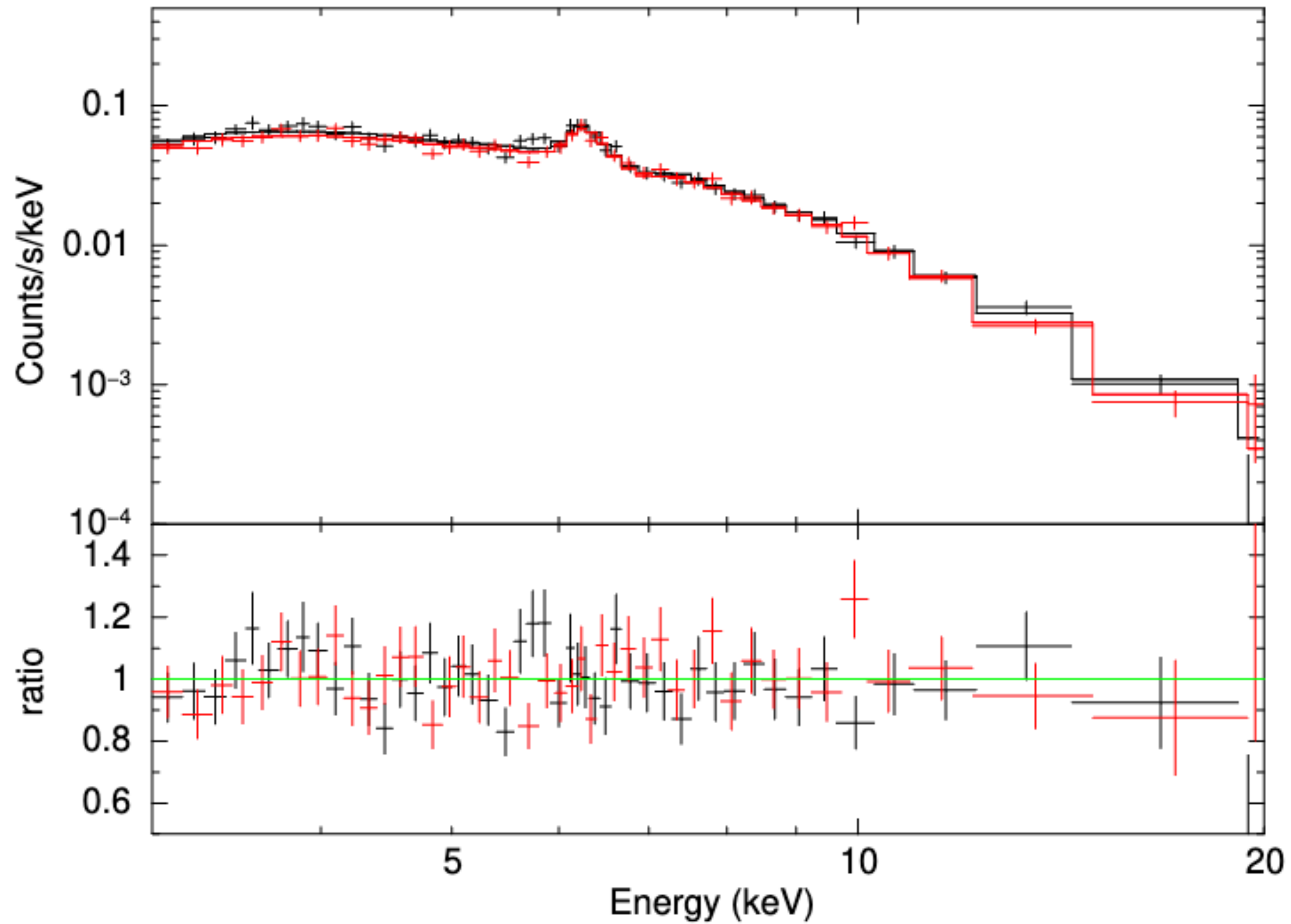


A1650

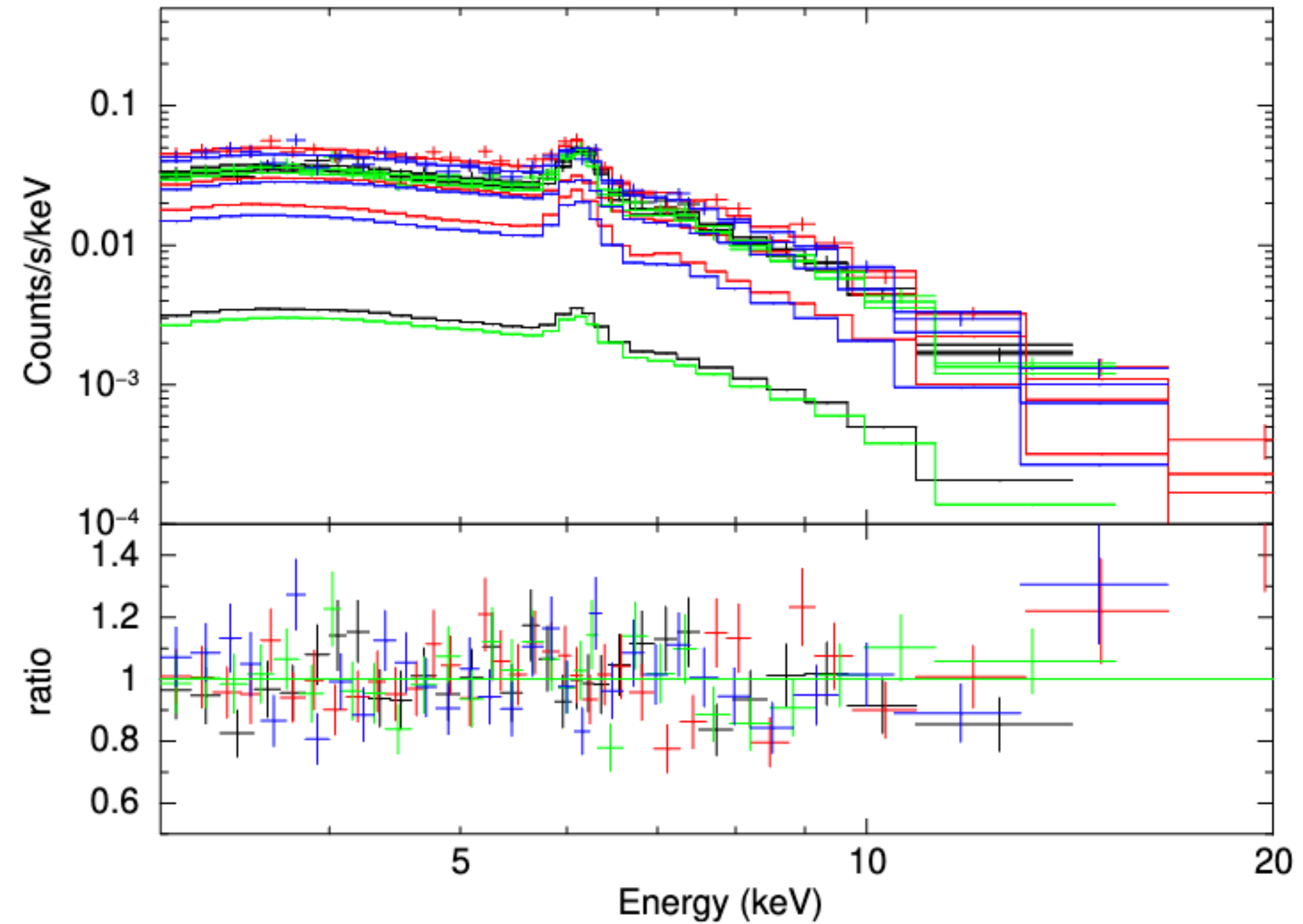


Snapshot Spectral Fits

A3158



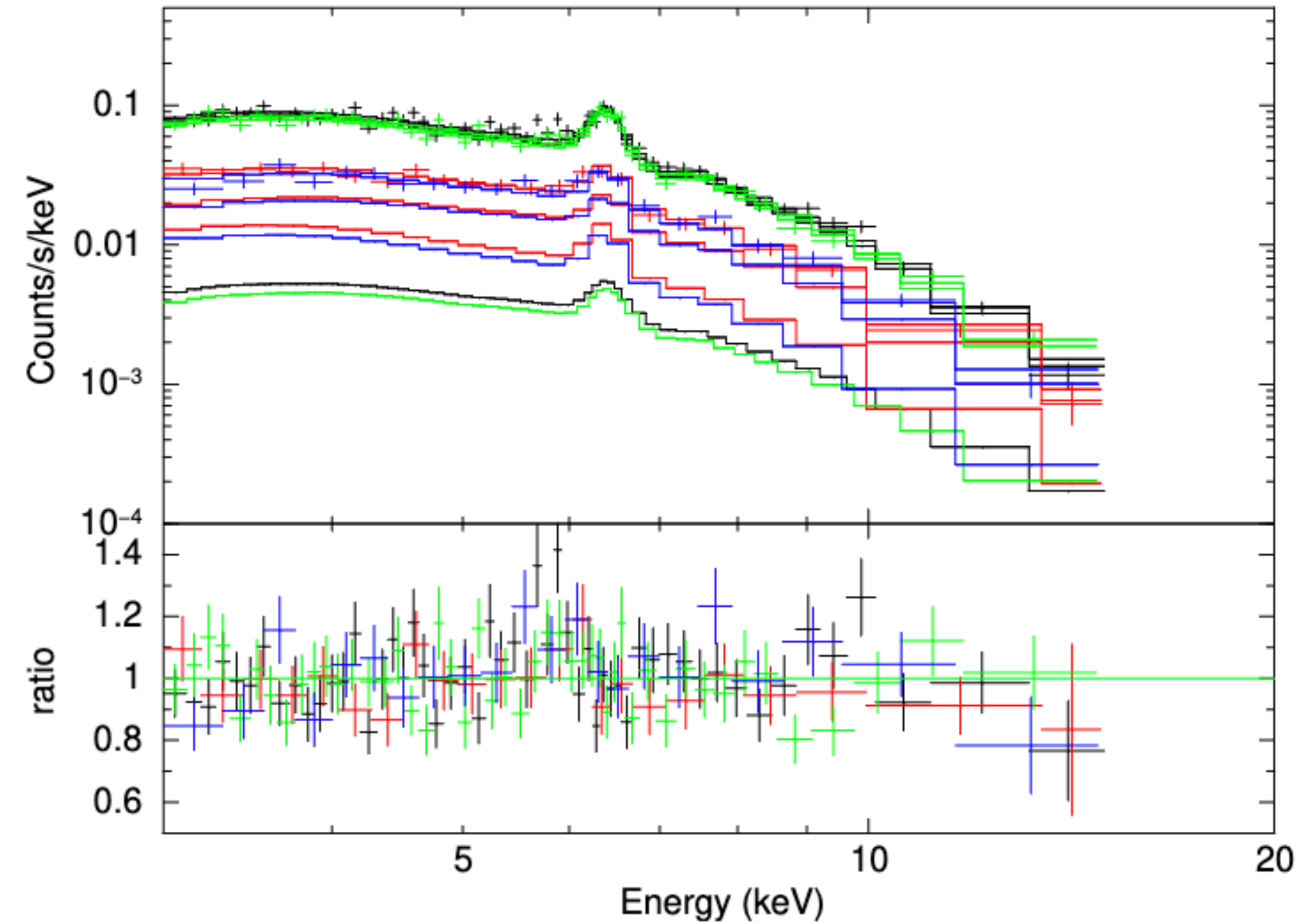
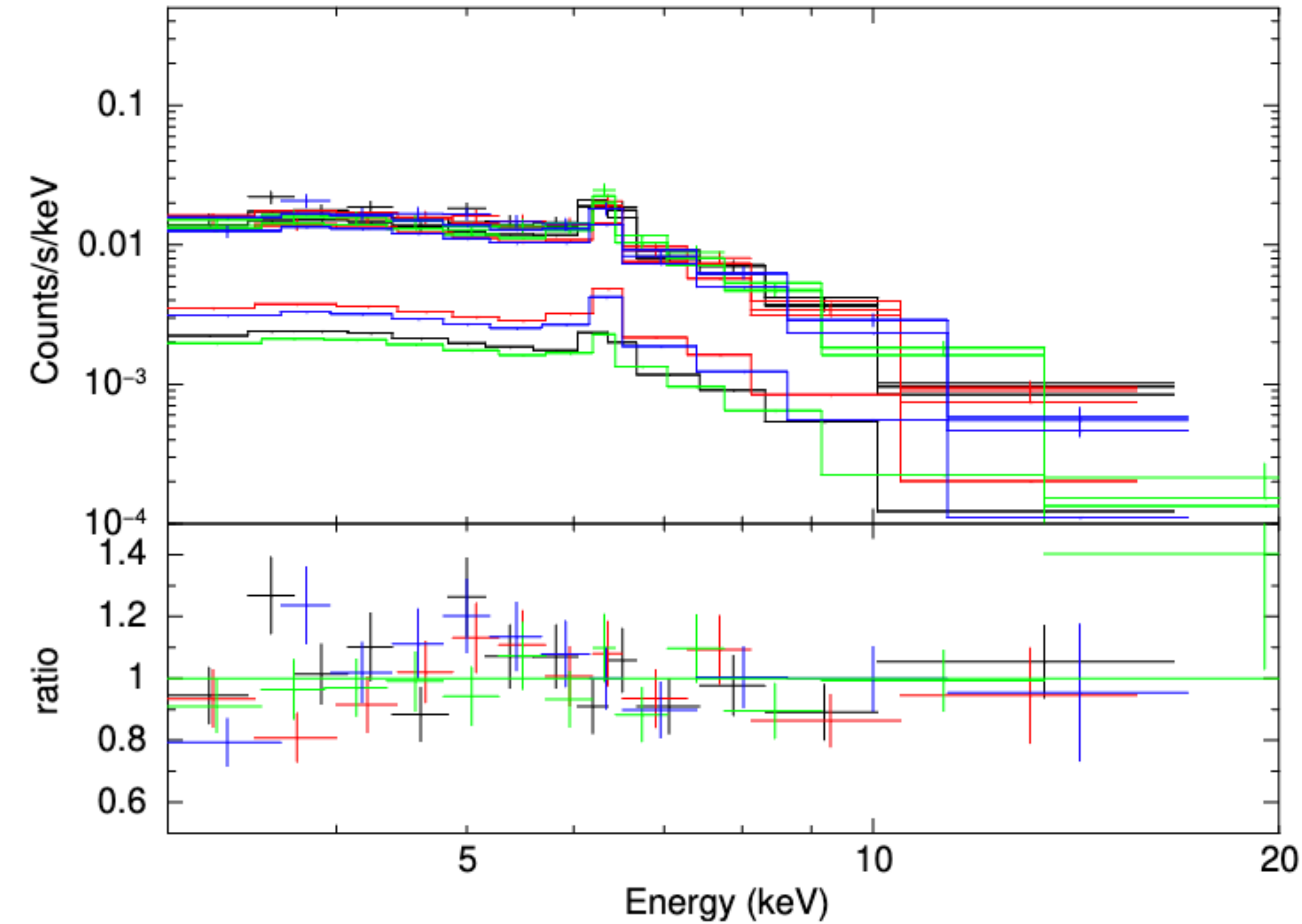
A3112



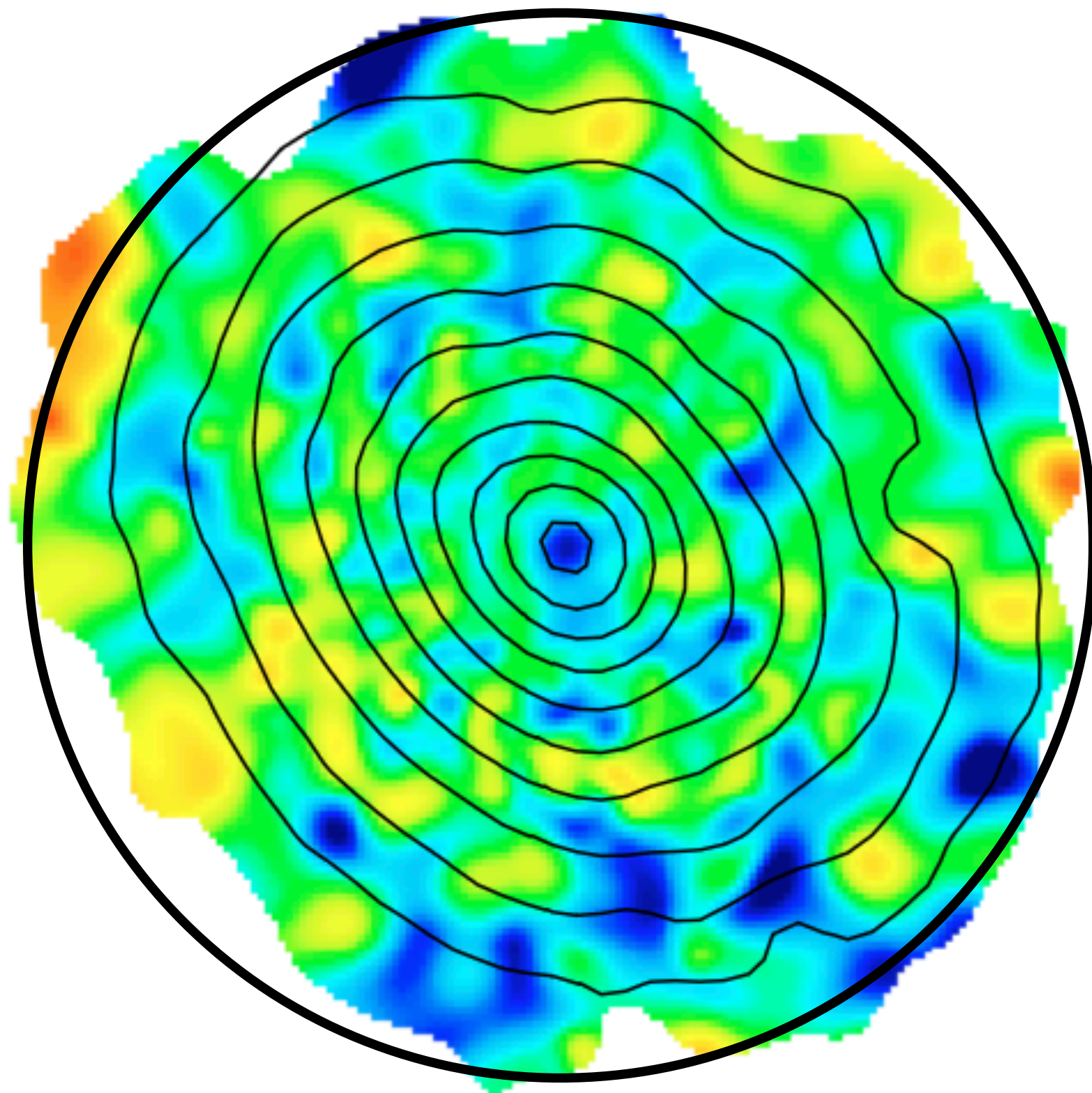
Snapshot Spectral Fits

A1644

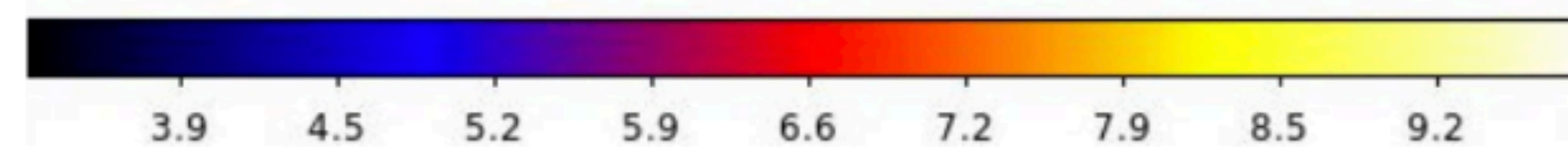
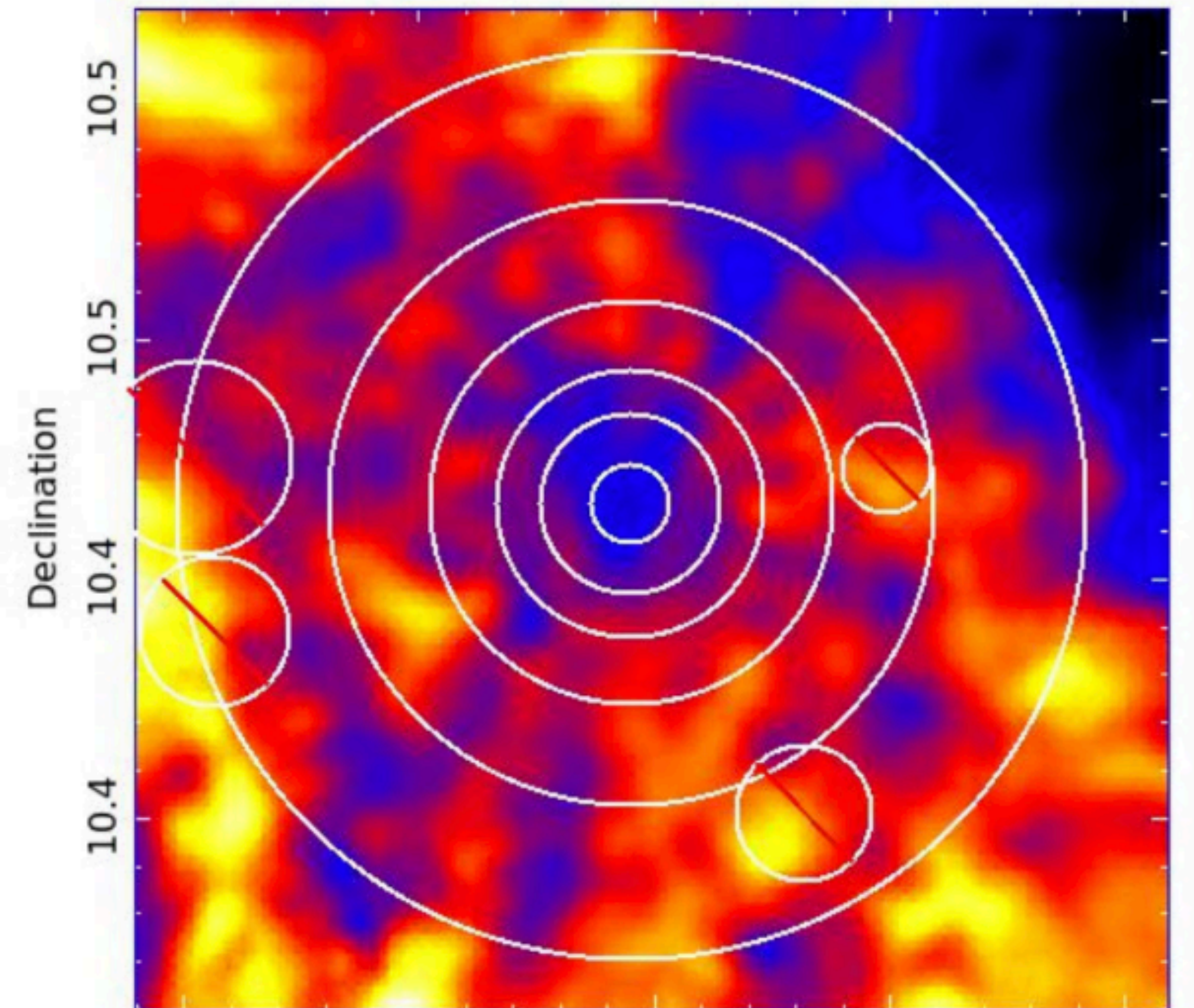
A496



Temperature Maps of A478

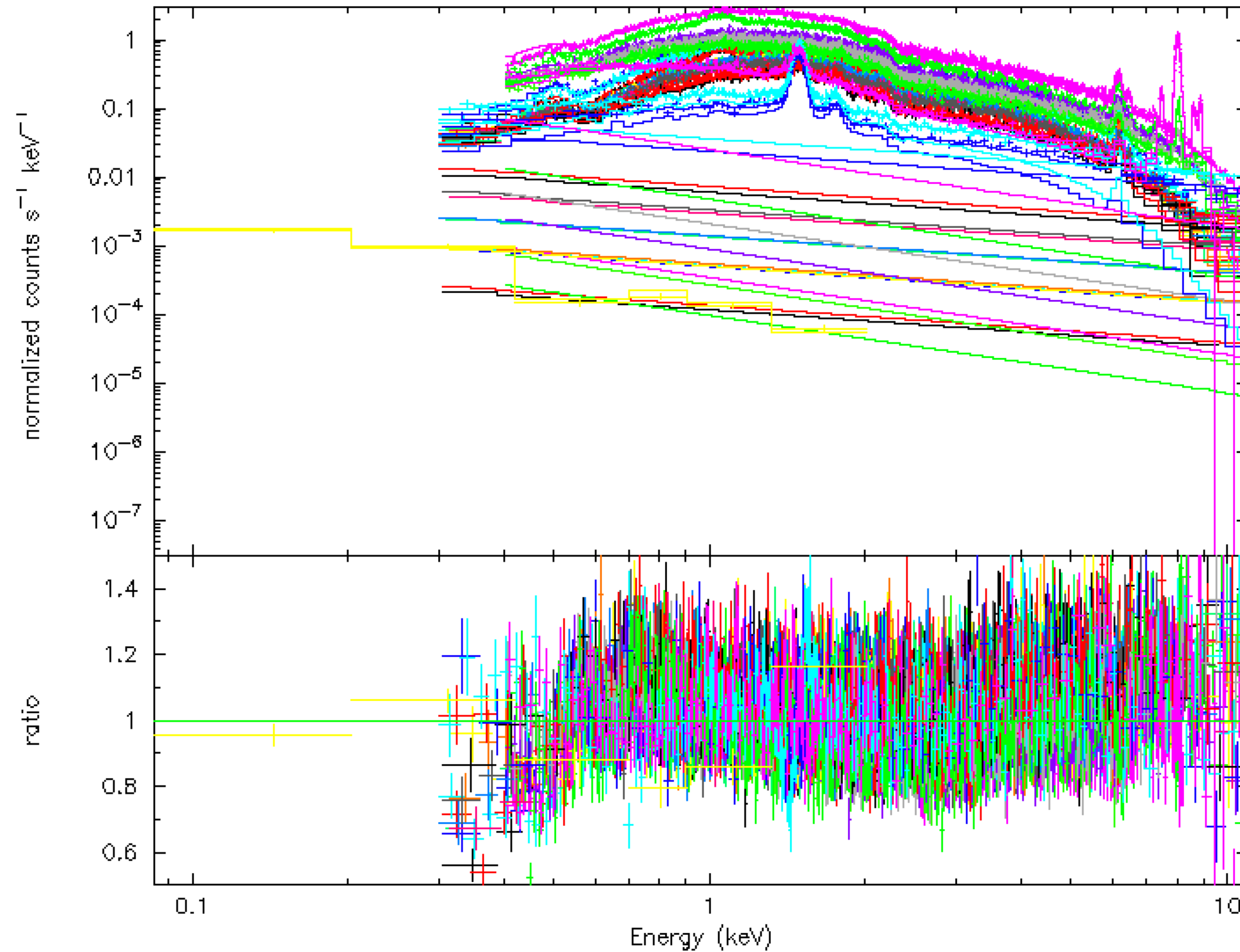


(<—hot) Hardness (cool—>)

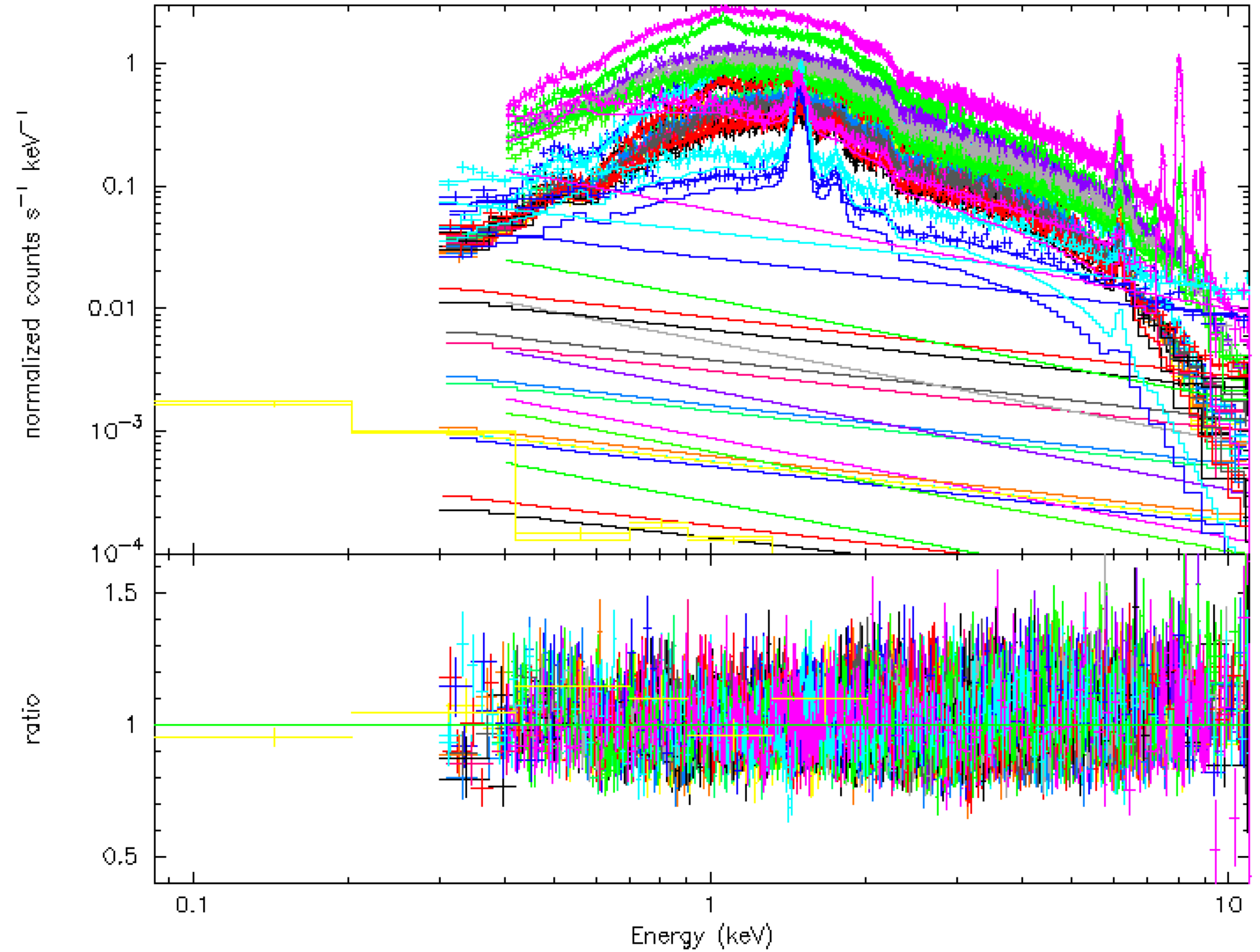
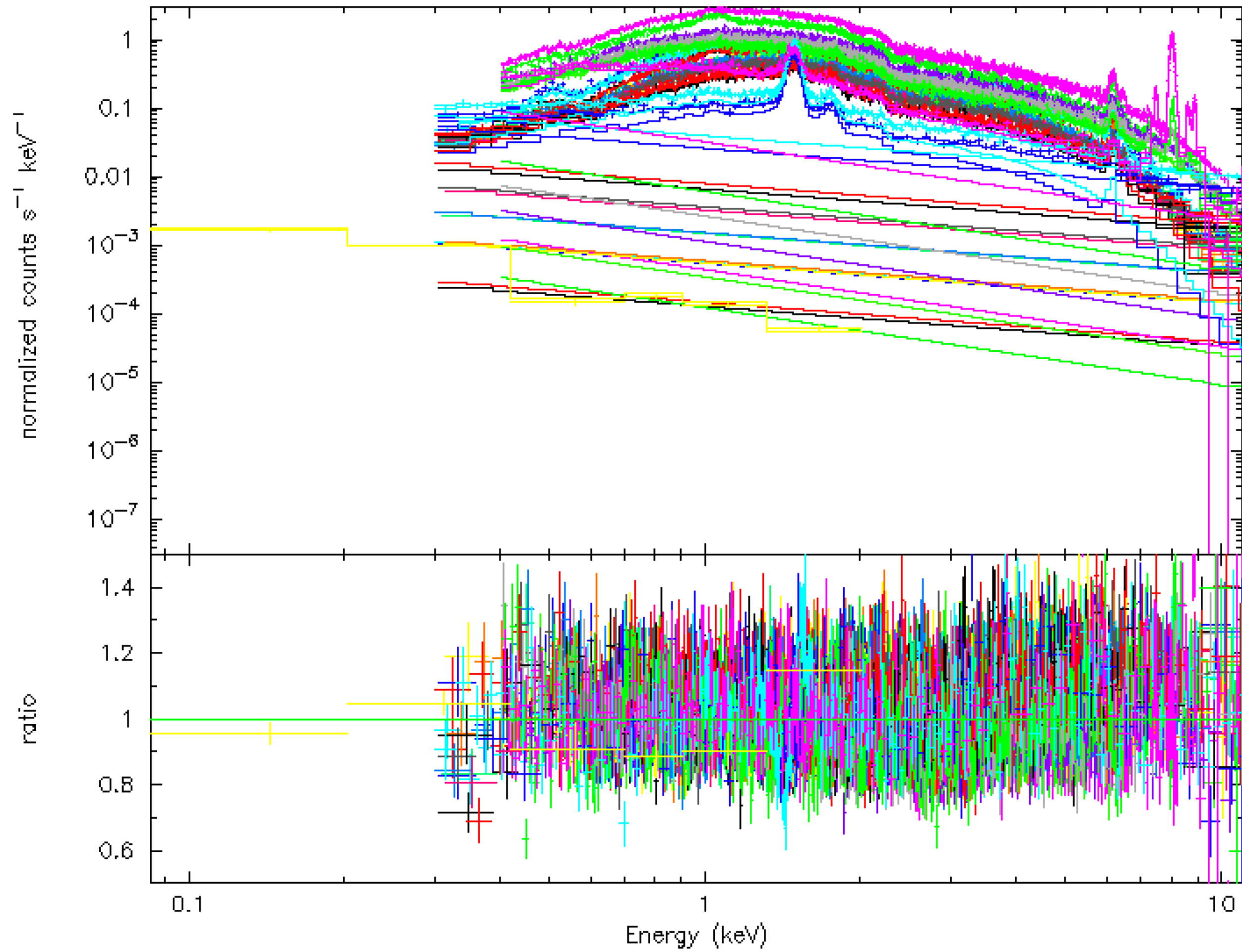


kT (keV)

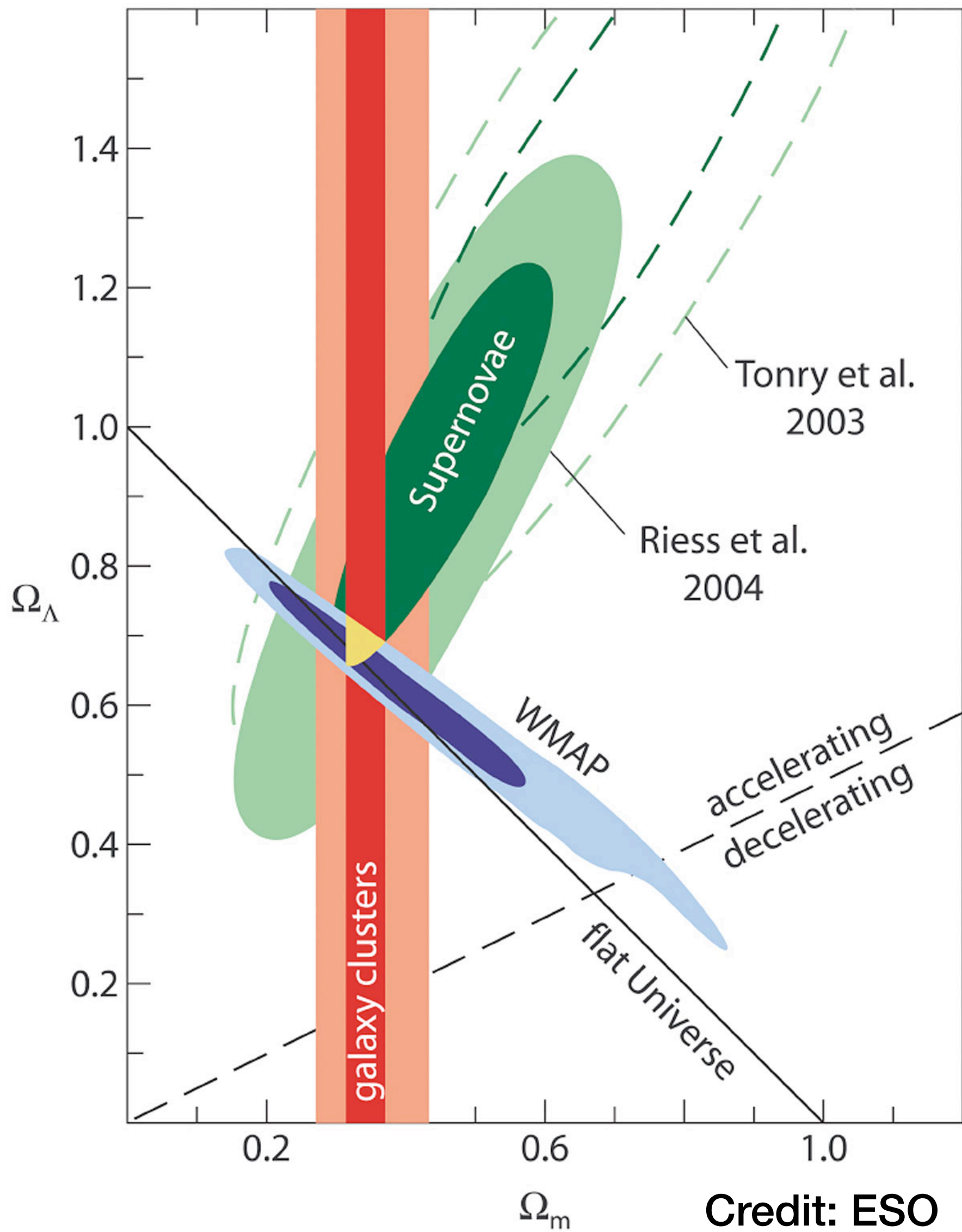
AnGr abund, wabs, no ARF correction



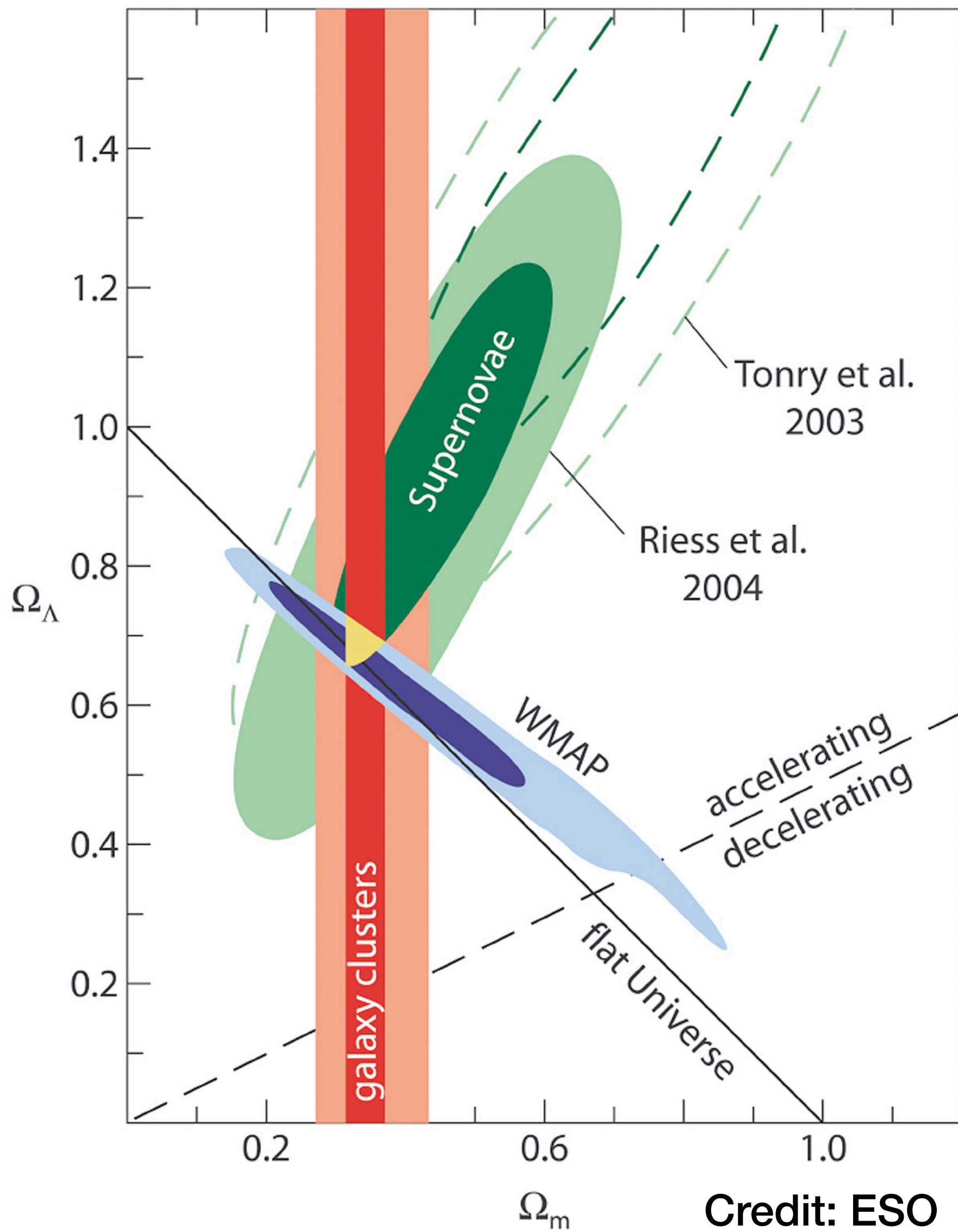
Abund Wilm, before & after ARF correction



Galaxy Clusters: Why Calibration?

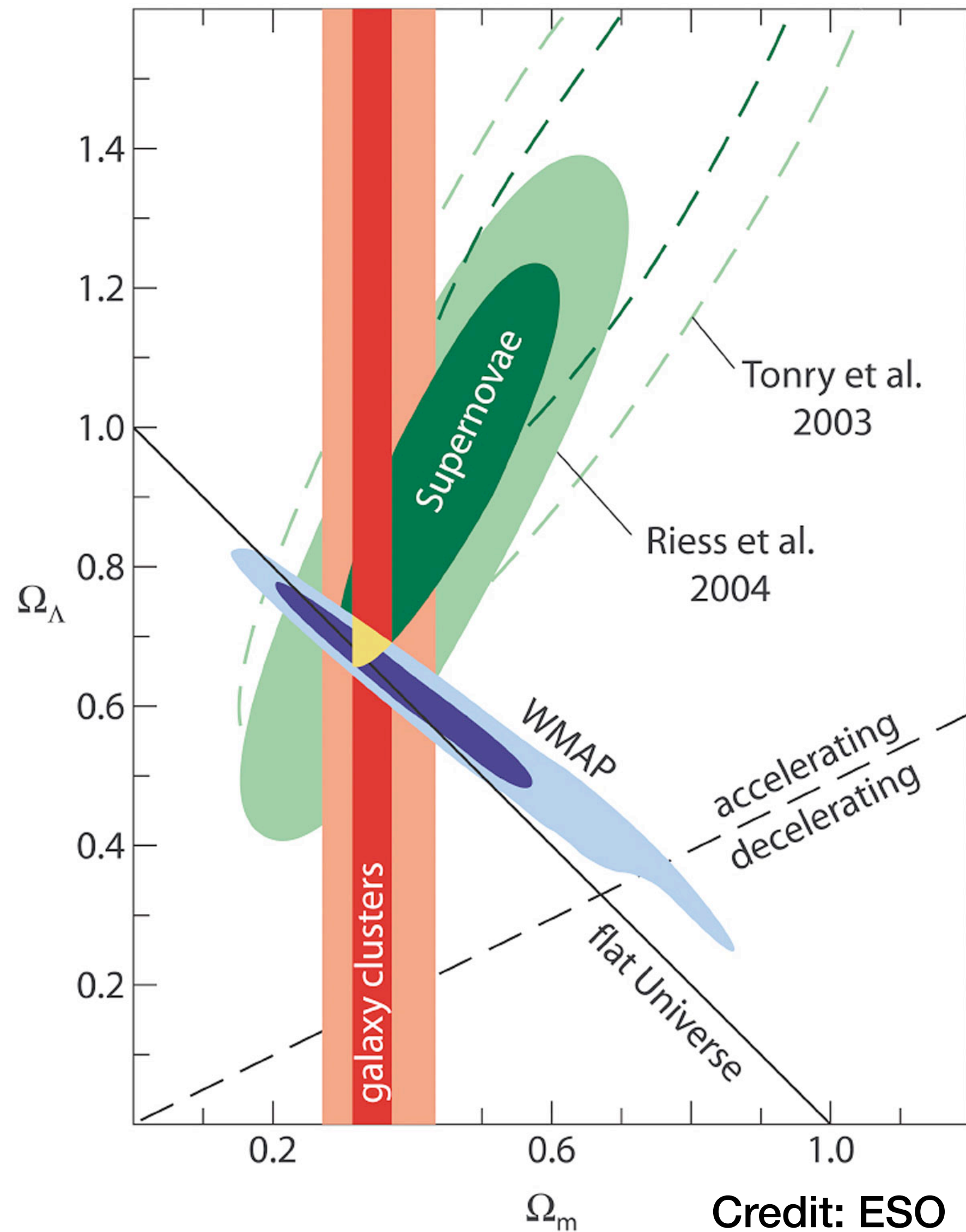


Galaxy Clusters: Why Calibration?

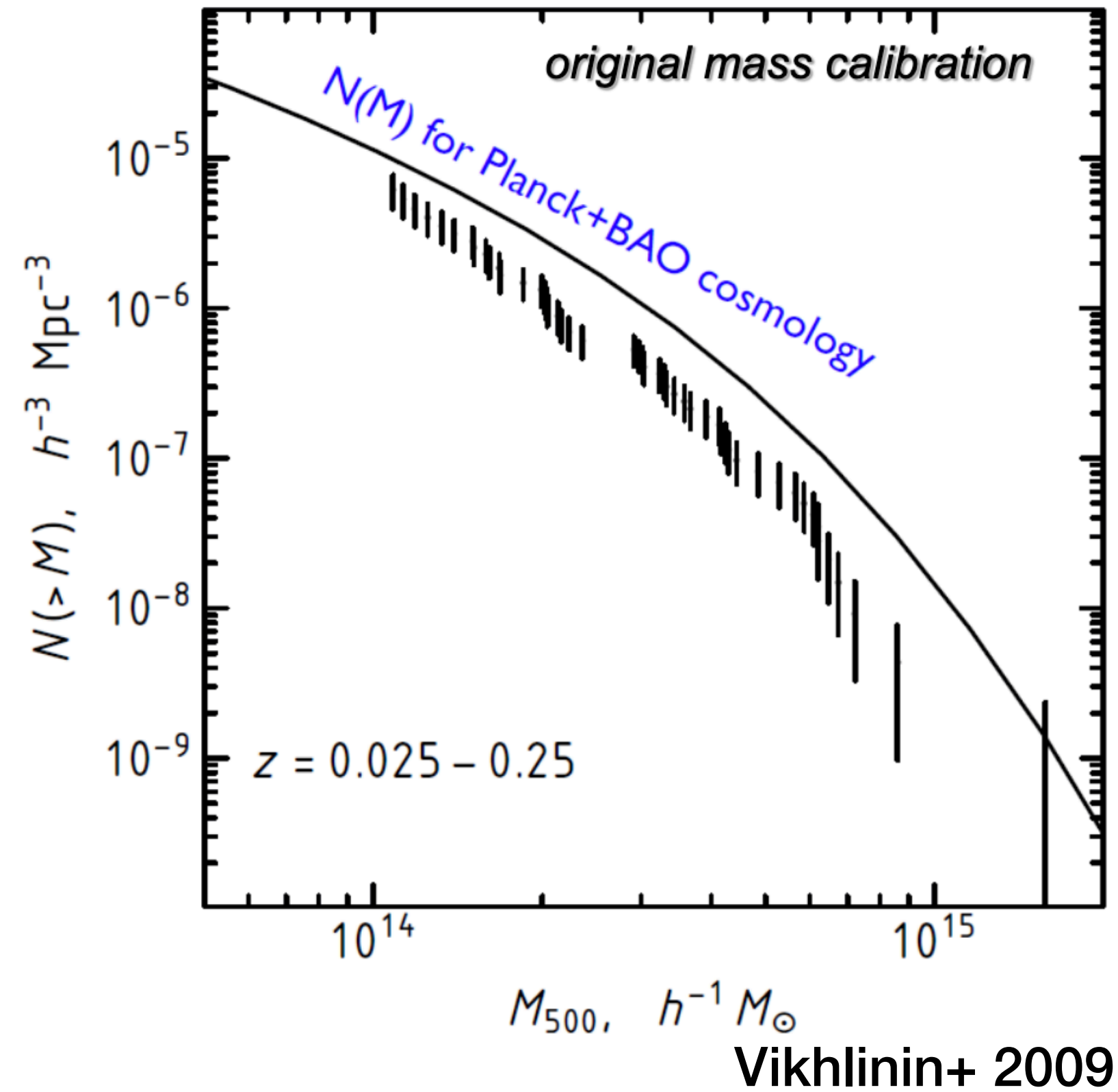


$$M(< r) = -\frac{kT(r)r}{G\mu m_p} \left[\frac{d \ln n_p}{d \ln r} + \frac{d \ln T}{d \ln r} \right] \propto T(r)r$$

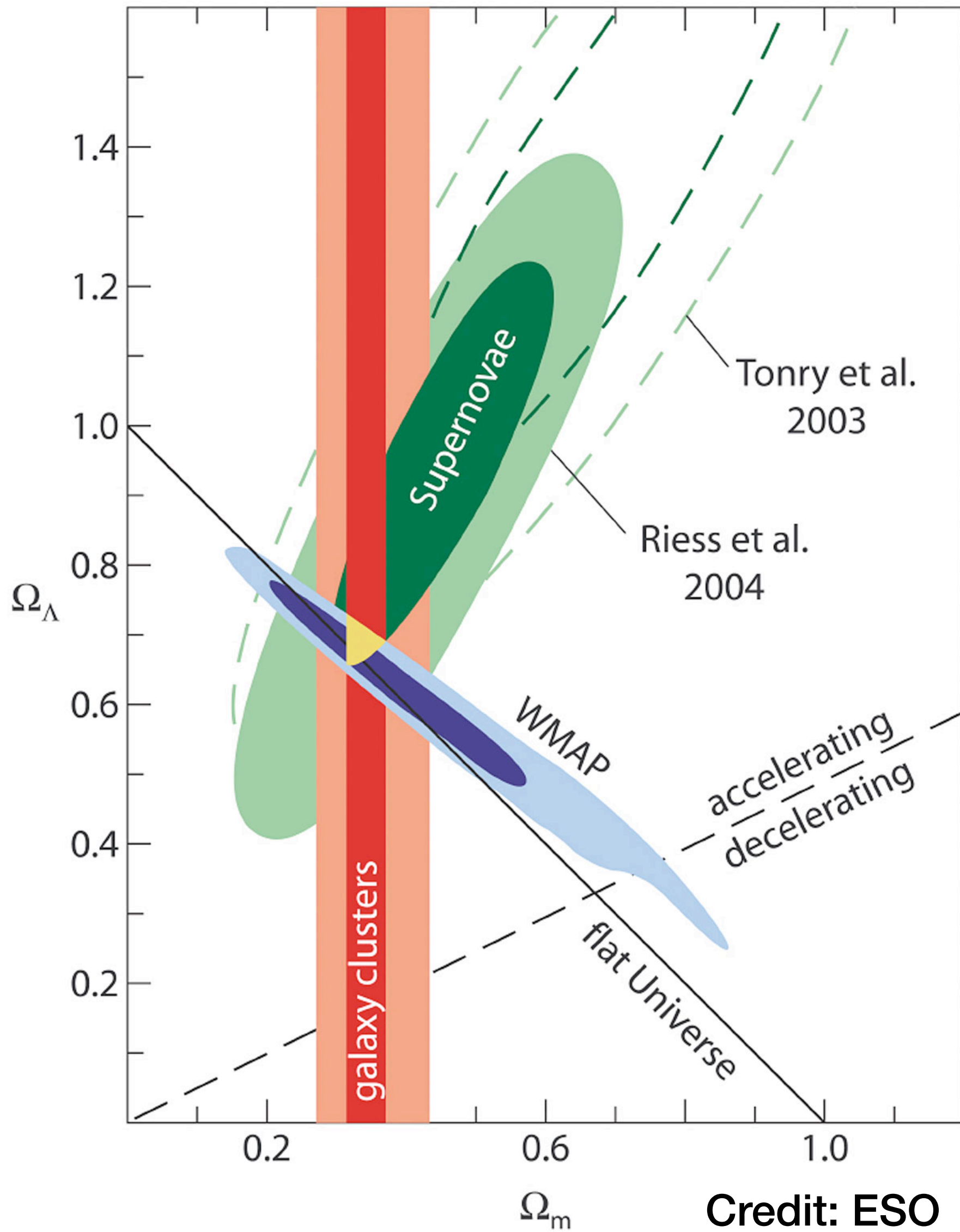
Galaxy Clusters: Why Calibration?



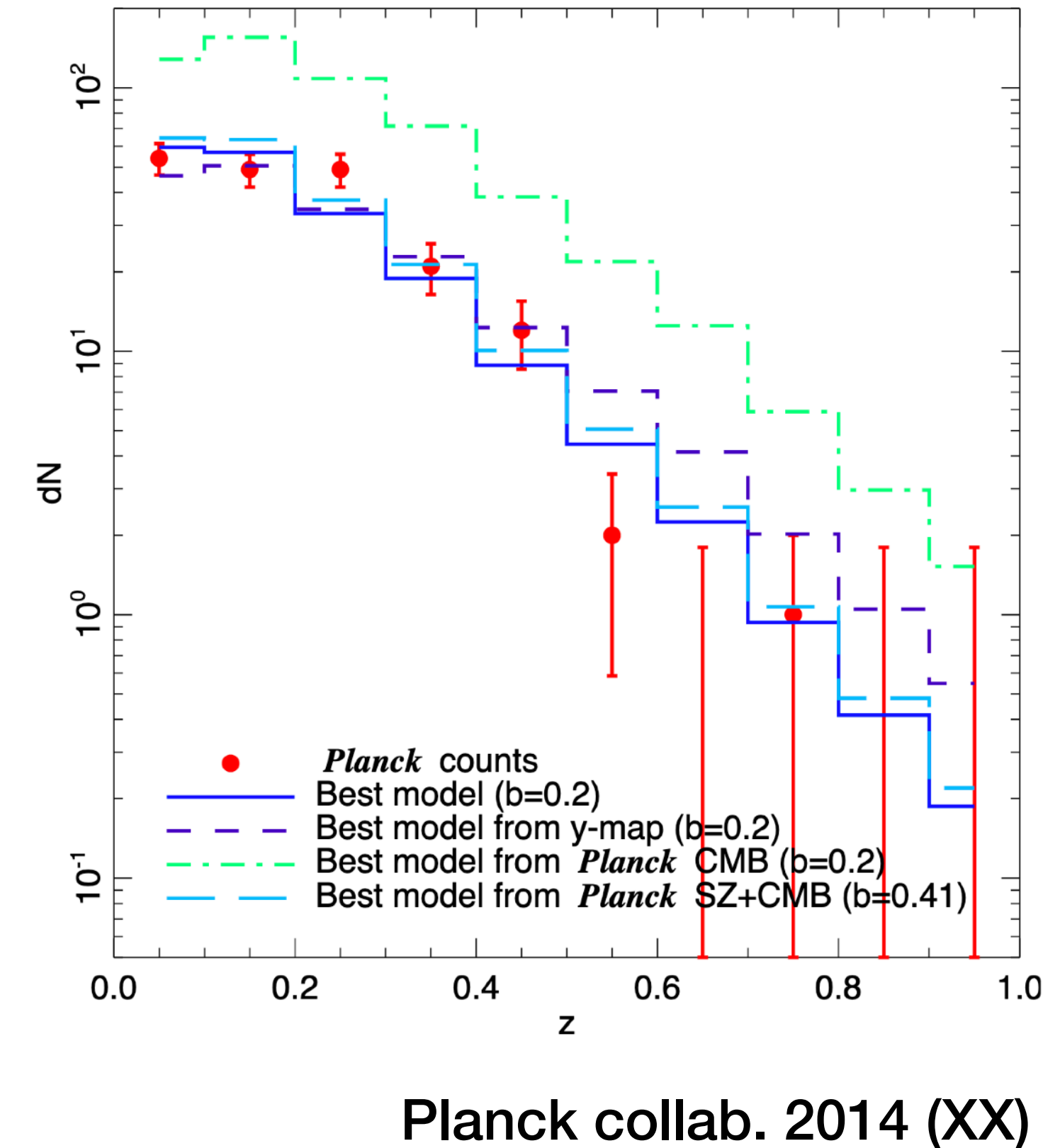
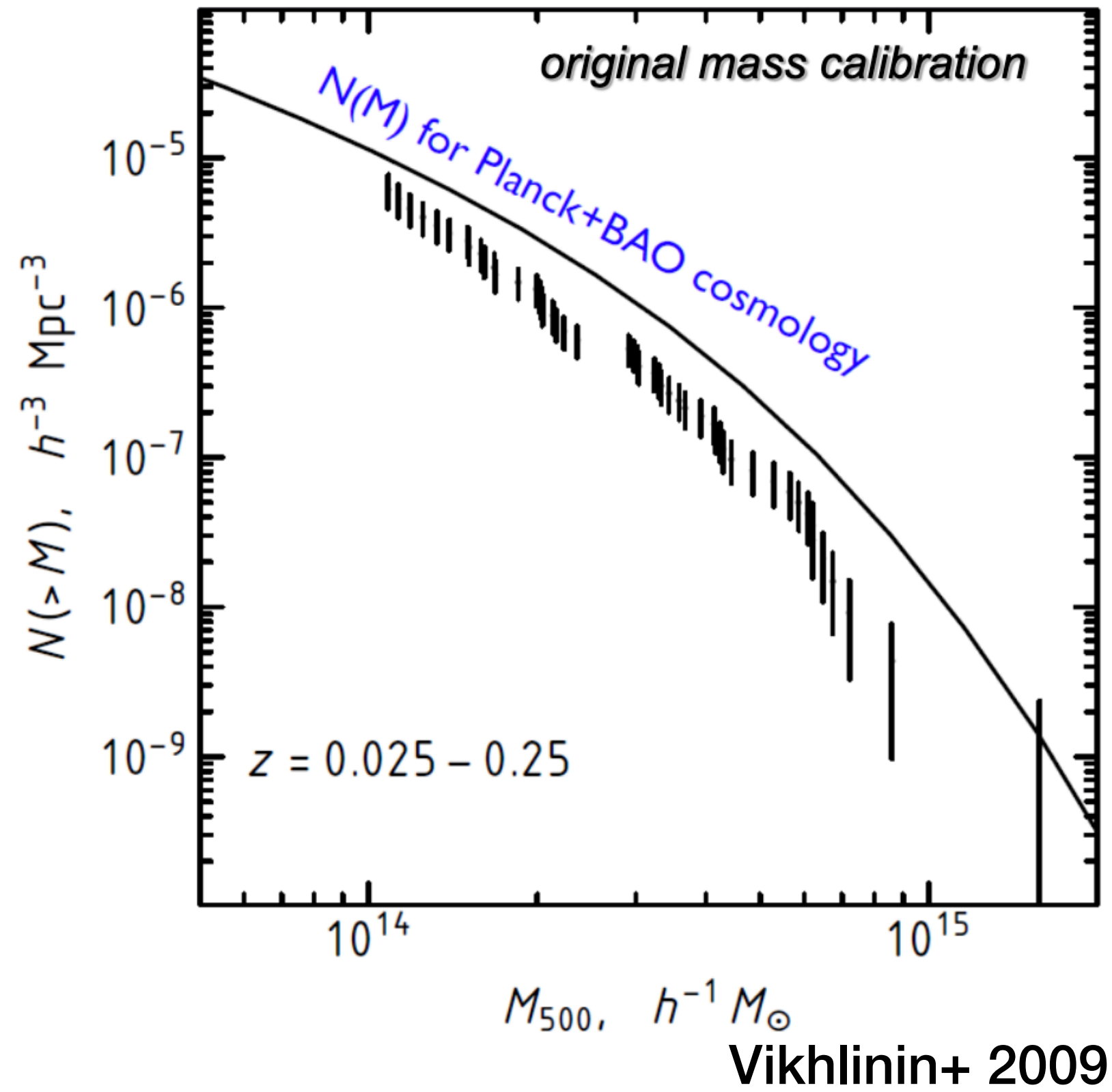
$$M(< r) = - \frac{kT(r)r}{G\mu m_p} \left[\frac{d \ln n_p}{d \ln r} + \frac{d \ln T}{d \ln r} \right] \propto T(r)r$$



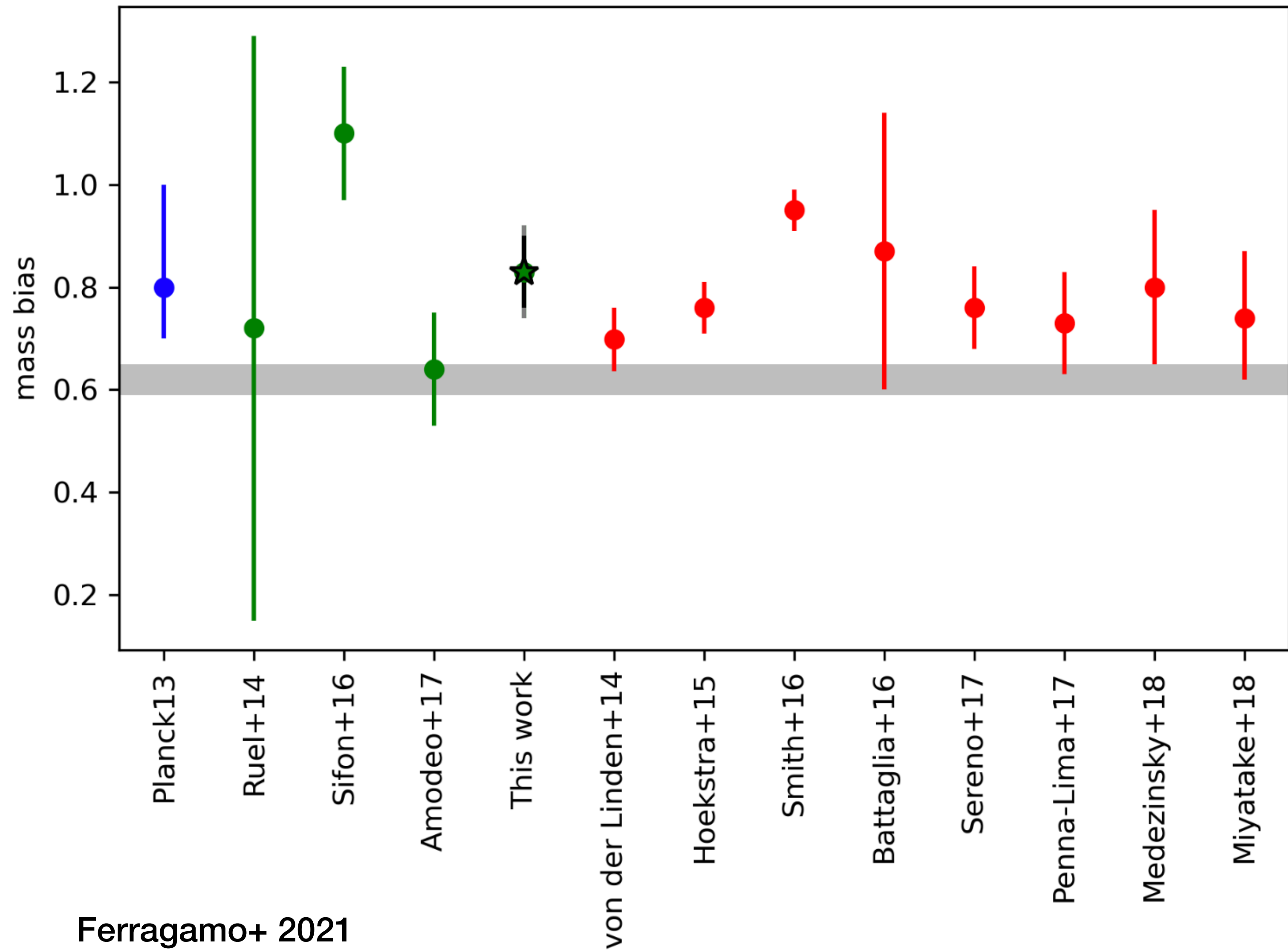
Galaxy Clusters: Why Calibration?



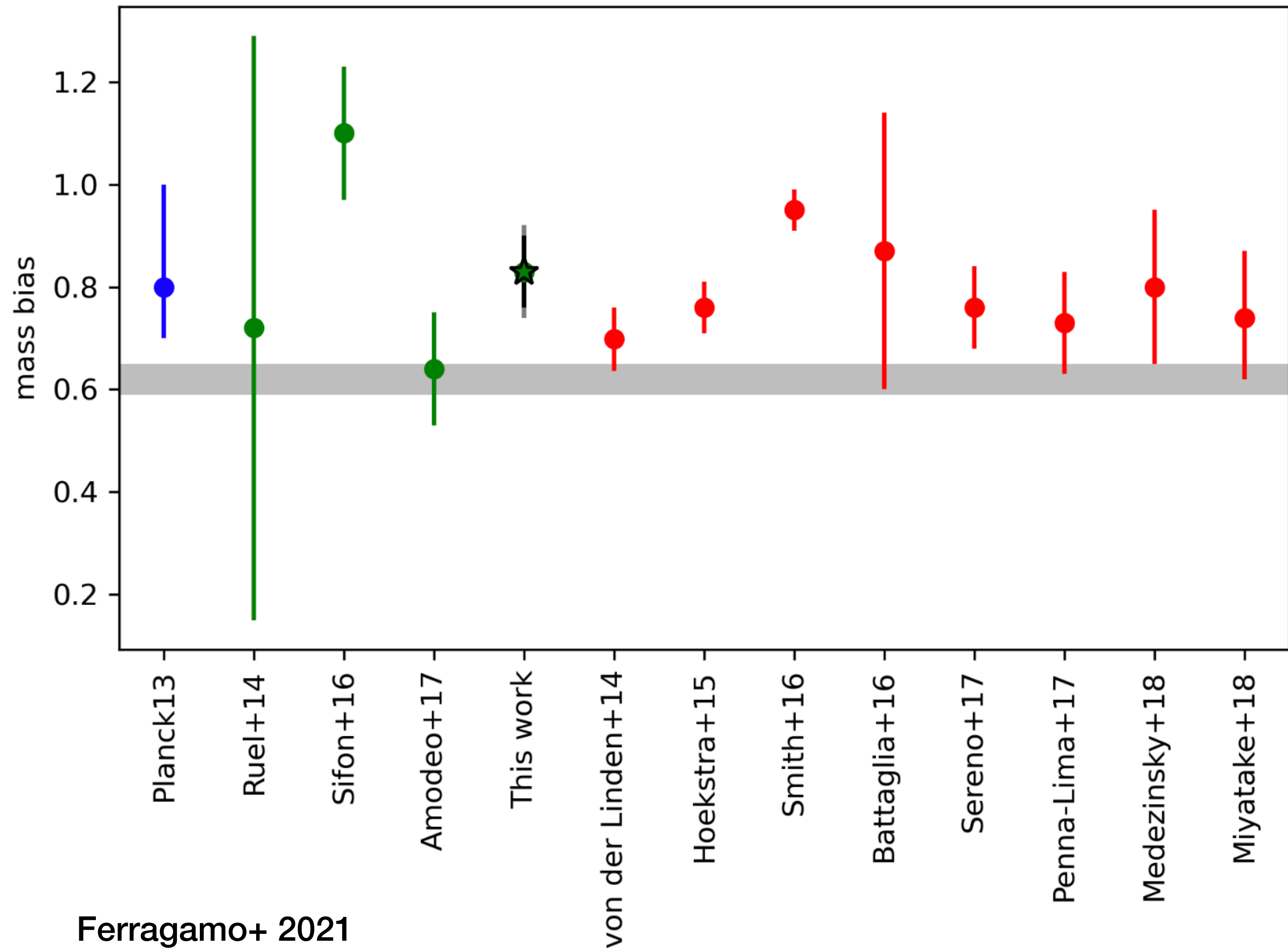
$$M(< r) = - \frac{kT(r)r}{G\mu m_p} \left[\frac{d \ln n_p}{d \ln r} + \frac{d \ln T}{d \ln r} \right] \propto T(r)r$$



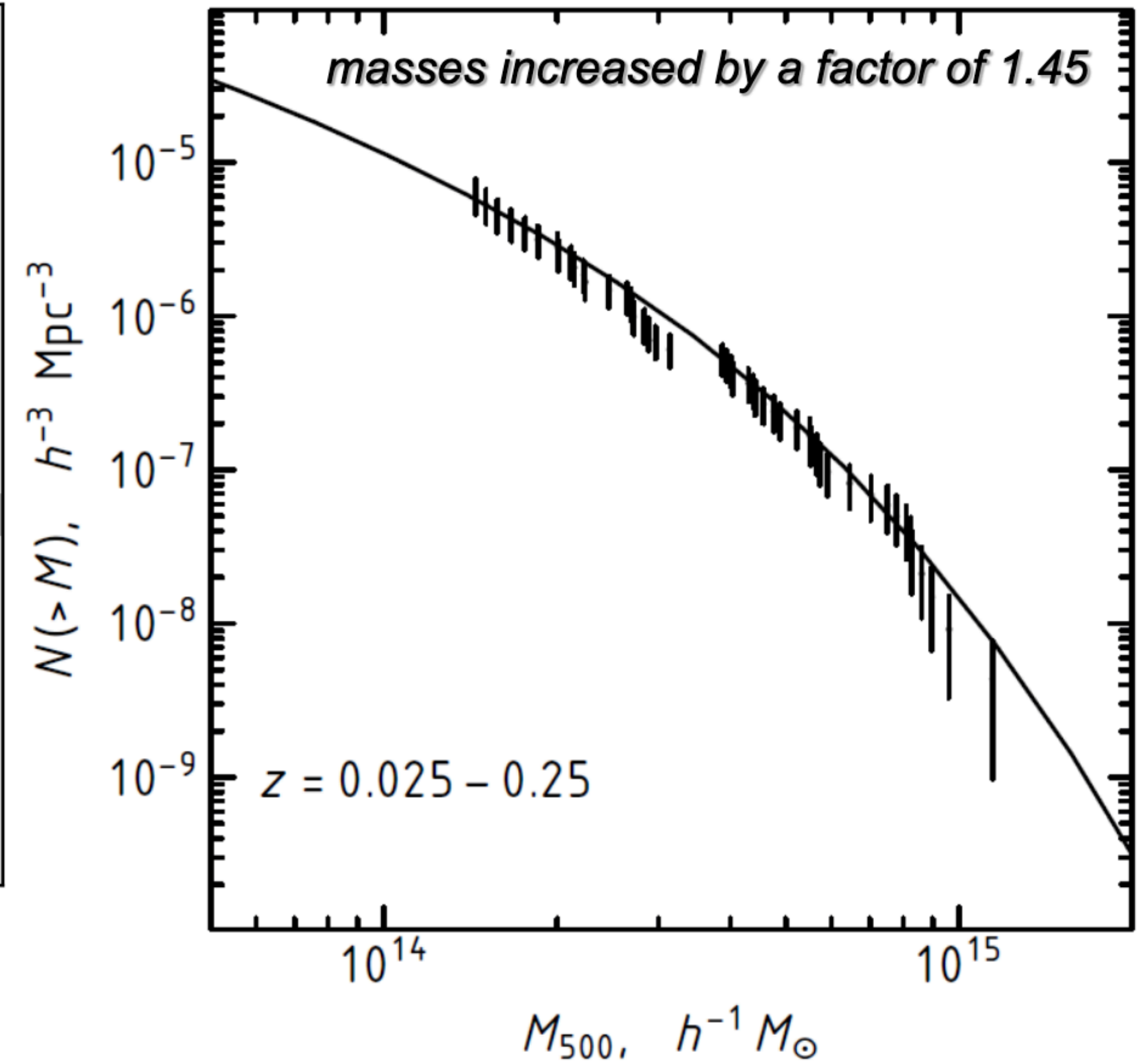
Galaxy Clusters: Why Calibration?



Galaxy Clusters: Why Calibration?

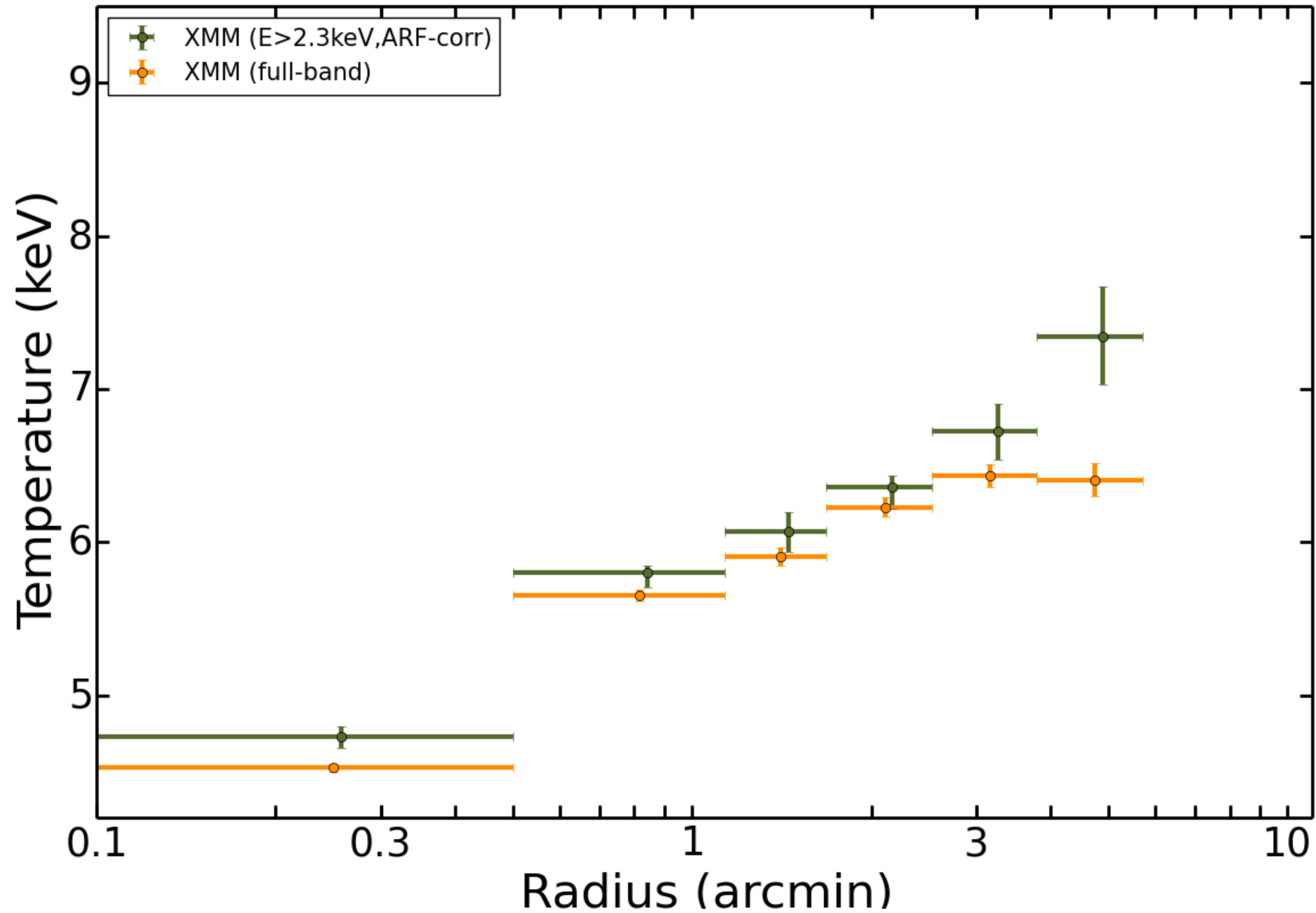


Ferragamo+ 2021

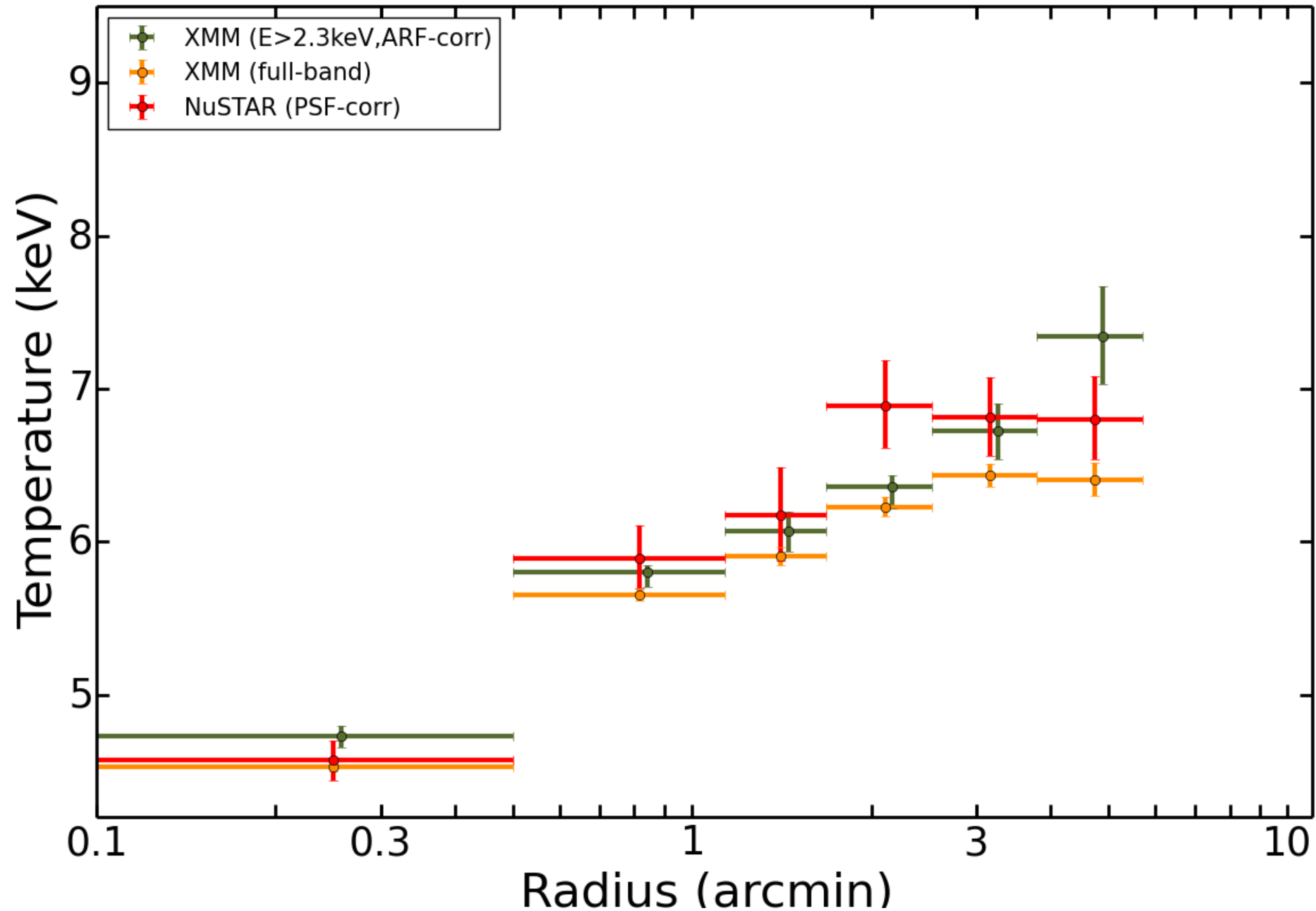


Vikhlinin+ 2009
 (Borrowed from 2016 KICP
 Workshop slide by Kravtsov)

XMM-Newton Self Consistency



XMM-Newton Self Consistency



Scattered & Stray Light

